

Genome-wide association study identifies new loci associated with OCD

Nora I Strom^{1,2,3,4} , Matthew W Halvorsen⁵, Chao Tian⁶, Christian Rück³, Gerd Kvale^{7,8}, Bjarne Hansen^{7,8}, Jonas Bybjerg-Grauholm^{9,10}, Jakob Grove^{4,9,11,12}, Julia Boberg³, Judith Becker Nissen^{13,14}, Thomas Damm Als^{4,9,11}, Thomas Werge^{9,15,16,17}, Elles de Schipper³, Bengt Fundin¹⁸, Christina Hultman¹⁸, Kira D. Höffler^{7,19,20}, Nancy Pedersen²¹, Sven Sandin^{21,22}, Cynthia Bulik^{21,23,24}, Mikael Landén²⁵, Elinor Karlsson^{26,27}, Kristen Hagen^{7,28,29}, Kerstin Lindblad-Toh²⁷, Nordic OCD and Related Disorders Consortium (NORDiC), 23andMe Research Team⁶, PGC TS/OCD working group, David M. Hougaard^{9,10}, Sandra M. Meier³⁰, Stéphanie Le Hellard^{7,19}, Ole Mors³¹, Anders D. Børglum^{4,9,11}, Jan Haavik^{7,32}, David A. Hinds⁶, David Mataix-Cols³, James J Crowley^{3,5,23}, and Manuel Mattheisen^{2,3,4,33} 

¹Department of Psychology, Humboldt-Universität zu Berlin, Berlin, Germany

²Institute of Psychiatric Phenomics and Genomics (IPPG), University Hospital of Munich, Munich, Germany

³Department of Clinical Neuroscience, Centre for Psychiatry Research, Karolinska Institutet, Stockholm, Sweden

⁴Department of Biomedicine, Aarhus University, Aarhus, Denmark

⁵Department of Genetics, University of North Carolina At Chapel Hill, Chapel Hill, NC, USA

⁶23andMe, Inc, Sunnyvale, Ca

⁷Bergen Center for Brain Plasticity, Division of Psychiatry, Haukeland University Hospital, Bergen, Norway

⁸Department of Clinical Psychology, University of Bergen, Bergen, Norway

⁹The Lundbeck Foundation Initiative for Integrative Psychiatric Research, iPSYCH, Aarhus, Denmark

¹⁰Center for Neonatal Screening, Department for Congenital Disorders, Statens Serum Institut, Copenhagen, Denmark

¹¹Center for Genomics and Personalized Medicine, Aarhus, Denmark

¹²Bioinformatics Research Centre, Aarhus University, Aarhus, Denmark

¹³Departments of Child and Adolescent Psychiatry, Aarhus University Hospital, Psychiatry, Aarhus, Denmark

¹⁴Institute of Clinical Medicine, Health, Aarhus University, Health, Aarhus University, Aarhus, Denmark

¹⁵Institute of Biological Psychiatry, Mental Health Services Copenhagen, Copenhagen University Hospital, Copenhagen, Denmark

¹⁶Department of Clinical Medicine, Faculty of Health Science, University of Copenhagen, Copenhagen, Denmark

¹⁷GLOBE Institute, Center for GeoGenetics, University of Copenhagen, Copenhagen, Denmark

¹⁸Department of Medical Epidemiology and Biostatistics, Center for Eating Disorders Innovation, Karolinska Institutet, Stockholm, Sweden

¹⁹Department of Clinical Science, University of Bergen, Bergen, Norway

²⁰Department of Medical Genetics, Haukeland University Hospital, Bergen, Norway

²¹Department of Medical Epidemiology and Biostatistics, Karolinska Institutet, Stockholm, Sweden

²²Department of Psychiatry, Icahn School of Medicine at Mount Sinai, NY, USA

²³Department of Psychiatry, University of North Carolina At Chapel Hill, Chapel Hill, NC, USA

²⁴Department of Nutrition, University of North Carolina at Chapel Hill, NC, USA

²⁵Department of Psychiatry and Neurochemistry, Institute of Neuroscience and Physiology, University of Gothenburg, Gothenburg, Sweden

²⁶Department of Bioinformatics and Integrative Biology, University of Massachusetts Medical School, Worcester, MA, USA

²⁷Department of Vertebrate Genomics, Broad Institute of MIT and Harvard, Cambridge, MA, USA

²⁸Department of Psychiatry, Møre og Romsdal Hospital Trust, Molde, Møre og Romsdal, Norway

²⁹Department of Mental Health, Norwegian University for Science and Technology, Trondheim, Sweden

³⁰Department of Psychiatry, Dalhousie University, Halifax, NS, Canada

³¹Psychosis Research Unit, Aarhus University Hospital - Psychiatry, Aarhus Denmark

³²Department of Biomedicine, University of Bergen, Bergen, Norway

³³Department of Community Health and Epidemiology and Faculty of Computer Science, Dalhousie University, Halifax, NS, Canada

To date, four genome-wide association studies (GWAS) of obsessive-compulsive disorder (OCD) have been published, reporting a high single-nucleotide polymorphism (SNP)-heritability of 28% but finding only one significant SNP. A substantial increase in sample size will likely lead to further identification of SNPs, genes, and biological pathways mediating the susceptibility to OCD. We conducted a GWAS meta-analysis with a 2-3-fold increase in case sample size (OCD cases: $N = 37,015$, controls: $N = 948,616$) compared to the last OCD GWAS, including six previously published cohorts (OCAS, IOCDF-GC, IOCDF-GC-trio, NORDiC-nor, NORDiC-swe, and iPSYCH) and unpublished self-report data from 23andMe Inc. We explored the genetic architecture of OCD by conducting gene-based tests, tissue and celltype enrichment analyses, and estimating heritability and genetic correlations with 74 phenotypes. To examine a potential heterogeneity in our data, we conducted multivariable GWASs with MTAG. We found support for 15 independent genome-wide significant loci (14 new) and 79 protein-coding genes. Tissue enrichment analyses implicate multiple cortical regions, the amygdala, and hypothalamus, while cell type analyses yielded 12 cell types linked to OCD (all neurons). The SNP-based heritability of OCD was estimated

to be 0.08. Using MTAG we found evidence for specific genetic underpinnings characteristic of different cohort-ascertainment and identified additional significant SNPs. OCD was genetically correlated with 40 disorders or traits- positively with all psychiatric disorders and negatively with BMI, age at first birth and multiple autoimmune diseases. The GWAS meta-analysis identified several biologically informative genes as important contributors to the aetiology of OCD. Overall, we have begun laying the groundwork through which the biology of OCD will be understood and described.

Obsessive-compulsive disorder | OCD | GWAS

Correspondence: Nora I. Strom, Department of Psychology, Humboldt-Universität zu Berlin, Berlin, Germany. nora.strom@hu-berlin.de
Manuel Mattheisen, MD, Department of Community Health and Epidemiology and Faculty of Computer Science, Dalhousie University, Halifax, Nova Scotia, Canada. manuel.mattheisen@dal.ca

Introduction

Obsessive-compulsive disorder (OCD) is a neuropsychiatric disorder characterized by recurrent, unwanted thoughts and/or repetitive behaviors^{1,2}. It is relatively common (1-3%

prevalence³, often begins in childhood and although medication and behavioral therapy are useful, symptom control is imperfect, and the course is often chronic. Most individuals with OCD also have a comorbid psychiatric disorder (e.g., tic disorders, anorexia nervosa, mood-, and/or anxiety disorders)^{3,4} and early onset and tic-related OCD may be etiologically meaningful subtypes of the disorder^{5,6}. OCD is responsible for profound personal and societal costs⁷ and patients are at a substantial risk of suicide (~10 times higher than the population prevalence)⁸ and show an increase in general mortality⁹. OCD is highly heritable (~50%)^{10,11}, and first-degree relatives of affected individuals have a 4-8 times increased risk of developing the disorder¹¹⁻¹³. It is hoped that the identification of specific genes and biological pathways mediating susceptibility to OCD will lead to improved understanding and perhaps to improved detection, differential diagnosis, and/or treatment of OCD. Unfortunately, several OCD linkage studies (reviewed by Pauls et al.¹⁴) and >100 candidate gene studies (meta-analyzed by Taylor et al.¹⁵) have produced inconsistent results. More recently, there have been four published genome-wide association studies (GWAS) of OCD. The first¹⁶ included 1,465 cases, 5,557 controls, and 400 trios. No genome-wide significant loci were identified, but polygenic risk analysis revealed overlap with Tourette syndrome and indicated that increased sample size will likely reveal significant loci¹⁷. A second OCD GWAS¹⁸ had 1,406 cases and 3,655 controls and although a third GWAS meta-analysis¹⁹ of these two studies revealed substantial heritability of OCD risk based on common variation (0.28 ± 0.04), it failed to identify genome-wide significant loci. The fourth GWAS, recently published on medRxiv²⁰, was comprised of a total of 14,140 OCD cases and 562,117 controls and revealed the first genome-wide significant hit for OCD on chromosome 3. Sample size has clearly been the limiting factor for gene discovery in OCD. Here we present GWAS results obtained from a sample with a ~ 2-3 fold increase in case sample size (37,015 cases and 948,616 controls) over the recent medRxiv paper. Cases and controls were derived from 1) a previous OCD GWAS meta-analysis mentioned above¹⁹, 2) ongoing studies in Scandinavia (NORDiC²¹ and the Danish iPSYCH cohort^{22,23}), which were also included in the most recent OCD GWAS meta-analysis²⁰, and 3) unpublished self-report OCD cases and controls from 23andMe Inc.

Methods

Samples

We analysed genomic data from seven OCD case-control cohorts of European ancestry. The meta-analysis included 1) partially published data from Scandinavia including NORDiC-NOR (365 OCD cases, 315 controls), NORDiC-SWE (977 OCD cases, 3,200 controls²¹), and iPSYCH (2,678 OCD cases, 10,410 controls) (data was included in the recently published OCD GWAS²⁰; 2) the three datasets from the previously published OCD PGC-freeze 1¹⁹), com-

prised of OCGAS¹⁸ (986 OCD cases, 1,023 controls; with changed control-inclusion compared to the original publication), IOCDF-GC (1,519 OCD cases, 3,541 controls¹⁶), and IOCDF-GC-trio (323 complete trios); and 3) unpublished self-report OCD cases and controls from 23andMe (30,167 OCD cases, 929,804 controls). Together, the GWAS meta-analysis included 37,015 OCD cases and 948,616 controls of European ancestry. We further conducted three separate GWAS analyses, a) combining all clinical cases primarily ascertained for OCD (OCD PGC-freeze1 and NORDiC samples (NORDiC-NOR and NORDiC-SWE), in the following referred to as "freeze1+NORDiC"), b) clinical cases obtained through a population-based sample primarily ascertained for another comorbid psychiatric disorder (iPSYCH), and c) self-report samples (23andMe). We also conducted three multivariable GWAS analyses with MTAG for the same subgroups as described above. Cohort specific sample and analytic details can be found in the following and Supplementary Table S1 provides an overview of the individual cohorts. Data collections were approved by the relevant institutional review boards at all participating sites. Where required, all participants provided written informed consent.

GWAS analysis NORDiC-NOR & NORDiC-SWE

pre-GWAS Quality Control (QC)

We assembled two separate NORDiC case/control datasets from genotype array data for our GWAS. The first consisted of 647,335 variant calls across a total of 1,107 NORDiC-SWE case and 3,500 Swedish control samples. The second consisted of 482 NORDiC-NOR case and 343 Norwegian-ancestry control samples. The Swedish GWAS was a merger across a total of four different cohorts (one case-only, three control-only) whereas the Norwegian GWAS was a merger across 3 cohorts (two case-only, one control-only). Variant-level QC on the data removed SNP markers where there was evidence of excess missingness in any of the input cohorts, case/control missingness difference, or evidence of clustering artifact. Sample-level QC on the data removed individuals with excess missingness and instances of cryptic relatedness. Sample-level QC also identified a subset of samples of likely European ancestry based on clustering with 1000 genomes data²⁴, ensuring the construction of datasets that are homogeneous and less prone to potential effects of population stratification. The process left us with 492,554 QC-passing variants across the NORDiC-SWE GWAS data (1,107 cases and 3,500 controls) and 479,358 QC-passing variants across the NORDiC-NOR data (407 cases and 340 controls). Please refer to the section 'GWAS details for NORDiC-NOR & NORDiC-SWE' in the supplemental text for details specific to the Swedish and Norwegian QC and GWAS analyses.

QC and imputation implemented in RICOPILI

We used the Rapid Imputation and Computational Pipeline for Genome-Wide Association Studies (RICOPILI,²⁵) to run an automated round of pre-imputation QC on the genotype data from 492,554 QC-passing variants across the full unpruned datasets of NORDiC-SWE (1,107 cases

and 3,500 controls) and 479,358 QC-passing variants across NORDIC-NOR (407 cases and 340 controls), and conducted imputation on the genotype data using the Haplotype Reference Consortium (HRC) reference panel. All subsets of the analysis were done using RICOPIILI v2018_Dec_7.001. The pre-imputation RICOPIILI QC step involved a series of hard filters on variant and sample level data, including removing variants with pre-sample pruning call rate < 0.95, samples with call rate < 0.98, FHET outside of +/- 0.20, samples with discrepancies between reported and derived sex, and post sample-pruning variants that met any of the following: 1) call rate < 0.98, 2) missing difference > 0.02, 3) invariant positions, 4) minor allele frequency (MAF) > 0.01, 5) Hardy-Weinberg equilibrium (HWE) $p < 1 \times 10^{-6}$ in controls, and 6) HWE $p < 1 \times 10^{-10}$ in cases. After the QC described we were left with 481,323 QC-passing variants across 1,077 cases and 3,486 controls in NORDiC-SWE, and 469,618 QC-passing variants across 404 cases and 340 controls in NORDiC-NOR.

After sample and variant pruning we next used RICOPIILI's impute_dirsub module to perform imputation using HRC genotypes as a reference panel. In our imputation run we used eagle v2.3.5 for pre-phasing, and minimac3 v2.0.1 for imputation. We derived 3 different imputed callsets from this process: 1) a set of high confidence imputed genotypes (2,771,425 in NORDiC-SWE, 3,043,464 in NORDiC-NOR), 2) a set of imputed best-guess genotypes with medium level accuracy (7,112,906 in NORDiCSWE, 7,277,174 in NORDiC-NOR), and 3) a set of variants for which imputation accuracy was lowered in order to increase the total number of variants included in the imputation (9,021,638 in NORDiC-SWE, 8,964,589 in NORDiC-NOR).

GWAS

We ran our GWAS across the largest dataset of imputed variants that were generated during the imputation process on a subset of samples that were of European ancestry. We intersected the RICOPIILI QC-pruned set of samples with our own set of relatedness-pruned European ancestry samples described earlier to obtain a set of 977 cases and 3,200 controls for NORDiC-SWE GWAS, and 365 cases and 315 controls for NORDiC-NOR OCD GWAS. We conducted principle component analysis (PCA) on these samples across high-confidence imputed genotypes using the pacer_sub RICOPIILI module and tested the first 20 PCs for significant association with sample case/control status (significant = p -value < 0.05/20). We identified PCs 1, 3 and 14 as significant predictors and used them as covariates in the NORDiC-SWE GWAS. Along the same lines we identified PCs 1, 2, 3 and 4 as significant predictors and used them as covariates in the NORDiC-NOR GWAS.

GWAS analysis iPSYCH

Danish nation-wide population-based case-control samples were collected in the scope of the 'Danish OCD and Tourette

Study' (DOTS) within 'The Lundbeck Foundation Initiative for Integrative Psychiatric Research' (iPSYCH). Individuals were not primarily ascertained for OCD; OCD cases were drawn from cases that also presented a diagnosis of another psychiatric disorder and from controls with a diagnosis of OCD.

Heel prick blood samples had been collected from all babies in Denmark born between 1981 and 2005. Genetic information was obtained by the Statens Serum Institut (SSI) at the Danish Neonatal Screening Biobank (DNSB). The genetic information was linked with the Danish Civil Registration System and thereby coupled with the Danish Psychiatric Central Research Register which collects patient data of individuals treated in psychiatric hospitals or in outpatient psychiatric clinics. OCD cases met ICD10 (F42) criteria, controls were randomly selected from the same birth cohorts and excluded individuals with a F42 diagnosis.

Genotyping was performed on the PsychChip v 1.0 array (Illumina, San Diego, CA, USA) at the Broad Institute of MIT and Harvard (Cambridge, MA, USA). Genotyping and data analysis was performed in 25 batches. Genotype data was processed using RICOPIILI performing stringent QC. Samples with a call rate below 95%, with a sex mismatch, between the sex obtained from genotype data and from the register data, as well as related individuals were removed. Principle component analysis was used to exclude ancestral outliers from non-European descent. The data was imputed using the HRC reference panel. The final data set included 2,678 OCD cases and 10,410 controls.

The study was approved by the Regional Scientific Ethics Committee in Denmark and the Danish Data Protection Agency. All analyses of the samples were performed on the secured national GenomeDK high performance-computing cluster in Denmark (<https://genome.au.dk>). Details of the cohort, data QC and GWAS analysis have been described elsewhere^{22,26}.

GWAS analysis OCD PGC-freeze1

The OCD PGC-freeze1 cohort refers to the OCD GWAS meta-analysis previously published by the PGC, comprising data from the 'OCD Foundation-Genetics Consortium' (IOCDF-GC) and 'The OCD Collaborative Genetics Association Study' (OC GAS). Details of the cohorts and analysis can be found in the primary publications^{16;18;27}. Here, we used the OC GAS and IOCDF-GC data from a recent meta-analysis for which the data was re-analyzed with newly matched controls²⁰.

The IOCDF-GC cohort consists of a case-control sample and a trio sample. The case-control cohort consists of 1,519 European OCD cases and 3,541 matched controls. Part of the controls were drawn from previously genotyped cohorts including the Alzheimer's Disease Genetics Initiative²⁸, the Center for Applied Genomics (CAG) at Children's Hospi-

tal of Philadelphia (CHOP)²⁹, and the Breast and Prostate Cancer Cohort Consortium (BPC3)³⁰. The trio sample consists of 323 complete trios of European ancestry. Cases and trios were predominantly recruited from OCD specialty clinics. Controls were recruited from Bonn, Germany and from Capetown, South Africa. All cases met DSM-IV diagnosis of OCD, while the controls from Bonn had no lifetime history of any axis I disorders and the controls from Cape Town were unscreened.

Genotyping was performed on the Illumina Human610-QuadV1_B array (Illumina, San Diego, CA, USA). Standard QC was performed using PLINK2³¹. Samples with a call rate <98%, sex discrepancy or ambiguous genomic sex, and related samples ($\text{pihat} > 0.2$) were removed. SNPs with a genotyping rate <98%, with a MAF < .01, monomorphic SNPs, CNV-targeted SNP probes, strand-ambiguous SNPs with significant allele frequency differences or aberrant LD correlations with neighbouring SNPs based on the entire HapMap2 reference panel, SNPs with differential missing rate between cases and controls (> 0.02), SNPs with $P < 1 \times 10^{-6}$ (controls) or $P < 1 \times 10^{-10}$ (cases) in HWE, and SNPs with batch effect ($P < 1 \times 10^{-5}$) in control cohorts were removed. The same QC was performed on the trios, additionally removing SNPs with Mendelian errors. For each trio, the transmitted and untransmitted alleles were converted into one case and one pseudo-control. Multidimensional scaling analysis (MDS) was performed and samples with significant outliers in the first five dimensions or when there were no matching cases and controls for each dimension, were removed. Phasing was done with SHAPEIT2³² and imputation was performed with Minimac3³³. HRC reference release 1.1 was used as a reference panel. PLINK2 was used to run the GWAS, including SNPs with imputation score > 0.8 and MAF < 0.01, using logistic regression and the first five and the 7th MDS components as covariates. For the trio analysis, phasing and imputation were performed in the same way, GWAS was conducted without covariates.

Participants for the OCGAS study were recruited at five different participating sites of the National Institute for Mental Health at Johns Hopkins University School of Medicine, Brown Medical School, New York State Psychiatric Institute and College of Physicians and Surgeons at Columbia University, University of California Los Angeles (UCLA) School of Medicine, Massachusetts General Hospital and Harvard Medical School, National Institute of Mental Health, and Keck School of Medicine at the University of Southern California and was approved by each site's IRB boards. Data was collected between 2007 and 2014 and is comprised of trios (affected proband and both parents) or a proband and an unaffected sibling. MD- or PhD-level clinical psychologists evaluated each individual using the Structured Clinical Interview for DSM-IV (SCID), the checklist of obsessions and compulsions from the Y-BOCS, refined to include the age of onset, age of offset, severity of each symptom, as well as the Y-BOCS scores for the worst episode (lifetime), further including course and treatment response variables. Children

older than 8 years were assessed in the same way, but using the Kiddie-SADS instead of the SCID. Diagnostic status was assigned based on the consensus of two psychiatrists or psychologists independently evaluating each proband, and was further reviewed by one of five members of the JHU diagnostic consensus committee to ensure comparability across all five participating sites. The chance-corrected percent agreement between the diagnosticians for the diagnosis of OCD was $K = 0.92$; for age at onset of OCD, $K = 0.88$ (for age ± 5 years), and Pearson's $r = 0.71$. Cases were required to meet DSM-IV criteria for OCD, with an onset of symptoms before the age of 18 ($\text{mean} = 9.4$ years; $SD = 6.35$). Individuals with a later age-of-onset, or with a diagnosis of schizophrenia, brain tumors, Huntington's disease, Parkinson's disease, Alzheimer's disease, severe mental retardation, not permitting an evaluation of psychiatric disorders, or Tourette's disorder or OCD occurring exclusively in the context of depression (secondary OCD) were excluded. Samples were genotyped on the Illumina PsychChip array at USC.

GWAS analysis 23andMe

Population

Samples of European ancestry were drawn from the research participant base of 23andMe, a private consumer genetics and research company. The cohort has been described in detail elsewhere³⁴. All participants provided informed consent, and answered online surveys. The cohort was selected from participant data available on 1st September 2017 and the analysis was reviewed and approved by a private institutional review board (www.eandireview.com). All individuals identified as cases have reported being diagnosed with OCD, while controls have reported not having been diagnosed with OCD. 30,167 OCD cases and 929,804 controls were included in the final GWAS. Of the cases, 10,808 (35.83%) were male and 19,359 (64.17%) were female. Of the controls, 443,336 (47.68%) were male and 486,468 (52.32%) were female. Of the cases, 7,040 (23.34%) individuals were below the age of 30, 11,087 (36.75%) between 30 and 45, 7,056 (23.39%) between 45 and 60, and 4,984 (16.52%) above the age of 60. Of the controls, 91,287 (9.82%) individuals were below the age of 30, 230,696 (24.81%) between 30 and 45, 257,793 between 45 and 60, and 350,028 (27.73%) above the age of 60.

Genotyping, QC, and imputation

Extraction of DNA and genotyping was performed by the National Genetics Institute (NGI), a CLIA licensed clinical laboratory and a subsidiary of Laboratory Corporation of America. Individuals were genotyped on four different genotype platforms. Two (V1, V2) platforms were variants of the Illumina HumanHap550+ BeadChip, including 25,000 custom SNPs, one platform (V3) was the Illumina OmniExpress+ BeadChip, with custom SNPs to increase overlap with V2, and one platform (V4) is in current use and a fully customized array. Individuals that failed to meet

a 98.5% call rate were re-analyzed. Only individuals with > 97% European ancestry were included in the analysis. European ancestry was determined through an analysis of local ancestry using a support vector machine to classify individual haplotypes into one of 31 reference populations. Those classifications were then fed into a hidden Markov model (HMM) which accounts for incorrect assignments and switch errors, thereby giving probabilities for each reference population per window (100 SNPs). Simulated admixed individuals were then used to re-calibrate the HMM probabilities so the assigned ancestries were consistent with the simulated individuals. Publicly available datasets (Human Genome Diversity Project, HapMap, and 1000 Genomes) and 23andMe research participants with four grandparents from the same country served as the reference population. Identity-by-descent (IBD) estimation was used to define a maximal set of unrelated individuals for each analysis. Individuals who shared less than 700 cM IBD were defined as unrelated (e.g. approximately less related than first cousins).

The merged UK10K and 1000 Genomes Phase 3 panel was used for imputation. Finch, an internally developed tool, that implements the Beagle haplotype graph-based phasing algorithm, modified to separate the steps of graph construction and phasing, was used for phasing. Imputation was then performed as an estimated allele dosage averaged over a set of possible imputed haplotypes for each individual.

GWAS

Genetic association testing was performed using logistic regression, assuming an additive model for allelic effects, including age, sex, first five PCs, and the genotype platform as covariates. For imputed data, the imputed dosages rather than the best-guess genotypes were used. The association p-value was computed using a likelihood ratio test.

GWAS meta-analysis

Before the above described datasets were combined in an OCD GWAS meta-analysis, each file was filtered and formatted in a way that they could be more easily combined. This involved aligning each SNP to the HRC genome³⁵ and excluding ambiguous SNPs and SNPs of likely poor quality. All variants had to meet the following criteria for inclusion: Case and control minor allele frequency > 1%, imputation-score > 0.8 and < 1.2. Strand-ambiguous A/T and C/G SNPs were removed if they had a frequency between 0.4 and 0.6. Was their frequency outside of that range, their frequency was compared to the frequency in the reference dataset. It was only retained if the frequency was either below 0.4 or above 0.6 in both, the OCD summary statistic and the reference dataset. If a variant did not overlap with the variants in the HRC reference, it was removed.

To combine the seven OCD case-control datasets we conducted an inverse variance weighted meta-analysis using METAL³⁶. The genome-wide significance threshold for the

GWAS was set at a p-value of 5.0×10^{-8} . For each individual GWAS as well as for the meta-analysis we calculated the genomic inflation factor (λ_{1000}) to identify any residual population stratification of systematic technical artifact. We further calculated the linkage disequilibrium score (LDSC) regression intercept to evaluate the relative contribution of polygenic effects and residual artefacts such as population stratification and cryptic relatedness. For the analysis we used pre-computed LD scores from European-ancestry samples in the 1000 Genomes Projects (see web resources) and filtered our dataset on high-quality common SNPs with an INFO score > 0.9. The influence of confounding factors was evaluated by comparing the estimated intercept of the LD score regression to one. One is the expected value of the LDSC intercept under the null hypothesis of no confounding (e.g. from population stratification). Heterogeneity in test-statistic across the seven datasets was assessed with Cochran's I^2 statistic. To identify any cohort in which the summary statistics significantly deviated from the rest of the cohorts, we performed sign test analyses for the top SNPs (inclusion threshold of $p = 1.00 \times 10^{-4}$, $p = 1.00 \times 10^{-5}$, $p = 1.00 \times 10^{-6}$, and $p = 5.00 \times 10^{-8}$) between each cohort and leave-one out meta-analyses of the remaining 6 datasets.

Gene-based tests

All gene-based tests were conducted using MAGMA v1.08³⁷. Gene units were defined using three separate models: 1) the standard MAGMA model based on proximity, with a SNP falling within the general gene region, here defined as 35kb upstream of the transcription start site to 10kb downstream of the transcription start site; 2) a model where genes units are formed across 13 different brain tissues from GTEx by defining SNPs as eQTLs for genes in each tissue in question³⁸; 3) a model defined by SNPs linked to gene regions via 3D chromatin interactions across eight brain tissue datasets³⁹. All MAGMA gene-based tests used the following inclusion filters: MAF ≥ 0.01 , INFO ≥ 0.9 , and additional MAGMA parameters 'use=SNP,P ncol=Neff_half'. The 'use=SNP,P' means that the SNP IDs are derived from the 'SNP' column of input daner files, and that p-values were derived from the 'P' column of these files. The 'ncol=Neff_half' refers to the definition of N per SNP as the effective sample size and can be defined as $4 * N_{ca} * N_{co} / (2 * (N_{ca} + N_{co}))$ in a single cohort. A Bonferroni threshold for significance was set based on the total number of tests performed across these three models combined (45,664) and was equal to $0.05 / 45,664 = 1.09 \times 10^{-6}$.

Tissue / celltype enrichment analyses

We followed a tissue / celltype enrichment analysis protocol recently described in Bryois et al.⁴⁰. Consistent with this we utilized the codebase for this analysis, and in particular the sets of genes that mark different highlighted tissue and celltype datasets, that were made available by the manuscript authors at https://github.com/jbryois/scRNA_disease.

We selected 3 datasets that had been preprocessed by Bryois et al.⁴⁰ for inclusion in this analysis. The first features tissue-specific gene expression data derived from GTEx⁴¹, with a total of 37 tissues represented in the data. The second and third are derived from Zeisel et al.⁴², and represent broad celltype groups across the entirety of the mouse nervous system, along with a high resolution single celltype map of the same data. In Zeisel et al.⁴², a total of 39 broad celltype groups and 265 individual celltypes are represented.

We followed the analysis protocol described in Bryois et al.⁴⁰ for the analyses of 37 tissues from GTEx and 39 broad celltype groups from Zeisel et al.⁴², and utilized a simplified approach for the analysis of each of the 265 individual celltypes from Zeisel et al.⁴². For the tissue and broad celltype group datasets, we conducted the full protocol from Bryois et al.⁴⁰ which included analyzing tissue/celltype enrichment using both LDSC⁴³ and MAGMA⁴⁴. We only considered a tissue / celltype significantly enriched if the FDR-adjusted p-value was less than 0.05 in both the LDSC and MAGMA-based tests. Due to the high computational demands of testing 265 individual celltypes across the mouse nervous system with LDSC, we limited the protocol to only include the MAGMA assessment. We considered a celltype significant if it had an FDR-adjusted p-value less than 0.05.

All statistical analysis downstream of LDSC and MAGMA (namely, p-value adjustment) was done using R v4.0.0, and all plotting was done inside of R v4.0.0 using the package ggplot2 v3.3.2. FDR p-value adjustments were performed using the R function `p.adjust(method="fdr")`. Bonferroni p-value adjustments were performed using the R function `p.adjust(method="Bonferroni")`.

Multivariable GWAS with MTAG

We used MTAG⁴⁵ to conduct multivariable GWAS analyses for the OCD samples. MTAG combines related traits into a meta-analysis by leveraging the shared heritability among the different traits. For this purpose we included the same summary statistics that also formed the basis for the meta-analysis using METAL, i.e., the freeze 1 data from the original meta-analysis together with the NORDiC samples (freeze1+NORDiC, see above), the iPSYCH dataset, and the 23andMe dataset. But unlike with the METAL-based meta-analysis, the MTAG analysis results in three subgroup-specific estimates (i.e., freeze1+NORDiC, iPSYCH, and 23andMe) that gain power by exploiting the high shared heritability across all subgroups compared to separate subgroup specific analysis. Through this approach we aimed to address potential concerns about heterogeneity in our phenotyping strategies for the three individual sub datasets (see below in the discussion). We performed maxFDR analyses to approximate the upper bound on the FDR of MTAG results.

SNP-based heritability and genetic correlation with other disorders and traits

LDSC⁴³ was used to evaluate the contribution of all included SNPs on the variance in liability to OCD (SNP-based heritability). The analysis was performed using pre-computed LDscores from samples restricted to European-ancestry in the 1000 Genomes Project^{43;46}, filtered for SNPs included in the HapMap3 reference panel⁴⁷. SNP-heritability was estimated based on the slope of the LD score regression, with heritability on the liability scale calculated assuming a 3% population prevalence of OCD. SNP-heritability was calculated for the whole OCD sample as well as for a) clinical samples (NORDiC-SWE, NORDiC-NOR, and freeze1), b) samples not primarily ascertained for OCD (iPSYCH), and c) self-reported biobank samples (23andMe). Cross-trait LDSC regression was used to estimate the genetic correlations of OCD with 74 other phenotypes (see Supplementary Table S7 for an overview of all tested traits). LDSC estimates the genetic correlation between two traits by regressing the product of the Z-scores from GWASs on the LD score which represents the genetic co-variation between the two traits based on all polygenic effects captured by the included SNPs. Again, European-ancestry LD-scores from the 1000Genomes project, restricted to SNPs included in the HapMap3 reference panel, were used. Cross-trait genetic correlations were calculated for the whole OCD sample, for the same three sub-samples used in the SNP heritability analysis, and for the three MTAG analyses.

Results

GWAS meta-analysis

We conducted a GWAS meta-analysis of seven European-ancestry case-control cohorts, including a total of 37,015 OCD cases and 948,616 controls with 6,829,695 autosomal SNPs. Five datasets have been published in previous OCD-GWASs - the OCGAS and IOCDF-GC cohorts have been included in the first OCD GWASs^{16;18;19}, while the NORDiC-SWE, NORDiC-NOR, and iPSYCH cohorts have been included in a recent preprint²⁰. For this GWAS, additional samples from 23andMe (30,167 cases and 929,804 controls) were added to these previously published datasets. The QQ-plot (Figure 1B) and Lambda ($\lambda = 1.241$; $\lambda_{1000} = 1.003$) of the meta-analysis was in accordance with the assumption of polygenicity and did not show any evidence for residual stratification effects. 15 independent SNPs exceeded the genome-wide threshold for significance (See Figure 1, Supplementary Figures S2-S16 for regional association plots and forest-plots). The genome-wide significant SNPs were located on chromosomes 1, 2, 3, 4, 5, 6, 8, 11, 12, 15, and 21. The SNP with the lowest p-value was rs10877425 on chromosome 12 ($P = 1.14 \times 10^{-10}$) and there were an additional 27 SNPs that were genome-wide significant in this locus.

Gene-based tests

Gene-based tests were conducted using MAGMA v1.08 to determine if, based on various criteria, any single protein-coding genes carried a load of common variation in OCD relative to controls that passed the Bonferroni threshold for significance. We conducted three sets of tests, each one linking common variation to individual genes via different means. The first was the standard MAGMA approach, considering SNPs as part of the signal for a given gene if it falls within the region 35kb upstream of the gene transcription start site to 10kb downstream of the transcript stop site (18,048 tests total). The second, e-MAGMA, considered SNPs as members of a gene if they were called as eQTLs in at least one brain tissue type assessed in GTEx (9240 tests total). The third, h-MAGMA, considered SNPs as members of a gene if they fell within gene exons or promoters, or alternatively if they were in distal intronic/intergenic regions but overlapped with a chromatin interaction detected in fetal or adult brain that linked back to the gene body (18,376 tests total). The threshold for significance was set based on the sum of the described tests performed ($0.05/45,664 = 1.1 \times 10^{-6}$).

We identified a total of 101 tests that passed the Bonferroni threshold for significance, mapping back to a total of 79 distinct protein-coding genes (Figure 2). Only one of these genes, *WDR6*, was observed as significant across all tests. Results from c-MAGMA, e-MAGMA and h-MAGMA captured overlapping and unique significant single-gene results (Figure 3). In some instances, the extended versions of MAGMA (e-MAGMA and h-MAGMA) provide additional context to the gene-based signal. For example, h-MAGMA suggests that the significantly associated gene *HCN1* is concentrated within promoter, exonic and chromatin-interacting loci. In another example, only e-MAGMA implicates a set of 6 genes within a region on chromosome 6, suggesting that the eQTLs that are a part of this signal could not be captured via simple gene overlap or 3D chromatin interactions. All gene-based test results are provided in Supplementary Table S2-S5.

Tissue / celltype enrichment analyses

In our enrichment analyses focused on broad tissues as defined by GTEx⁴¹ we identified five different tissues that carried a significant amount of OCD heritability enrichment. All tissues were found within the brain, and included the Anterior cingulate Cortex, Frontal Cortex, Amygdala, and Hypothalamus (Figure 4).

Enrichment analyses focused on broad celltypes were carried out in the same manner as tissue enrichment analyses and identified a total of five broad celltypes that are significant based on the methods used (see methods). Significant results included telencephalon projecting excitatory and inhibitory neurons, di- and mesencephalon excitatory and inhibitory neurons, and dentate gyrus granule neurons (Figure 4).

We conducted these enrichment analyses on a total of 265 fine-grain celltypes from the mouse nervous system⁴², and identified a total of 44 that survived FDR correction (Supplementary Table S10). We formed 35 groups of single cell types where $N \geq 2$ based on the 'Description' column from the table in <http://mousebrain.org/celltypes/>. We then took the mean $-\log_{10}$ p-value from each group, and performed FDR correction on these aggregated statistics in order to determine if any of these groups carried a significant excess. We identified a total of seven significant classifications, with key results including D1 and D2 medium spiny neurons, along with excitatory neurons from hippocampus C1, and cerebral cortex (Figure 5).

MTAG analyses

Leveraging the shared heritability among the three characteristically differing OCD sub-samples (freeze1+Nordic, iPSYCH, 23andMe), we performed three separate multi-trait analysis with MTAG, with the aim to extract specific genetic underpinnings characteristic of a) clinically ascertained OCD cases (freeze1+Nordic) b) OCD cases comorbid with another psychiatric disorder (iPSYCH), and c) self-report OCD status (23andMe).

For freeze1+NORDiC (clinically ascertained) we identified seven genome-wide significant associated SNPs (see figure 1C for the Manhattan plot and figure 1D for the qq-plot). Four of these SNPs overlap with the original GWAS meta-analysis of OCD, one genetic region overlaps with the MTAG analysis focusing on the iPSYCH sample (comorbid ascertainment) and the MTAG analysis focusing on the 23andMe sample (self-report), one SNP overlaps with the MTAG analysis focusing on the iPSYCH sample, and one is unique for clinically ascertained OCD cases. Max FDR was calculated at 0.0371. For iPSYCH we identified 15 significant SNPs, of which 11 regions (the most significant SNP in a region varied) overlap with the original GWAS meta-analysis, one overlaps with the other two MTAG analyses, and four SNPs overlap with one of the other two MTAG analyses. Max FDR was calculated at 0.0154. For 23andMe we identified 18 genome-wide significant SNPs, of which 12 regions overlapped with the original GWAS meta-analysis, three overlapped with at least one of the other MTAG analyses and three were uniquely significant in this analysis. Max FDR was calculated at 0.0035.

A total of five loci were significant in all three runs of MTAG (one locus was tagged by two different SNPs: rs13262595 in freeze1+NORDiC and rs4129585 in iPSYCH and 23andMe) and four of these were significant in the original meta-analysis of these samples. Overall p-values of the lead SNPs appeared more significant in the MTAG analyses when compared to the original GWAS meta-analysis. See Supplementary Table S6 for an overview of all significant SNPs in the MTAG analyses compared to the original GWAS meta-analysis.

SNP-based heritability and genetic correlation with other disorders and traits

The SNP-based heritability of OCD, calculated using LD-score regression (LDSC), was estimated to be 0.085 ($SE = 0.004$) for the whole sample, assuming a 3% population prevalence. Subdividing the sample into the three subsets (freeze1+NORDiC, iPSYCH, 23andMe) and keeping the population prevalence at 3% yielded liability scale heritability estimates of 0.321 ($SE = 0.039$), 0.25 ($SE = 0.045$), and 0.081 ($SE = 0.005$), respectively. Genetic correlations between the three sub-samples were high, reaching $rg = 0.88$ ($SE = 0.13$, $P = 2.01 \times 10^{-12}$) between freeze1+NORDiC and iPSYCH, $rg = 0.64$ ($SE = 0.06$, $P = 5.56 \times 10^{-29}$) between freeze1+NORDiC and 23andMe, and $rg = 0.85$ ($SE = 0.09$, $P = 1.52 \times 10^{-21}$) between iPSYCH and 23andMe.

Of the genetic correlations between OCD and 74 psychiatric, personality, psychological, substance-use, neurological, cognition, socioeconomic status, autoimmune, cardiovascular, anthropomorphic, and fertility traits, 40 exceeded the FDR-corrected significance threshold (Figure 6, Supplementary Table S7). OCD positively correlated with all psychiatric disorders, with especially high correlations with ANX, depressive disorder/MDD, PTSD, AN, and TS. Also, alcohol- and nicotine dependence correlated positively with OCD, as well as several other smoking related phenotypes. While intelligence and educational attainment correlated negatively, OCD correlated positively with memory. Moreover, OCD was significantly positively genetically correlated with neuroticism (especially with the worry sub-cluster), conscientiousness, loneliness, and tiredness, while the genetic correlation with household income, subjective well-being, self-rated health, and sleep duration was negative. Notable are also the significant negative correlations with the three autoimmune disorders ulcerative colitis, Crohn's disease, and inflammatory bowel disease and a positive correlation with adult-onset asthma. Moreover, OCD showed a positive genetic correlation with ALS and childhood maltreatment and a negative correlation with BMI and age at first birth. Correlations with other neurological, cardiovascular, anthropomorphic and fertility traits did not demonstrate a significant correlation with OCD.

We further examined the genetic correlations of the three OCD sub-samples, freeze1+NORDiC, iPSYCH, and 23andMe, and the 74 traits (Supplementary Figure S17, and Supplementary Table S8). All three sub-samples showed significant genetic correlations in the same direction for most psychiatric disorders (except ADHD and PTSD), neuroticism, neuroticism worry sub-cluster, and subjective well-being. Across all trait-categories, the correlations of the clinically ascertained sub-sample were generally lower than the correlations of the other two sub-samples, with the exception of the three autoimmune disorders ulcerative colitis, Crohn's disease, and inflammatory bowel disease, as well as several anthropomorphic traits. Also for the substance-use

phenotypes we found divergence in the correlation pattern - only the self-reported samples show a negative correlation with IQ, educational attainment, verbal-numerical reasoning and household income.

We also repeated the genetic correlation analyses for the OCD summary statistics resulting from the three MTAG analyses (Supplementary Figure S18, and Supplementary Table S9). As expected, correlations with all three OCD MTAG summary statistics were more uniform than the correlations with the individual sub-samples (Supplementary Figure SS17) and similar to the genetic correlation estimates of the over all OCD GWAS meta-analysis (Figure 6).

Discussion

Here we report results from the largest OCD GWAS to date. We find support for 15 independent genome-wide significant loci (14 new) and 79 protein coding genes in gene-based tests. Tissue enrichment analyses implicate multiple cortical regions, the amygdala and hypothalamus while cell type analyses yielded 12 cell types linked to OCD (all neurons). The SNP heritability of clinically ascertained samples (freeze1+NORDiC; 0.318) was comparable to samples ascertained for a different co-morbid disorder (iPSYCH; 0.254) but higher than self-reported OCD samples (23andMe; 0.081), although all three sub-samples were highly correlated. OCD was genetically correlated with 40 disorders or traits - positively with all psychiatric disorders and negatively with BMI, age at first birth and multiple related autoimmune diseases. Overall, OCD appears to be on a trajectory similar to other psychiatric disorders in terms of common-variant discovery as sample size grows.

We replicated the one previously described²⁰ genome-wide significant locus for OCD at (rs2581789 at 3p21.1) and refined this hit (rs2564930 is now the lead SNP; see Supplementary Figure S6). As described before²⁰, this region has previously been associated with a broad range of other psychiatric disorders and related traits, including schizophrenia⁴⁸, well-being⁴⁹, and the worry-subcluster of neuroticism⁵⁰. This variant was genome-wide significant in all three MTAG analyses. We also describe, for the first time, an association between OCD and the major histocompatibility complex (MHC) region of chromosome 6 (Supplementary Figure S7). The lead SNP, rs9265969, is just 6kb away from the HLA-B gene. This is notable for multiple reasons. First, much attention has been devoted to the possible alterations of the immune system in OCD⁵¹ and there is a familial link between autoimmune diseases and OCD⁵². Second, other psychiatric disorders (e.g., schizophrenia and bipolar disorder) have shown association with the MHC^{48;53}, with schizophrenia's association with the MHC locus arising in substantial part from many structurally diverse alleles of the complement component 4 (C4) genes⁵⁴. It will be interesting to see whether imputation of C4 alleles using SNP data uncovers an association with OCD, or like bipolar disorder, reveals no association with C4.

We further found OCD to be associated with rs4702 in the 5' UTR of the gene *FURIN* (Supplementary Figure S9). This variant is a known eQTL, with the OCD risk variant (G) associated with decreased expression in the brain⁵⁵. Of note, the same variant has previously been associated with schizophrenia and bipolar disorder with the same direction of effect^{48,53}. There were 12 other genome-wide significant hits, including 2 intergenic loci, 3 that are multigenic, and 7 where a single gene is contained within the genome-wide significant region (these 7 genes are *HCNI*, *LINC00970*, *UNC5D*, *LINC02106*, *BRWD1*, *SLC39A8* and *LINC01122*). Little is known about the 3 *LINC* RNA genes, although *LINC01122* is highly expressed in the brain relative to other tissues in GTEx. *HCNI* encodes a hyperpolarization-activated cation channel that contributes to spontaneous rhythmic activity in both heart and brain and rare variants in this gene have been associated with epilepsy⁵⁶. *UNC5D* is a receptor for netrin-1 and is thought to play a role in axon guidance by mediating axon repulsion of neuronal growth cones in the developing nervous system⁵⁷. *BRWD1* is thought to act as a transcriptional regulator involved in chromatin remodeling and is located within the Down syndrome region-2 on chromosome 21⁵⁸. *SLC39A8* encodes a plasma membrane transporter mediating the cellular uptake of zinc and manganese, two divalent metal cations important for development, tissue homeostasis and immunity⁵⁹. Of note, in a small study zinc was used as an adjuvant to fluoxetine and produced improved response⁶⁰.

We performed three sets of gene-based tests using MAGMA (standard MAGMA⁴⁴, e-MAGMA⁶¹ and h-MAGMA³⁹) to link common variation to protein-coding genes. A total of 79 genes were implicated, including 21 genes that were found with at least two versions of MAGMA, and one gene (*WDR6*) that was found with all three methods (see Figure 2 and Figure 3). *WDR6* is a member of the WD repeat protein family which is implicated in cell growth arrest⁶². We further performed three sets of multivariable GWAS (MTAG) to obtain ascertainment specific estimates while gaining power through leveraging the shared heritability among the subgroups. A total of five loci were significant in all three runs of MTAG (see Supplementary Table S6) and four of these were significant in the standard GWAS. The one MTAG-significant locus that was not significant in the standard GWAS contains *TSNARE1*, which encodes a protein thought to play a crucial role in intracellular protein transport and synaptic transmission⁶³ and has been repeatedly associated with schizophrenia and other neuropsychiatric traits⁶⁴.

We used MTAG⁴⁵ to conduct multivariable GWAS analyses for the OCD samples. MTAG combines related traits into a meta-analysis by leveraging the shared heritability among the different traits. For this purpose we included the same summary statistics that also formed the basis for the meta-analysis using METAL, i.e., the freeze 1 data from the original meta-analysis together with the NORDiC samples (freeze1+NORDiC, see above), the iPSYCH dataset, and the 23andMe dataset. But unlike with the METAL-based meta-analysis, the MTAG analysis results in three subgroup-

specific estimates (i.e., freeze1+NORDiC, iPSYCH, and 23andMe) that gain power by exploiting the high shared heritability across all subgroups compared to separate subgroup specific analysis. Through this approach we aimed to address potential concerns about heterogeneity in our phenotyping strategies for the three individual sub datasets (see below in the discussion). We performed maxFDR analyses to approximate the upper bound on the FDR of MTAG results.

Our tissue enrichment results are consistent with other psychiatric disorders in that only brain tissues were found to be enriched for OCD heritability (Figure 4). Specific tissues were the anterior cingulate cortex, frontal cortex, amygdala, and hypothalamus, although a number of other brain regions approached significance, including sub-components of the striatum. Imaging studies as well as neuropsychological and treatment studies have implicated a cortico-thalamo-striato-cortical (CTSC) circuit in the pathophysiology of OCD¹⁴. Therefore, while there is some overlap in brain regions implicated by OCD genetics and imaging, larger studies and more precise brain tissue expression data are needed to clarify this relationship. We next sought to identify cell-types enriched for OCD heritability using single-cell RNA sequencing data. As shown in Figure 5, a total of 12 cell types reached significance, including multiple types of cortical neurons and both dopamine D1 and D2 receptor-expressing medium spiny neurons (MSNs) of the striatum. MSNs are a special type of GABAergic inhibitory cells representing 95% of neurons within the human striatum, a central structure of the CTSC circuit mentioned above.

With regards to the difference in reported liability-scale heritability for the three sub samples there could be multiple reasons. For example, on average our freeze1+NORDiC sub sample (as well as the iPSYCH sub sample) likely includes more severely and more chronically affected individuals in contrast to the 23andMe sub sample (which might represent on average healthier individuals within the OCD spectrum). The effect of such a difference on heritability estimates and variance explained has been reported before^{65,66}.

Our LDSC results revealed that OCD was genetically correlated with 40 disorders or traits (Figure 6). This included positive correlations with all psychiatric disorders, most notably anxiety, depression, PTSD, anorexia and Tourette syndrome. These results are consistent with prior studies of OCD as well as known comorbidities. Negative correlations were found for BMI and age at first birth (as described before²⁰) as well three related autoimmune disorders (ulcerative colitis, Crohn's disease and inflammatory bowel disease), which is perhaps surprising given the association with the MHC and the familial link between autoimmune diseases and OCD.

In summary, we report 15 independent genome-wide significant loci associated with OCD. The GWAS meta-analysis implicates the MHC region, *FURIN* and other biologically informative genes as important contributors to the etiology of OCD. The results also highlight strong overlap with the genetics of OCD-related disorders and traits in the population, encouraging a multi-faceted view on the genetic underpinnings of OCD and potentially a continuum of

genetically distinctive sub-entities . Overall, we have begun laying the groundwork through which the biology of OCD and related phenotypes will be described.

<https://research.23andme.com/collaborate/dataset-access/> for more information and to apply to access the data.

FUNDING ACKNOWLEDGEMENTS

The iPSYCH team was supported by grants from the Lundbeck Foundation (R102-A9118, R155-2014-1724, and R248-2017-2003), NIH/NIMH (1R01MH124851-01 to A.D.B.) and the Universities and University Hospitals of Aarhus and Copenhagen. The Danish National Biobank resource was supported by the Novo Nordisk Foundation. High-performance computer capacity for handling and statistical analysis of iPSYCH data on the GenomeDK HPC facility was provided by the Center for Genomics and Personalized Medicine and the Centre for Integrative Sequencing, iSEQ, Aarhus University, Denmark (grant to A.D.B.). A.D.B. was also supported by the EU's HORIZON-HLTH-2021-STAYHLTH-01 programme, project number 101057385: Risk and Resilience in Developmental Diversity and Mental Health (R2D2-MH). The NORDiC study was supported by NIH grant R01MH110427 (PI: Crowley), NIMH R01 MH105500 (PI Crowley); the Swedish Research Council (grant numbers 2015-02271, 2018-02487) (PIs: Mataix-Cols and Rück), CIMED and Region Stockholm (PI: Rück). The computation was performed on resources provided by SNIC through Uppsala Multidisciplinary Center for Advanced Computational Science (UPPMAX) under Project sens2018605.

We would like to thank the research participants and employees of 23andMe for making this work possible. Participants provided informed consent and participated in the research online, under a protocol approved by the external AAHRPP-accredited IRB, Ethical Independent Review Services (EI Review). Participants were included in the analysis on the basis of consent status as checked at the time data analyses were initiated.

DISCLOSURES

David A. Hinds and Chao Tian are employed by and hold stock or stock options in 23andMe, Inc. ADB has received speaker fee from Lundbeck. JH has received lecture honoraria as part of continuing medical education programs sponsored by Shire, Takeda and Medice. DMC receives royalties for contributing articles to UpToDate, Wolters Kluwer Health, and personal fees for editorial work from Elsevier, all unrelated to the current work.

All other authors report to conflicts of interests.

DATA AVAILABILITY

GWAS summary statistics will be made available on the iPSYCH website (<https://ipsych.dk/en/research/downloads>), excluding 23andMe data. The full GWAS summary statistics for the 23andMe discovery data set will be made available through 23andMe to qualified researchers under an agreement with 23andMe that protects the privacy of the 23andMe participants. Please visit

Figures and Tables

DRAFT

Table 1. Top SNP results of OCD meta-analysis showing all significant SNPs, and corresponding chromosome (CHR), basepair position (BP), effect allele and non-effect allele (A1/A2), frequency of allele A1 for cases (FRQ cases), frequency of allele A1 for controls (FRQ controls), log odds ratio (log(OR) Meta), and p-value for association results (P Meta). Also listing protein coding genes and/or microRNAs in a LD region of $r^2=0.6$ around the lead SNP (± 50 kb) in brackets distance to index SNP in kb (Genes). If more than one gene is contained within that region, only selected genes with a known association with OCD or a related disorder together with the number of genes (in brackets) within that region are listed in the table, while the remaining genes are listed at the end of this description. Also listing FRQ cases, log(OR), and P separately for freeze1+NORDiC, including 4417 OCD cases from NORDiC-NOR, NORDiC-SWE, and freeze1 (OCGAS, IOCDF-GC, and IOCDF-GC_trios); for iPSYCH (including 2678 OCD cases), and for 23andMe (including 30167 OCD cases). Genome-wide significant p-values are in bold. * List of genes in a LD region of $r^2=0.6$ around the lead SNPs (± 50 kb): **rs674094**: *SERPING1*(-233.0), *MIR130A*(-206.6), *YPEL4*(-197.9), *CLP1*(-186.0), *ZDHHC5*(-146.7), *MED19*(-135.5), *TMX2*(-106.9), *TMX2-CTNND1*(-28.7), *SELENOH*(-104.3), *BTBD18*(-96.1), *CTNND1*(-28.3); **rs9840050**: *SLC26A6*(-410.4), *MIR6824*(-412.2), *CELSR3*(-383.0), *MIR4793*(-401.6), *LINC02585*(-376.7), *NCKIPSD*(-360.0), *IP6K2*(-328.6), *PRKAR2A*(-198.0), *PRKAR2A-AS1*(-193.9), *SLC25A20*(-147.0), *ARIH2OS*(-126.5), *ARIH2*(-59.5), *P4HTM*(-38.7), *WDR6*(-29.9), *DALRD3*(-24.8), *MIR425*(-25.6), *NDUFAF3*(-22.4), *MIR191*(-25.2), *IMPDH2*(-16.5), *QRICH1*(0.0), *QARS*(0.0), *MIR6890*(0.0), *USP19*(0.0), *LAMB2*(0.0), *LAMB2P1*(7.0), *CCDC71*(16.7), *KLHDC8B*(25.7), *C3orf84*(31.8), *CCDC36*(52.5), *C3orf62*(122.7), *MIR4271*(128.2), *USP4*(131.3); **rs2564930**: *NEK4*(-162.4), *ITIH1*(-141.2), *ITIH3*(-124.3), *ITIH4*(-102.6), *ITIH4-AS1*(-108.0), *MUSTN1*(-98.3), *STIMATE-MUSTN1*(-35.7), *STIMATE*(-35.7), *MIR8064*(-86.7), *SFMBT1*(0.0), *RFT1*(55.2), *PRKCD*(127.9); **rs9265969**: *HCG20*(-505.7), *LINC00243*(-467.3), *LINC02570*(-449.8), *DDR1*(-397.8), *MIR4640*(-407.0), *GTF2H4*(-383.8), *VARS2*(-371.5), *SFTA2*(-365.8), *MUCL3*(-343.7), *HCG21*(-343.1), *MUC21*(-308.0), *MUC22*(-262.5), *HCG22*(-238.1), *C6orf15*(-185.4), *PSORS1C1*(-157.8), *CDSN*(-177.5), *PSORS1C2*(-158.9), *CCHCR1*(-139.7), *TGF19*(-133.7), *POU5F1*(-127.2), *PSORS1C3*(-111.6), *HCG27*(-94.0), *HLA-C*(-25.8), *LINC02571*(0.0), *HLA-B*(0.0), *MIR6891*(0.0), *MICA-AS1*(0.0), *MICA*(2.8), *LINC01149*(43.7), *HCP5*(65.2), *HCG26*(73.3), *MICB-DT*(82.0), *MICB*(97.0), *MCCD1*(131.0), *ATP6V1G2-DDX39B*(132.3), *DDX39B*(132.3), *SNORD117*(138.4), *MICB*(143.2), *DDX39B-AS1*(144.4), *ATP6V1G2*(146.5), *NFKBIL1*(148.9), *LOC100287329*(161.6), *LTA*(174.2), *TNF*(177.6), *LTB*(182.6), *LST1*(188.3), *NCR3*(191.0), *AIF1*(217.3), *PRRC2A*(222.8), *SNORA38*(225.1), *MIR6832*(235.9), *BAG6*(241.1), *APOM*(254.5), *C6orf47*(260.4), *GPANK1*(263.3), *CSNK2B*(267.9), *LY6G5B*(273.0), *LY6G5C*(278.8), *ABHD16A*(289.0), *MIR4646*(303.1), *LY6G6F*(308.9), *LY6G6F-LY6G6D*(308.9), *LY6G6E*(314.0), *LY6G6D*(317.4), *LY6G6C*(320.7), *MPIG6B*(325.4), *DDAH2*(329.1), *CLIC1*(332.7), *MSH5*(342.0), *MSH5-SAPCD1*(342.0), *SAPCD1*(365.1), *SAPCD1-AS1*(366.2), *VWA7*(367.7), *VARS*(379.6), *LSM2*(399.5), *HSPA1L*(411.7), *HSPA1A*(417.6), *HSPA1B*(429.8), *SNHG32*(437.0), *SNORD48*(437.3), *SNORD52*(439.1), *NEU1*(459.7), *SLC44A4*(465.3), *EHMT2*(481.8), *C2*(499.9), *ZBTB12*(501.7), *C2-AS1*(536.5), *CFB*(548.0), *NELFE*(554.2), *MIR1236*(558.9), *SKIV2L*(561.2), *DXO*(571.9), *STK19*(573.2), *C4A*(584.1), *C4B*(584.1), *C4B_2*(584.1), *LOC110384692*(584.1), *CYP21A1P*(607.7), *TNXA*(610.5), *TNXB*(610.5), *CYP21A2*(640.4), *ATF6B*(717.3), *FKBPL*(730.8); **rs4702**: *FURIN*(0.0), *FES*(0.0), *MAN2A2*(0.0), *HDDC3*(0.0), *UNC45A*(0.0); **rs3899258**: *PARP8*(-64.2), *LINC02106*(0.0); **rs2836950**: *PSMG1*(0.0), *BRWD1*(0.0), *BRWD1-AS2*(31.4), *BRWD1-AS1*(33.2), *HMGN1*(59.8), *GET1*(97.7), *WRB-SH3BGR*(97.8); **rs4460629**: *DCST1*(-61.9), *DCST1-AS1*(-48.9), *ADAM15*(-50.1), *EFNA4*(-43.3), *EFNA3*(-25.3), *EFNA1*(0.0), *SLC50A1*(0.0), *DPM3*(0.0), *KRT-CAP2*(0.0), *TRIM46*(0.0), *MUC1*(0.0), *MIR92B*(0.0), *THBS3*(0.0), *MTX1*(0.0), *GBAP1*(0.0), *GBA*(18.9), *FAM189B*(31.7), *SCAMP3*(40.4)

SNP	CHR	BP	A1/A2	Meta				freeze1+NORDiC			iPSYCH			23andMe			Genes
				FRQ cases	FRQ controls	log(OR)	P	FRQ cases	log(OR)	P	FRQ cases	log(OR)	P	FRQ cases	log(OR)	P	
rs10877425	12	60751330	G/A	0.514	0.518	-0.051	1.14E-10	0.508	-0.044	0.128	0.481	-0.086	0.006	0.518	-0.049	9.16E-09	-
rs674094	11	57665336	C/A	0.701	0.705	-0.055	1.39E-10	0.691	-0.099	0.001	0.674	-0.122	2.44E-04	0.705	-0.046	8.06E-07	many (11)
rs11953498	5	45240783	G/C	0.18	0.184	-0.065	3.36E-10	0.172	-0.077	0.038	0.148	-0.064	0.138	0.184	-0.063	6.87E-09	HGN1(0.0)
rs9840050	3	49133310	G/A	0.655	0.66	-0.05	6.09E-10	0.639	-0.04	0.171	0.624	-0.064	0.046	0.66	-0.05	1.12E-08	CELSR3; many (31)
rs2564930	3	53017307	T/C	0.338	0.341	-0.051	7.45E-10	0.317	-0.143	1.98E-06	0.33	-0.063	0.057	0.341	-0.042	2.33E-06	many (12)
rs9265969	6	31315706	G/A	0.874	0.874	0.072	2.34E-09	0.881	0.082	0.057	0.86	0.077	0.079	0.874	0.07	5.57E-08	many (103)
rs6660196	1	168874798	T/G	0.638	0.637	0.048	3.26E-09	0.651	0.071	0.017	0.623	0.024	0.456	0.637	0.048	4.32E-08	LINC00970(0.0)
rs4702	15	91426560	G/A	0.456	0.456	0.045	5.82E-09	0.458	0.046	0.109	0.451	0.067	0.04	0.456	0.044	1.56E-07	many (5)
rs2198140	8	35039646	T/C	0.493	0.494	-0.046	6.39E-09	0.483	-0.045	0.113	0.497	-0.046	0.137	0.494	-0.046	7.24E-08	UNC5D(3.3)
rs3899258	5	50256551	G/A	0.779	0.777	0.055	6.90E-09	0.788	0.055	0.113	0.781	0.008	0.84	0.777	0.059	8.84E-09	many (2)
rs66818976	5	90900362	G/A	0.28	0.284	-0.05	1.45E-08	0.261	-0.092	0.005	0.275	-0.03	0.396	0.284	-0.048	4.25E-07	-
rs2836950	21	40604429	G/C	0.361	0.361	-0.046	2.40E-08	0.362	-0.008	0.795	0.363	-0.039	0.226	0.360	-0.05	1.88E-08	many (7)
rs35518360	4	103146890	T/A	0.0874	0.0899	0.076	3.78E-08	0.084	0.115	0.035	0.059	0.109	0.109	0.091	0.071	1.13E-06	SLC39A8(0.0)
rs4460629	1	155135335	T/C	0.526	0.526	0.043	3.96E-08	0.54	0.025	0.375	0.5	0.036	0.239	0.526	0.045	9.28E-08	many (18)
rs1922782	2	58916336	T/C	0.427	0.426	0.043	4.89E-08	0.44	0.098	5.8E-04	0.419	0.069	0.028	0.426	0.036	2.09E-05	LINC01122(0.0)

Fig. 1. Genome-wide association results for the OCD meta-analysis (37,015 OCD cases and 948,616 controls; Manhattan plot in (A) and quantile-quantile plot in (B)) and for the MTAG analysis with freeze1+NORDiC as the primary phenotype (Manhattan plot in (C) and quantile-quantile plot in (D)). The x-axis in (A) and (C) shows the position in the genome (chromosomes 1-22), while the y-axis represents $-\log_{10}(p)$ values for the association of variants with OCD. The horizontal red line represents the threshold for genome-wide significance. Each dot represents one SNP that was tested in the GWAS, with green diamonds indicating the lead SNP in regions harboring a genome-wide significant SNP. In (B) and (D) the expected $-\log_{10}(p)$ under the null is plotted against the observed $-\log_{10}(p)$, qq-plots (B) and (D) belong to Manhattan lots (A) and (C), respectively. The shading indicates 95% confidence region under the null. Lambda indicates the genomic inflation factor.

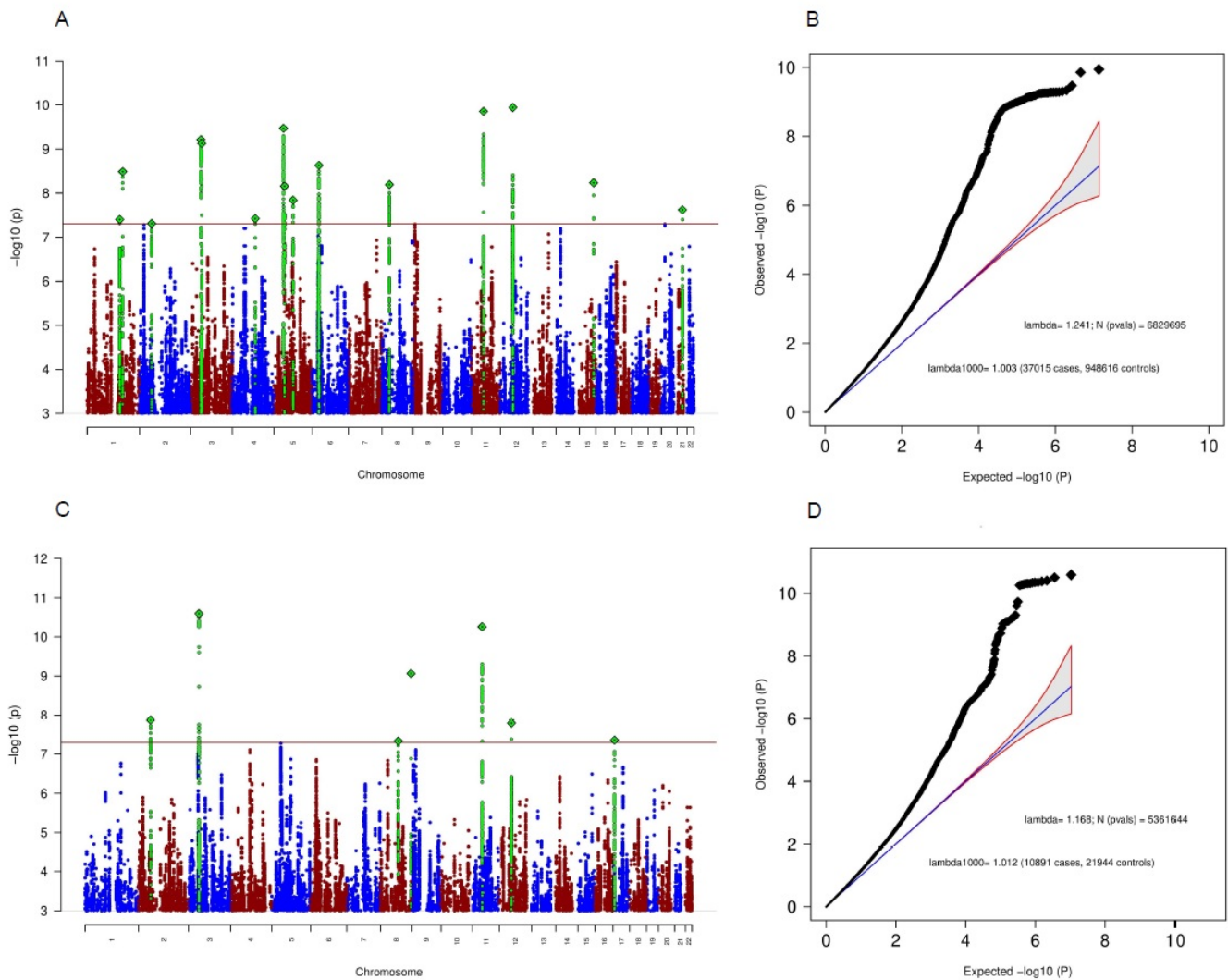


Fig. 3. Overlaps of genes called as significant in MAGMA, e-MAGMA and h-MAGMA. Overlaps between the three methods for conducting gene-based tests using GWAS summary statistics are depicted via a venn diagram, with the numbers representing the number of genes called as significant across methods.

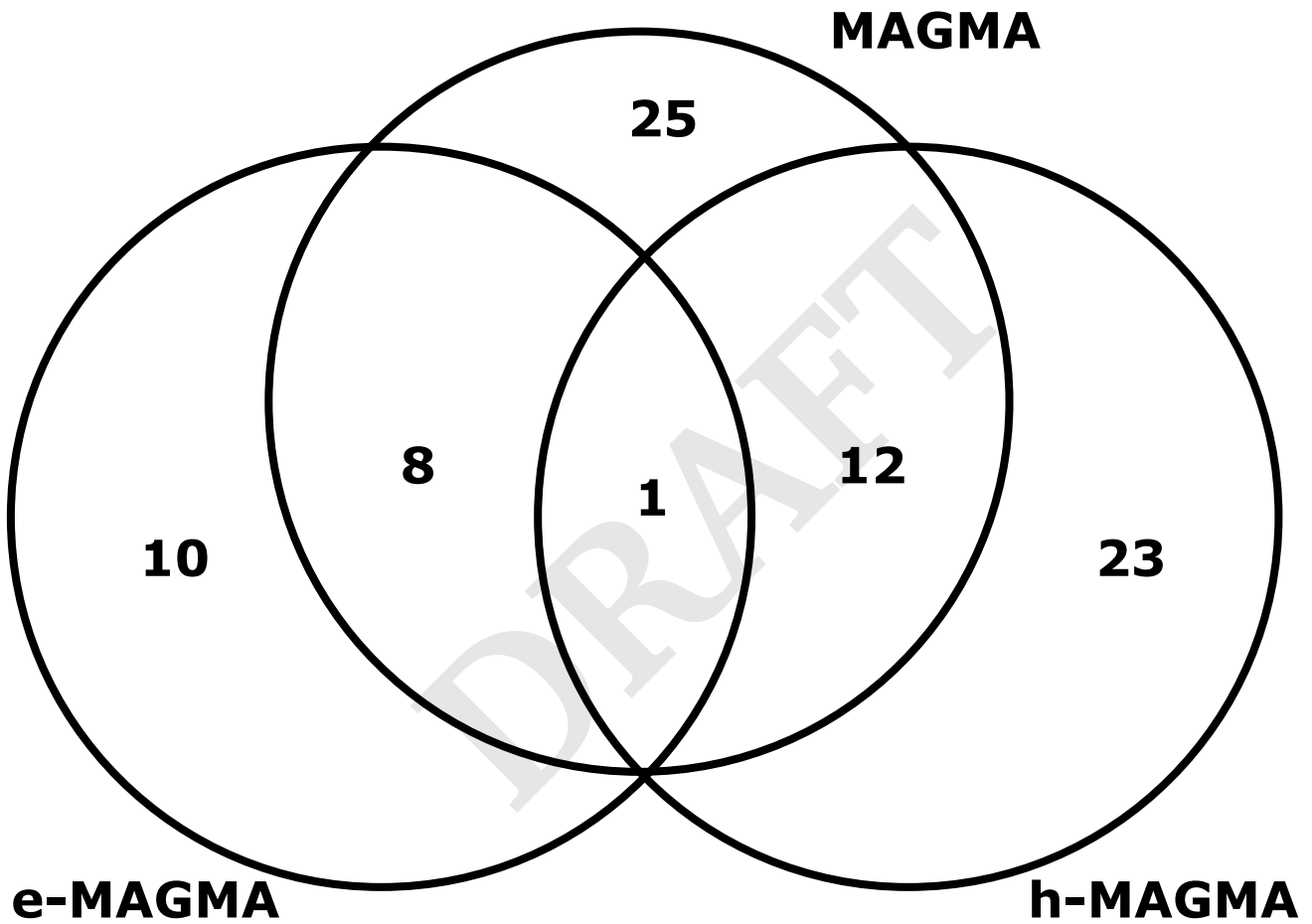


Fig. 4. OCD heritability enrichment p-values across tissue/celltype expression profiles. Test result p-values are shown for heritability enrichment tests with genes representing expression profiles of 37 different tissues from GTEx (left) and 39 broad nervous system celltypes from mice (right) The p-value shown for each result is averaged between MAGMA and LDSC approaches, and is considered to be significant only if FDR-adjusted $p < 0.05$ in both. A total of 5 broad tissue types from GTEx (all from brain), and a total of 5 broad neuronal celltypes from Zeisel et al. are significantly enriched for OCD heritability based on these criteria.

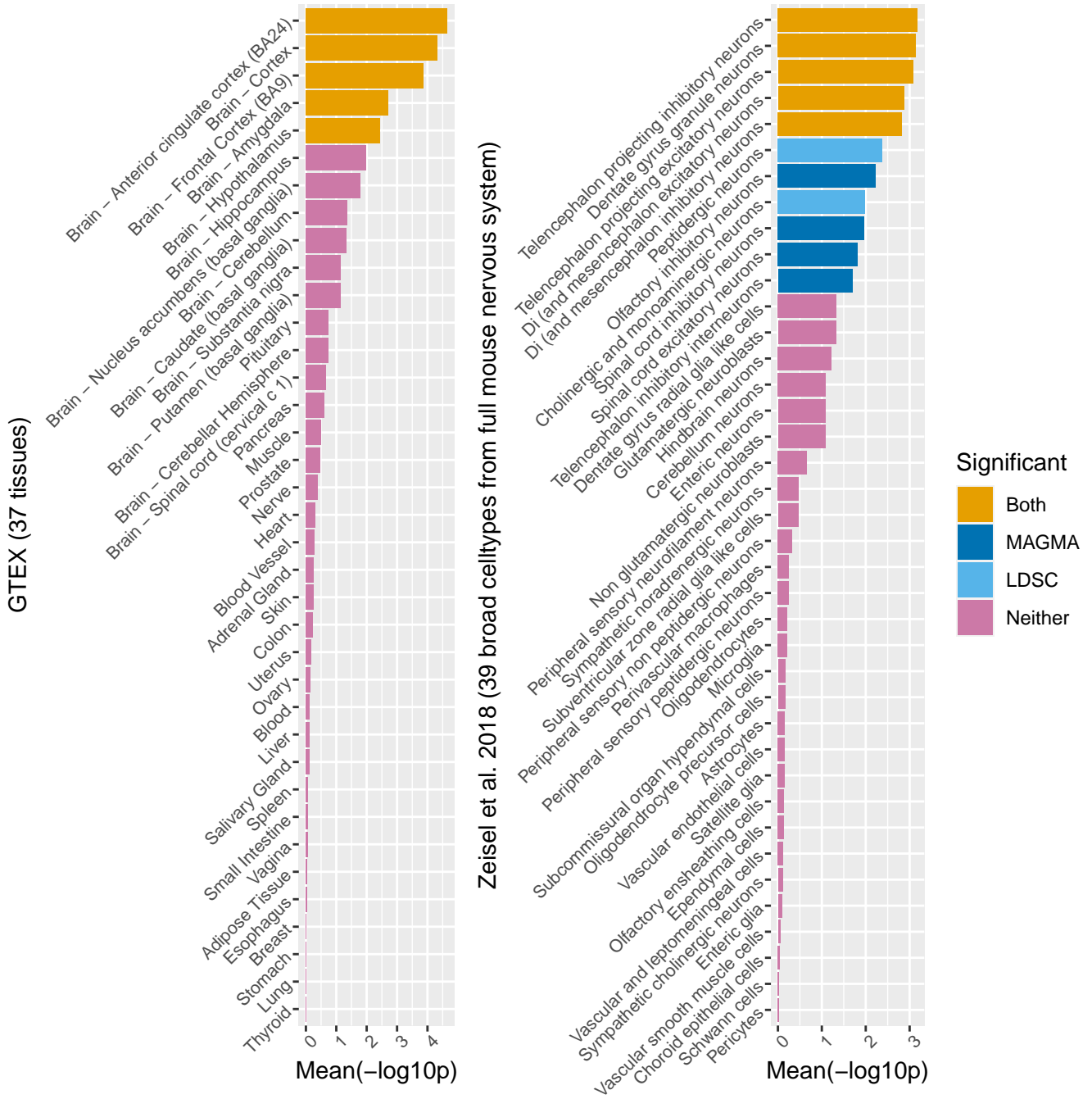


Fig. 5. Heritability enrichment p-values between OCD and neuronal celltype groups. P-values for OCD heritability enrichment across 265 celltypes from Zeisel et al. were generated, and grouped into 35 groups of single cell types where $n \geq 2$ based on the 'Description' column from the table in <http://mousebrain.org/celltypes/>. We first tested each of the 265 celltypes and found that a total of 44 were significant at an FDR < 0.05. We then took the mean $-\log_{10}$ p-value from each of the 35 groups and found that of these a total of 7 were significant at FDR < 0.05. We indicate in blue the single celltypes and overall celltype groups that are significant after FDR adjustment.

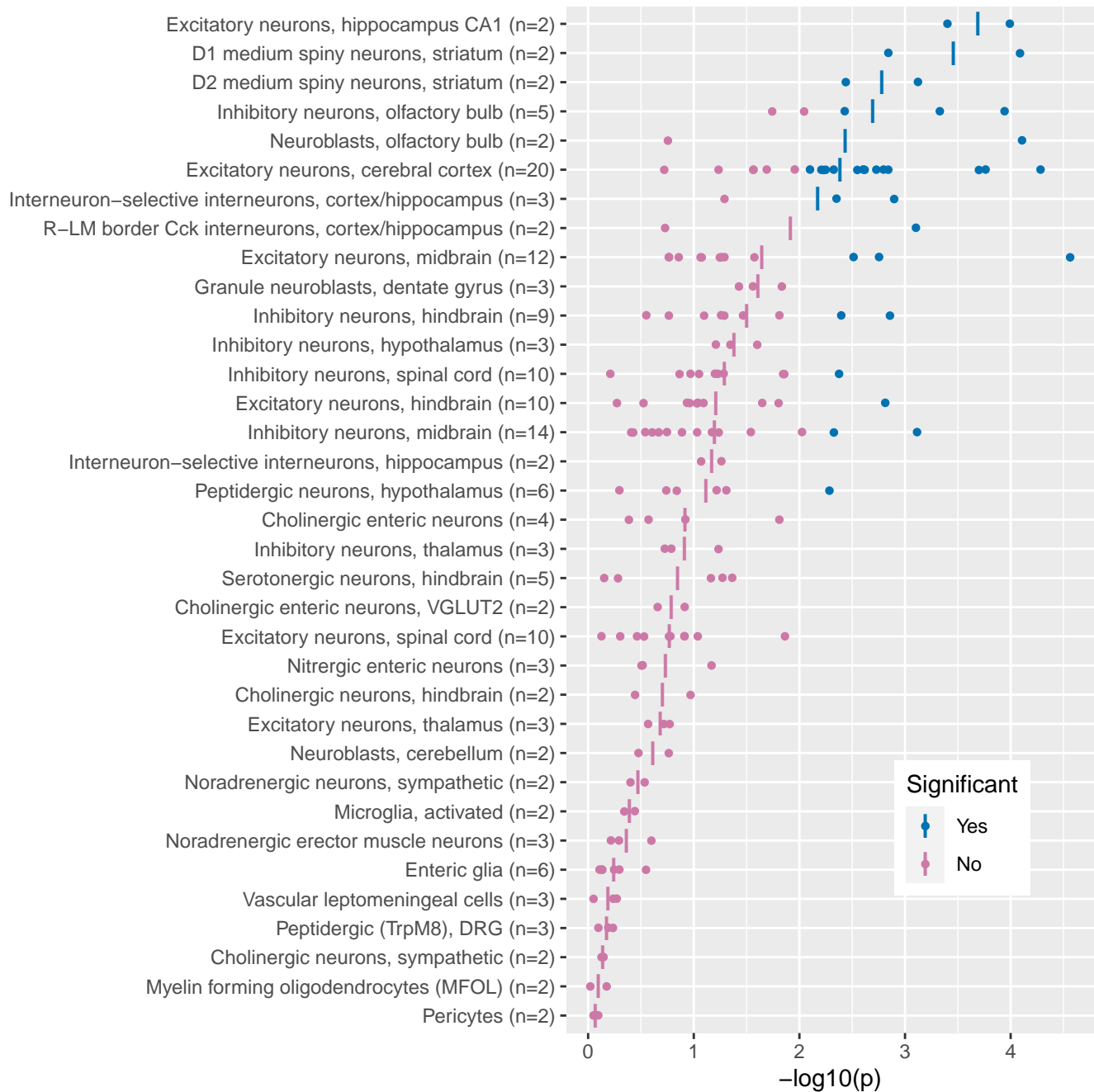
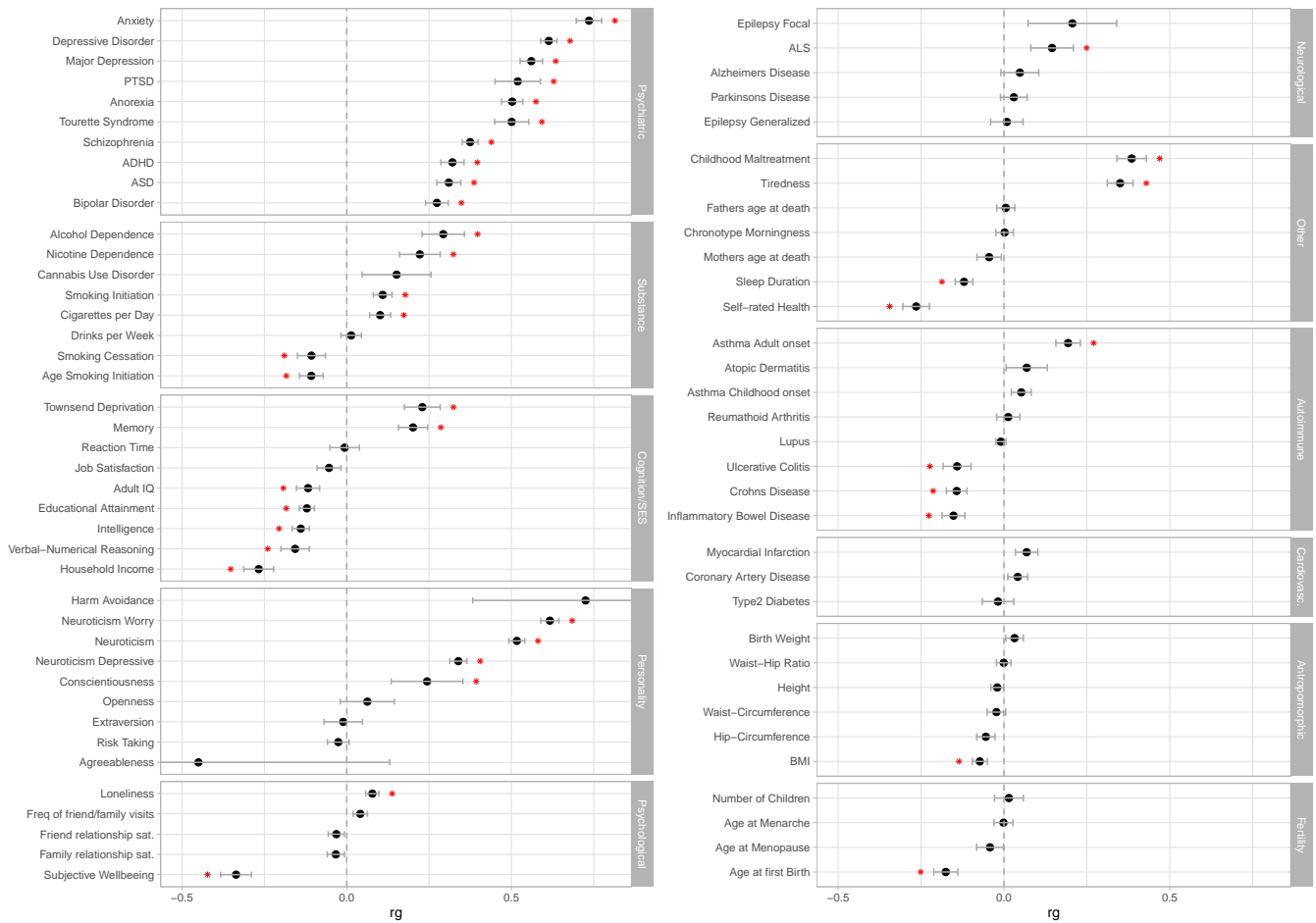


Fig. 6. Genetic correlations (rg) between OCD and 74 behavioral, cognitive, psychiatric, neurologic, immunologic, metabolic, and anthropomorphic phenotypes. Error bars represent standard errors and red asterisks indicate significant associations after FDR correction for multiple testing.



Bibliography

1. American Psychiatric Association. Diagnostic and statistical manual of mental disorders (5th ed.). Arlington, VA: American Psychiatric Publishing; 2013.
2. World Health Organization. The ICD-10 classification of mental and behavioural disorders: Clinical descriptions and diagnostic guidelines. Geneva: World Health Organization; 1992.
3. Ruscio AM, Stein DJ, Chiu WT, Kessler RC. The epidemiology of obsessive-compulsive disorder in the National Comorbidity Survey Replication. *Molecular Psychiatry*. 2010;15(1).
4. Fullana MA, Mataix-Cols D, Caspi A, Harrington H, Grisham JR, Moffitt TE, et al. Obsessions and Compulsions in the Community: Prevalence, Interference, Help-Seeking, Developmental Stability, and Co-Occurring Psychiatric Conditions. *American Journal of Psychiatry*. 2009 Mar;166(3):329–336. Available from: <http://psychiatryonline.org/doi/abs/10.1176/appi.ajp.2008.08071006>.
5. Leckman JF, Denys D, Simpson HB, Mataix-Cols D, Hollander E, Saxena S, et al. Obsessive-compulsive disorder: a review of the diagnostic criteria and possible subtypes and dimensional specifiers for DSM-V. *Depression and Anxiety*. 2010 Jun;27(6):507–527.
6. Brander G, Kuja-Halkola R, Rosenqvist MA, Rück C, Serlachius E, Fernández de la Cruz L, et al. A population-based family clustering study of tic-related obsessive-compulsive disorder. *Molecular Psychiatry*. 2019 Oct; Available from: <http://www.nature.com/articles/s41380-019-0532-z>.
7. World Health Organization. The Global Burden of Disease: 2004 Update. Geneva: WHO Press; 2008.
8. Fernández de la Cruz L, Rydell M, Runeson B, D'Onofrio BM, Brander G, Rück C, et al. Suicide in obsessive-compulsive disorder: a population-based study of 36788 Swedish patients. *Molecular Psychiatry*. 2017 Nov;22(11):1626–1632.
9. Meier S, Mattheisen M, Mors O, Schendel D, Mortensen P, Plessen K. Mortality Among Persons With Obsessive-Compulsive Disorder in Denmark. *JAMA psychiatry*. 2016 Mar;73(3):268–274. Publisher: JAMA Psychiatry. Available from: <https://pubmed.ncbi.nlm.nih.gov/26818216/>.
10. van Grootheest DS, Cath DC, Beekman AT, Boomsma DI. Twin Studies on Obsessive-Compulsive Disorder: A Review. *Twin Research and Human Genetics*. 2005 Oct;8(5):450–458. Available from: http://journals.cambridge.org/abstract_S1832427400005648.
11. Mataix-Cols D, Boman M, Monzani B, Rück C, Serlachius E, Långström N, et al. Population-Based, Multigenerational Family Clustering Study of Obsessive-compulsive Disorder. *JAMA Psychiatry*. 2013 Jul;70(7):709–709. Available from: <http://archpsyc.jamanetwork.com/article.aspx?doi=10.1001/jamapsychiatry.2013.3>.
12. Nestadt G, Samuels J, Riddle M, Bienvenu OJ, Liang KY, LaBuda M, et al. A Family Study of Obsessive-compulsive Disorder. *Archives of General Psychiatry*. 2000 Apr;57(4):358–358. Available from: <http://archpsyc.jamanetwork.com/article.aspx?doi=10.1001/archpsyc.57.4.358>.
13. Browne HA, Hansen SN, Buxbaum JD, Gair SL, Nissen JB, Nikolajsen KH, et al. Familial clustering of tic disorders and obsessive-compulsive disorder. *JAMA psychiatry*. 2015 Apr;72(4):359–366.
14. Pauls DL, Abramovitch A, Rauch SL, Geller DA. Obsessive-compulsive disorder: an integrative genetic and neurobiological perspective. *Nature Reviews Neuroscience*. 2014 Jun;15(6):410–424. Available from: <http://www.nature.com/articles/nrn3746>.
15. Taylor S. Molecular genetics of obsessive-compulsive disorder: a comprehensive meta-analysis of genetic association studies. *Molecular Psychiatry*. 2013 Jul;18(7):799–805. Available from: <http://www.nature.com/articles/mp201276>.
16. Stewart SE, Yu D, Scharf JM, Neale BM, Fagerness JA, Mathews CA, et al. Genome-wide association study of obsessive-compulsive disorder. *Molecular Psychiatry*. 2013 Jul;18(7):788–798.
17. Davis LK, Yu D, Keenan CL, Gamazon ER, Konkashbaev AI, Derks EM, et al. Partitioning the Heritability of Tourette Syndrome and Obsessive Compulsive Disorder Reveals Differences in Genetic Architecture. *PLoS Genetics*. 2013;9(10).
18. Mattheisen M, Samuels JF, Wang Y, Greenberg BD, Fyer AJ, McCracken JT, et al. Genome-wide association study in obsessive-compulsive disorder: Results from the OCGAS. *Molecular Psychiatry*. 2015 Mar;20(3):337–344. Publisher: Nature Publishing Group.
19. International Obsessive Compulsive Disorder Foundation Genetics Collaborative (IOCDF-GC) and OCD Collaborative Genetics Association Studies, OCGAS. Revealing the complex genetic architecture of obsessive-compulsive disorder using meta-analysis. *Mol Psychiatry*. 2017;23(5):1181–1188.
20. Strom NI, Yu D, Gerring ZF, Halvorsen MW, Abdellaoui A, Rodriguez-Fontenla C, et al. Genome-wide association study identifies new locus associated with OCD. *medRxiv*. 2021; Publisher: Bjarne K. A. Hansen 131. Available from: <https://doi.org/10.1101/2021.10.13.21261078>.
21. Mataix-Cols D, Hansen B, Mattheisen M, Karlsson EK, Addington AM, Boberg J, et al. Nordic OCD and Related Disorders Consortium: Rationale, design, and methods. *American Journal of Medical Genetics Part B: Neuropsychiatric Genetics*. 2020 Jan;183(1):38–50. Publisher: Blackwell Publishing Inc.
22. Pedersen CB, Bybjerg-Grauholm J, Pedersen MG, Grove J, Agerbo E, Bækvad-Hansen M, et al. The iPSYCH2012 case-cohort sample: New directions for unravelling genetic and environmental architectures of severe mental disorders. *Molecular Psychiatry*. 2018 Jan;23(1):6–14. Publisher: Nature Publishing Group.
23. Bybjerg-Grauholm J, Pedersen CB, Bækvad-Hansen M, Pedersen MG, Adamsen D, Hansen CS, et al. The iPSYCH2015 Case-Cohort sample: updated directions for unravelling genetic and environmental architectures of severe mental disorders. *medRxiv*; 2020. Pages: 2020.11.30.20237768. Available from: <https://www.medrxiv.org/content/10.1101/2020.11.30.20237768v1>.
24. Auton A, Abecasis GR, Altshuler DM, Durbin RM, Bentley DR, Chakravarti A, et al. A global reference for human genetic variation. *Nature*. 2015.
25. Lam M, Awasthi S, Watson HJ, Goldstein J, Panagiotaropoulou G, Trubetskoy V, et al. R1-COPILI: Rapid Imputation for COntortias PipelIne. *Bioinformatics*. 2020 Feb;36(3):930–933. Publisher: Oxford University Press. Available from: <https://pubmed.ncbi.nlm.nih.gov/31393554/>.
26. Strom NI, Grove J, Meier SM, Bækvad-Hansen M, Becker Nissen J, Damm Als T, et al. Polygenic Heterogeneity Across Obsessive-Compulsive Disorder Subgroups Defined by a Comorbid Diagnosis. *Frontiers in Genetics*. 2021 Aug;12:1504–1504. Publisher: Frontiers Media S.A.
27. Arnold PD, Askland KD, Barlassina C, Bellodi L, Bienvenu OJ, Black D, et al. Revealing the complex genetic architecture of obsessive-compulsive disorder using meta-analysis. *Molecular Psychiatry*. 2018 May;23(5):1181–1188. Publisher: Nature Publishing Group.
28. Lee JH, Cheng R, Graff-Radford N, Foroud T, Mayeux R, National Institute on Aging Late-Onset Alzheimer's Disease Family Study Group. Analyses of the National Institute on Aging Late-Onset Alzheimer's Disease Family Study: implication of additional loci. *Archives of Neurology*. 2008 Nov;65(11):1518–1526.
29. Gur RC, Richard J, Calkins ME, Chiavacci R, Hansen JA, Bilker WB, et al. Age group and sex differences in performance on a computerized neurocognitive battery in children age 8–21. *Neuropsychology*. 2012;26(2):251–265. Publisher: Neuropsychology.
30. Schumacher FR, Berndt SI, Siddiq A, Jacobs KB, Wang Z, Lindstrom S, et al. Genome-wide association study identifies new prostate cancer susceptibility loci. *Human Molecular Genetics*. 2011 Oct;20(19):3867–3875.
31. Purcell S, Neale B, Todd-Brown K, Thomas L, Ferreira MAR, Bender D, et al. PLINK: A tool set for whole-genome association and population-based linkage analyses. *American Journal of Human Genetics*. 2007;81(3):559–575. Publisher: Cell Press.
32. Delaneau O, Marchini J, Zagury JF. A linear complexity phasing method for thousands of genomes. *Nature Methods*. 2012;.
33. Das S, Forer L, Schönerr S, Sidore C, Locke AE, Kwong A, et al. Next-generation genotype imputation service and methods. *Nature Genetics*. 2016 Oct;48(10):1284–1287.
34. Hyde C, Nagle M, Tian C, Chen X, Paciga S, Wendland J, et al. Identification of 15 genetic loci associated with risk of major depression in individuals of European descent. *Nature genetics*. 2016 Sep;48(9):1031–1036. Publisher: Nat Genet. Available from: <https://pubmed.ncbi.nlm.nih.gov/27479909/>.
35. McCarthy S, Das S, Kretschmar W, Delaneau O, Wood AR, Teumer A, et al. A reference panel of 64,976 haplotypes for genotype imputation. *Nature Genetics*. 2016 Oct;48(10):1279–1283. Publisher: Nature Publishing Group.
36. Willer CJ, Li Y, Abecasis GR. METAL: Fast and efficient meta-analysis of genomewide association scans. *Bioinformatics*. 2010;26(17).
37. Leeuw CAD, Mooij JM, Heskes T, Posthuma D. MAGMA: Generalized Gene-Set Analysis of GWAS Data. *PLoS Computational Biology*. 2015 Apr;11(4):e1004219. Publisher: Public Library of Science, Available from: <https://journals.plos.org/ploscompbiol/article?id=10.1371/journal.pcbi.1004219>.
38. Gerring Z, Mina-Vargas A, Derks E. eMAGMA: an eQTL-informed method to identify risk genes using genome-wide association study summary statistics. *bioRxiv*. 2019 Nov;p. 854315–854315. Publisher: Cold Spring Harbor Laboratory. Available from: <https://doi.org/10.1101/854315>.
39. Sey NYA, Hu B, Mah W, Fauni H, McAfee JC, Rajarajan P, et al. A computational tool (H-MAGMA) for improved prediction of brain-disorder risk genes by incorporating brain chromatin interaction profiles. *Nature Neuroscience*. 2020 Apr;23(4):583–593. Publisher: Nature Research. Available from: <https://pubmed.ncbi.nlm.nih.gov/32152537/>.
40. Bryois J, Skene NG, Hansen TF, Kogelman LJA, Watson HJ, Liu Z, et al. Genetic identification of cell types underlying brain complex traits yields insights into the etiology of Parkinson's disease. *Nature Genetics*. 2020 May;52(5):482–493. Publisher: Nature Research. Available from: <https://pubmed.ncbi.nlm.nih.gov/32341526/>.
41. GTEx Consortium, Lead analysts: Aguet F, et al. Genetic effects on gene expression across human tissues. *Nature*. 2017 Oct;550(7675).
42. Zeisel A, Hochgerner H, Lönnerberg P, Johnson A, Memic F, van der Zwan J, et al. Molecular Architecture of the Mouse Nervous System. *Cell*. 2018 Aug;174(4):999–1014.e22. Publisher: Cell Press. Available from: <https://pubmed.ncbi.nlm.nih.gov/30096314/>.
43. Bulik-Sullivan B, Loh PR, Finucane HK, Ripke S, Yang J, Patterson N, et al. LD score regression distinguishes confounding from polygenicity in genome-wide association studies. *Nature Genetics*. 2015 Feb;47(3):291–295. Publisher: Nature Publishing Group.
44. de Leeuw CA, Mooij JM, Heskes T, Posthuma D. MAGMA: Generalized Gene-Set Analysis of GWAS Data. *PLoS Computational Biology*. 2015 Apr;11(4). Publisher: Public Library of Science. Available from: <https://pubmed.ncbi.nlm.nih.gov/25885710/>.
45. Turley P, Walters RK, Maghziyan O, Okbay A, Lee JJ, Fontana MA, et al. Multi-trait analysis of genome-wide association summary statistics using MTAG. *Nature Genetics*. 2018 Feb;50(2):229–237. Publisher: Nature Publishing Group. Available from: www.nature.com/naturegenetics.
46. Finucane HK, Bulik-Sullivan B, Gusev A, Trynka G, Reshef Y, Loh PR, et al. Partitioning heritability by functional annotation using genome-wide association summary statistics. *Nature Genetics*. 2015 Nov;47(11):1228–1235. Publisher: Nature Publishing Group. Available from: <https://pubmed.ncbi.nlm.nih.gov/26414678/>.
47. Altshuler DM, Gibbs RA, Peltonen L, Schaffner SF, Yu F, Dermitzakis E, et al. Integrating common and rare genetic variation in diverse human populations. *Nature*. 2010 Sep;467(7311):52–58. Publisher: Nature Publishing Group. Available from: <http://pmc/articles/PMC3173859/>.
48. Pardiñas AF, Holmans P, Pocklington AJ, Escott-Price V, Ripke S, Carrera N, et al. Common schizophrenia alleles are enriched in mutation-intolerant genes and in regions under strong background selection. *Nature Genetics*. 2018 Mar;50(3):381–389. Publisher: Nature Publishing Group. Available from: <https://pubmed.ncbi.nlm.nih.gov/29483656/>.
49. Watanabe K, Stringer S, Frei O, Umičević Mirkov M, de Leeuw C, Polderman TJC, et al. A global overview of pleiotropy and genetic architecture in complex traits. *Nature Genetics*. 2019 Sep;51(9):1339–1348. Publisher: Nature Publishing Group. Available from: <https://pubmed.ncbi.nlm.nih.gov/31427899/>.
50. Nagel M, Watanabe K, Stringer S, Posthuma D, Van Der Sluis S. Item-level analyses reveal genetic heterogeneity in neuroticism. *Nature Communications*. 2018 Dec;9(1). Publisher: Nature Publishing Group. Available from: <https://pubmed.ncbi.nlm.nih.gov/29500382/>.

51. Marazziti D, Mucci F, Fontenelle LF. Immune system and obsessive-compulsive disorder. *Psychoneuroendocrinology*. 2018 Jul;93:39–44. Publisher: Elsevier Ltd. Available from: <https://pubmed.ncbi.nlm.nih.gov/29689421/>.
52. Mataix-Cols D, Frans E, Pérez-Vigil A, Kuja-Halkola R, Gromark C, Isomura K, et al. A total-population multigenerational family clustering study of autoimmune diseases in obsessive-compulsive disorder and Tourette's/chronic tic disorders. *Molecular Psychiatry*. 2018 Jul;23(7):1652–1658. Publisher: Nature Publishing Group. Available from: <https://pubmed.ncbi.nlm.nih.gov/29133949/>.
53. Stahl EA, Breen G, Forstner AJ, McQuillin A, Ripke S, Trubetskov V, et al. Genome-wide association study identifies 30 loci associated with bipolar disorder. *Nature Genetics*. 2019 May;51(5):793–803. Publisher: Nature Publishing Group. Available from: <https://pubmed.ncbi.nlm.nih.gov/31043756/>.
54. Sekar A, Bialas AR, De Rivera H, Davis A, Hammond TR, Kamitaki N, et al. Schizophrenia risk from complex variation of complement component 4. *Nature*. 2016 Feb;530(7589):177–183. Publisher: Nature Publishing Group. Available from: <https://pubmed.ncbi.nlm.nih.gov/26814963/>.
55. Schrodde N, Ho SM, Yamamuro K, Dobbyn A, Huckins L, Matos MR, et al. Synergistic effects of common schizophrenia risk variants. *Nature Genetics*. 2019 Oct;51(10):1475–1485. Publisher: Nature Publishing Group. Available from: <https://pubmed.ncbi.nlm.nih.gov/31548722/>.
56. Biel M, Wahl-Schott C, Michalakis S, Zong X. Hyperpolarization-activated cation channels: From genes to function. *Physiological Reviews*. 2009 Jul;89(3):847–885. Publisher: Physiol Rev. Available from: <https://pubmed.ncbi.nlm.nih.gov/19584315/>.
57. Zhu Y, Li Y, Haraguchi S, Yu M, Ohira M, Ozaki T, et al. Dependence receptor UNC5D mediates nerve growth factor depletion-induced neuroblastoma regression. *Journal of Clinical Investigation*. 2013 Jul;123(7):2935–2947. Available from: <http://www.jci.org/articles/view/65988>.
58. Ramos VC, Vidal-Taboada JM, Bergoñon S, Egeo A, Fisher EMC, Scartezzini P, et al. Characterisation and expression analysis of the WDR9 gene, located in the Down critical region-2 of the human chromosome 21. *Biochimica et Biophysica Acta - Gene Structure and Expression*. 2002 Sep;1577(3):377–383. Publisher: Biochim Biophys Acta. Available from: <https://pubmed.ncbi.nlm.nih.gov/12359327/>.
59. Boycott KM, Beaulieu CL, Kernohan KD, Gebril OH, Mhanni A, Chudley AE, et al. Autosomal-Recessive Intellectual Disability with Cerebellar Atrophy Syndrome Caused by Mutation of the Manganese and Zinc Transporter Gene SLC39A8. *American Journal of Human Genetics*. 2015 Dec;97(6):886–893. Publisher: Cell Press. Available from: <https://pubmed.ncbi.nlm.nih.gov/26637978/>.
60. Sayyah M, Olapour A, Saeedabad Ys, Yazdan Parast R, Malayeri A. Evaluation of oral zinc sulfate effect on obsessive-compulsive disorder: A randomized placebo-controlled clinical trial. *Nutrition*. 2012 Sep;28(9):892–895. Publisher: Nutrition. Available from: <https://pubmed.ncbi.nlm.nih.gov/22465904/>.
61. Gerring ZF, Gamazon ER, Derks EM. A gene co-expression network-based analysis of multiple brain tissues reveals novel genes and molecular pathways underlying major depression. *PLoS Genetics*. 2019 Jul;15(7). Publisher: Public Library of Science. Available from: <https://pubmed.ncbi.nlm.nih.gov/31306407/>.
62. Xie X, Wang Z, Chen Y. Association of LKB1 with a WD-repeat protein WDR6 is implicated in cell growth arrest and p27Kip1 induction. *Molecular and Cellular Biochemistry*. 2007 Jul;301(1-2):115–122. Publisher: Mol Cell Biochem. Available from: <https://pubmed.ncbi.nlm.nih.gov/17216128/>.
63. Sleiman P, Wang D, Glessner J, Hadley D, Gur RE, Cohen N, et al. GWAS meta analysis identifies TSNARE1 as a novel Schizophrenia / Bipolar susceptibility locus. *Scientific Reports*. 2013 Oct;3:3075–3075. Publisher: Nature Publishing Group. Available from: <https://www.ncbi.nlm.nih.gov/pmc/articles/PMC4166486/?tool=EBI>.
64. Trubetskov V, Pardiñas AF, Qi T, Panagiotaropoulou G, Awasthi S, Bigdeli TB, et al. Mapping genomic loci implicates genes and synaptic biology in schizophrenia. *Nature*. 2022 Apr;604(7906):502–508. Number: 7906 Publisher: Nature Publishing Group. Available from: <https://www.nature.com/articles/s41586-022-04434-5>.
65. Wray NR, Ripke S, Mattheisen M, Trzaskowski M, Byrne EM, Abdellaoui A, et al. Genome-wide association analyses identify 44 risk variants and refine the genetic architecture of major depression. *Nature Genetics* 2018 50:5. 2018 Apr;50(5):668–681. Publisher: Nature Publishing Group. Available from: <https://www.nature.com/articles/s41588-018-0090-3>.
66. Meier S, Agerbo E, Maier R, Pedersen C, Lang M, Grove J, et al. High loading of polygenic risk in cases with chronic schizophrenia. *Molecular Psychiatry*. 2015 Sep;21(7):969–974. Publisher: Nature Publishing Group. Available from: <http://europepmc.org/article/MED/26324100>.

Supplementary

CONSORTIA

Members of the Nordic OCD & Related Disorders Consortium (NORDiC):

Julia Boberg, Long Long Chen, James J. Crowley, Elles de Schipper, Diana R. Djurfeldt, Jan Haavik, Kristen Hagen, Matthew W. Halvorsen, Bjarne Hansen, Kira D. Höffler, Anna K. Kähler, Elinor K. Karlsson, Gerd Kvale, Paul Lightenstein, Kerstin Lindblad-Toh, Manuel Mattheisen, David Mataix-Cols, Kathleen Morrill, Hyun Ji Noh, Christian Rück, Stian Solem, Nora I. Strom, Tetyana Zayats

23andMe Research Team:

The following members of the 23andMe Research Team contributed to this study: Stella Aslibekyan, Adam Auton, Elizabeth Babalola, Robert K. Bell, Jessica Bielenberg, Katarzyna Bryc, Emily Bullis, Daniella Coker, Gabriel Cuellar Partida, Devika Dhamija, Sayantan Das, Sarah L. Elson, Teresa Filshtein, Kipper Fletez-Brant, Pierre Fontanillas, Will Freyman, Pooja M. Gandhi, Karl Heilbron, Barry Hicks, David A. Hinds, Ethan M. Jewett, Yunxuan Jiang, Katelyn Kukar, Keng-Han Lin, Maya Lowe, Jey C. McCreight, Matthew H. McIntyre, Steven J. Micheletti, Meghan E. Moreno, Joanna L. Mountain, Priyanka Nandakumar, Elizabeth S. Noblin, Jared O'Connell, Aaron A. Petrakovitz, G. David Poznik, Morgan Schumacher, Anjali J. Shastri, Janie F. Shelton, Jingchunzi Shi, Suyash Shringarpure, Vinh Tran, Joyce Y. Tung, Xin Wang, Wei Wang, Catherine H. Weldon, Peter Wilton, Alejandro Hernandez, Corinna Wong, Christophe Toukam Tchakouté.

PGC TS/OCD working group

Nora I. Strom^{1,2,3,4}, Dongmei Yu^{5,6}, Zachary F. Gerring⁷, Matthew W. Halvorsen⁸, Abdel Abdellaoui⁹, Cristina Rodriguez-Fontenla¹⁰, Julia M. Sealock¹¹, Tim Bigdeli¹², Jonathan R. I. Coleman^{13,14}, Behrang Mahjani^{15,16}, Jackson G. Thorp¹⁷, Katharina Bey¹⁸, Christie L. Burton¹⁹, Jurjen J. Luykx^{20,21}, Gwyneth Zai^{22,23}, Kathleen D. Askland²⁴, Cristina Barlassina²⁵, Judith Becker Nissen^{26,27}, Laura Bellodi²⁸, O. Joseph Bienvenu²⁹, Donald Black³⁰, Michael Bloch³¹, Julia Boberg³², Rosa Bosch³³, Michael Breen^{15,34,35}, Brian P. Brennan³⁶, Helena Brentani³⁷, Joseph D. Buxbaum¹⁵, Jonas Bybjerg-Grauholm³⁸, Enda M. Byrne^{39,40}, Beatriz Camarena⁴¹, Adrian Camarena⁴², Carolina Cappi^{15,37}, Angel Carracedo⁴³, Miguel Casas^{44,45}, Maria C. Cavallini⁴⁶, Valentina Ciullo⁴⁷, Edwin H. Cook⁴⁸, Vladimir Coric³¹, Bernadette A. Cullen²⁹, Elles J. De Schipper³, Bernie Devlin⁴⁹, Srdjan Djurovic^{50,51}, Jason A. Elias³⁶, Lauren Erdman⁵², Xavier Estivil⁵³, Martha J. Falkenstein⁵⁴, Bengt T. Fundin¹⁶, Maiken E. Gabrielsen⁵⁵, Fernando S. Goes²⁹, Marco A. Grados²⁹, Jakob Grove^{56,57}, Wei Guo^{58,59}, Jan Haavik^{60,61}, Kristen Hagen^{62,63}, Alexandra Havdahl^{64,65,66}, Ana G. Hounie³⁷, Donald Hucks^{11,67}, Christina Hultman¹⁶, Magdalena Janecka^{15,34}, Michael Jenike⁶⁸, Elinor K. Karlsson^{69,70}, Julia Klawohn¹, Lambertus Klei⁷¹, Janice Krasnow⁷², Kristi

Krebs⁷³, Jason Kropfingger³⁶, Nuria Lanzagorta⁷⁴, Fabio Macciardi⁷⁵, Brion Maher⁷⁶, Evonne McArthur¹¹, Nathaniel McGregor⁷⁷, Nicole C. McLaughlin⁷⁸, Sandra Meier⁷⁹, Euripedes C. Miguel³⁷, Maureen Mulhern^{15,34}, Paul S. Nestadt²⁹, Erika L. Nurmi⁸⁰, Kevin S. O'Connell^{81,82}, Lisa Osiecki^{5,83}, Teemu Palviainen⁸⁴, Fabrizio Piras⁴⁷, Federica Piras⁴⁷, Ann E. Pulver²⁹, Raquel Rabionet⁵³, Alfredo Ramirez^{85,86,87,88}, Scott Rauch⁵⁴, Abraham Reichenberg⁸⁹, Jennifer Reichert^{15,34}, Mark A. Riddle²⁹, Stephan Ripke^{6,90,91}, Aline S. Sampaio^{37,92}, Miriam A. Schiele⁹³, Laura G. Sloofman¹⁵, Jan Smit⁹⁴, Janet L. Sobell⁹⁵, María Soler Artigas^{96,97,98,99}, Laurent F. Thomas^{100,101}, Homero Vallada^{37,102}, Jeremy Veenstra-VanderWeele¹⁰³, Nienke N. C. C. Vulink⁹, Christopher P. Walker¹⁰⁴, Ying Wang²⁹, Jens R. Wendland¹⁰⁵, Bendik S. Winsvold^{106,107,108}, Yin Yao¹⁰⁹, Pino Alonso¹¹⁰, Götz Berberich¹¹¹, Cynthia M. Bulik^{16,112,113}, Danielle Cath^{114,115}, Daniele Cusi¹¹⁶, Richard Delorme¹¹⁷, Damiaan Denys¹¹⁸, Valsamma Eapen¹¹⁹, Peter Falkai¹²⁰, Thomas V. Fernandez³¹, Abby J. Fyer^{121,122}, Daniel A. Geller^{5,123}, Hans J. Grabe¹²⁴, Benjamin D. Greenberg^{77,78,125}, Gregory L. Hanna¹²⁶, Ian M. Hickie¹²⁷, David M. Hougaard^{38,57}, Norbert Kathmann¹, James Kennedy²³, Liang Kung-Yee^{128,129}, Mikael Landén^{16,130}, Stéphanie Le Hellard^{131,132}, Marion Leboyer¹³³, Christine Lochner¹³⁴, James T. McCracken⁸⁰, Sarah E. Medland⁷, Preben B. Mortensen^{57,135,136}, Benjamin Neale^{83,137,138}, Humberto Nicolini^{139,140}, Merete Nordentoft^{141,142}, Michele Pato¹⁴³, Carlos Pato¹⁴³, David L. Pauls¹⁴⁴, Nancy L. Pedersen¹⁶, John Piacentini⁸⁰, Christopher Pittenger¹⁴⁵, Danielle Posthuma¹⁴⁶, Josep A. Ramos-Quiroga^{147,148,149,150}, Steven A. Rasmussen⁷⁸, Kerry J. Ressler³⁶, Margaret A. Richter^{23,151}, Maria C. Rosário¹⁵², David R. Rosenberg¹⁵³, Stephan Ruhrmann⁸⁵, Jack F. Samuels²⁹, Sven Sandin^{15,16}, Paul Sandor²³, Gianfranco Spalletta^{47,154}, Dan J. Stein¹⁵⁵, S. Evelyn Stewart¹⁵⁶, Eric A. Storch¹⁵⁴, Barbara E. Stranger^{157,158}, Maurizio Turiel¹⁵⁹, Thomas Werge^{57,142,160,161}, Ole A. Andreassen^{82,162}, Anders D. Børglum^{56,57}, Susanne Walitza^{163,164,165}, Bjarne K. A. Hansen^{131,166}, Christian P. Rück³, Nicholas G. Martin¹⁷, Lili Milani⁷³, Ole Mors¹⁶⁷, Ted Reichborn-Kjennerud^{64,162}, Marta Ribasés^{97,168,169,170}, Gerd Kvale^{131,166}, David Mataix-Cols³, Katharina Domschke^{93,171}, Edna Grünblatt^{163,164,165}, Michael Wagner¹⁸, John-Anker Zwart^{106,107,172}, Gerome Breen^{13,14}, Gerald Nestadt²⁹, Andres Metspalu⁷³, Jaakko Kaprio¹⁷³, Paul D. Arnold^{174,175}, Dorothy E. Grice¹⁵, James A. Knowles¹⁷⁶, Helga Ask⁶⁴, Karin J. H. Verweij⁹, Lea K. Davis⁶⁷, Dirk J. A. Smit¹⁷⁷, James J. Crowley^{3,8,112}, Carol A. Mathews¹⁷⁸, Eske M. Derks¹⁷, Jeremiah M. Scharf^{5,6}, and Manuel Mattheisen^{2,4,180}

¹Department of Psychology, Humboldt-Universität zu Berlin, Berlin, Germany ²Institute of Psychiatric Phenomics and Genomics (IPPG), University Hospital of Munich, Munich, Germany ³Department of Clinical Neuroscience, Karolinska Institutet, Stockholm, Sweden ⁴Department of Biomedicine, Aarhus University, Aarhus, Denmark

⁵Department of Psychiatry, Massachusetts General Hospital, Boston, MA, USA ⁶Stanley Center for Psychiatric Research, Broad Institute of MIT and Harvard, Cambridge, MA, USA ⁷Department of Mental Health, QIMR Berghofer Medical Research Institute, Brisbane, QLD, Australia ⁸Department of Genetics, University of North Carolina At Chapel Hill, Chapel Hill, NC, USA ⁹Department of Psychiatry, Amsterdam UMC, University of Amsterdam, Amsterdam, The Netherlands ¹⁰CIMUS (centre for Research In Molecular Medicine and Chronic Diseases), University of Santiago De Compostela, Santiago De Compostela, A Coruña, Spain ¹¹Vanderbilt Genetics Institute, Vanderbilt University Medical Center, Nashville, TN, USA ¹²Departments of Psychiatry and Behavioral Sciences, SUNY Downstate Health Sciences University, Brooklyn, NY, USA ¹³Social, Genetic and Developmental Psychiatry Centre, King's College London, London, United Kingdom ¹⁴Departments of South London and Maudsley NHS Trust, NIHR Maudsley Biomedical Research Centre, London, United Kingdom ¹⁵Department of Psychiatry, Icahn School of Medicine At Mount Sinai, New York, NY, USA ¹⁶Departments of Medical Epidemiology and Biostatistics, Karolinska Institutet, Stockholm, Sweden ¹⁷Departments of Genetics and Computational Biology, QIMR Berghofer Medical Research Institute, Brisbane, QLD, Australia ¹⁸Departments of Psychiatry and Psychotherapy, University Hospital Bonn, Bonn, Germany ¹⁹Departments of Neurosciences and Mental Health, Hospital for Sick Children, Toronto, ON, Canada ²⁰Department of Psychiatry, University Medical Center Utrecht, Utrecht, The Netherlands ²¹Second Opinion Outpatient Clinic, Ggnet, Warnsveld, The Netherlands ²²Molecular Brain Science Department, Campbell Family Mental Health Research Institute, Centre for Addiction and Mental Health, Toronto, ON, Canada ²³Department of Psychiatry, University of Toronto, Toronto, ON, Canada ²⁴Waypoint Research Institute AND Outpatient Assessment and Treatment Services,, Waypoint Centre for Mental Health Care, Penetanguishene, ON, Canada ²⁵Department of Heath Sciences, University of Milano, Milano, Milano, Italy ²⁶Departments of Child and Adolescent Psychiatry, Aarhus University Hospital, Psychiatry, Denmark, Aarhus University Hospital, Psychiatry, Aarhus, Denmark ²⁷Institute of Clinical Medicine, Health, Aarhus University, Health, Aarhus University, Aarhus, Denmark ²⁸Department of Neuropsychiatric Sciences, Università Vita-salute San Raffaele Milano Italy, Milano, Italy ²⁹Departments of Psychiatry and Behavioral Sciences, Johns Hopkins University, Baltimore, MD, USA ³⁰Departments of Roy J. and Lucille A. Carver College of Medicine, University of Iowa, Iowa City, IA, USA ³¹Child Study Center and Psychiatry, Yale University, New Haven, CT, USA ³²Center for Psychiatric Research, Institution of Clinical Neuroscience, Stockholm, Sweden ³³Department of MIND SCHOOLS, HOSPITAL SANT JOAN DE DEU, ESPLUGUES DE LLOBREGAT, BARCELONA, Spain ³⁴Seaver Autism Center for Research and Treatment, Icahn School of Medicine At Mount Sinai, New York, NY, USA ³⁵The Mindich Child Health and Development Institute, Icahn School of

Medicine Mount Sinai, New York, NY, USA ³⁶Department of Mclean Hospital, Harvard Medical School, Belmont, MA, USA ³⁷Department of Psychiatry, Universidade De São Paulo, São Paulo, Brazil ³⁸Department of Congenital Disorders, Statens Serum Institut, Copenhagen, Denmark ³⁹Institute for Molecular Bioscience, University of Queensland, Brisbane, Queensland, Australia ⁴⁰Child Health Research Centre, University of Queensland, Brisbane, QLD, Australia ⁴¹Department of Pharmacogenetics, Instituto Nacional De Psiquitria Ramon De La Fuente Muñiz, Mexico City, Mexico ⁴²Department of Surgery, Duke University, Durham, NC, USA ⁴³Genomics Group, University of Santiago De Compostela, Santiago De Compostela, A Coruña, Spain ⁴⁴Programa MIND Escolles, Hospital Sant Joan De Déu, ESPLUGUES DE LLOBREGAT, Barcelona, Spain ⁴⁵Department of Departamento De Psiquiatria Y Medicina Legal, Universitat Autònoma De Barcelona, Bellaterra, Barcelona, Spain ⁴⁶Department of Psychiatry, Ospedale San Raffaele, Milano, Italy ⁴⁷Laboratory of Neuropsychiatry, IRCCS Santa Lucia Foundation, Rome, Italy ⁴⁸Department of Psychiatry, University of Illinois At Chicago, Chicago, IL, USA ⁴⁹Department of Psychiatry, University of Pittsburgh School of Medicine, Pittsburgh, PA, USA ⁵⁰Department of Medical Genetics, Oslo University Hospital, Oslo, Norway ⁵¹NORMENT, Clinical Science, University of Bergen, Bergen, Norway ⁵²Departments of Genetics and Genome Biology, The Hospital for Sick Children, Toronto, ON, Canada ⁵³Department of Genetics, University of Barcelona, Barcelona, Spain ⁵⁴Department of Psychiatry, Mclean Hospital, Harvard Medical School, Belmont, MA, USA ⁵⁵Departments of Public Health and Nursing, Norwegian University of Science and Technology, Trondheim, Norway ⁵⁶Biomedicine and The iSEQ Center, Aarhus University, Aarhus, Denmark ⁵⁷The Lundbeck Foundation Initiative for Integrative Psychiatric Research, Ipsych, , Denmark ⁵⁸National Institute of Mental Health, National Institutes of Health, Bethesda, MD, USA ⁵⁹Genetic Epidemiology Research Branch, National Institute of Mental Health, National Institutes of Health, Bethesda, MD, Bethesda, MD, USA ⁶⁰Department of Biomedicine, University of Bergen, Bergen, Norway ⁶¹Department of Division of Psychiatry, Haukeland University Hospital, Bergen, Norway ⁶²Department of Molde Hospital, Møre Og Romsdal Hospital Trust, Molde, Norway ⁶³Department of Mental Health, Norwegian University of Science and Technology, Trondheim, Norway ⁶⁴Department of Mental Disorders, Norwegian Institute of Public Health, Oslo, Norway ⁶⁵Nic Waals Institute, Lovisenberg Diaconal Hospital, Oslo, Norway ⁶⁶PROMENTA Research Center, Psychology, University of Oslo, Oslo, Norway ⁶⁷Department of Medicine, Vanderbilt University Medical Center, Nashville, TN, USA ⁶⁸Department of Psychiatry, Massachusetts General Hospital and Harvard Medical School, Boston, MA, USA ⁶⁹Departments of Bioinformatics and Integrative Biology, University of Massachusetts Medical School, Worcester, MA, USA ⁷⁰Department of Vertebrate Genomics, Broad Institute of MIT and Harvard, Cambridge, MA, USA ⁷¹Department of Psychiatry, University of

Pittsburgh, Pittsburgh, PA, USA ⁷²Department of Psychiatry, Johns Hopkins University, Baltimore, MD, USA ⁷³Institute of Genomics, University of Tartu, Tartu, Estonia ⁷⁴Carracci Medical Group, Mexico City, Mexico ⁷⁵Departments of Psychiatry and Human Behavior, University of California Irvine (UCI), Irvine, CA, USA ⁷⁶Department of Mental Health, Johns Hopkins Bloomberg School of Public Health, Baltimore, MD, USA ⁷⁷COBRE Center for Neuromodulation, Butler Hospital, Providence, RI, USA ⁷⁸Departments of Psychiatry and Human Behavior, Alpert Medical School, Brown University, Providence, RI, USA ⁷⁹Department of Psychiatry, Dalhousie University, Halifax, NS, Canada ⁸⁰Departments of Psychiatry and Biobehavioral Sciences, University of California, Los Angeles, Los Angeles, CA, USA ⁸¹NORMENT Center of Excellence (coe), Institute of Clinical Medicine, University of Oslo, Oslo, Norway ⁸²Departments of Division of Mental Health and Addiction, Oslo University Hospital, Oslo, Norway ⁸³Psychiatric and Neurodevelopmental Genetics Unit, Harvard Medical School, Boston, MA, USA ⁸⁴Institute for Molecular Medicine Finland - FIMM, University of Helsinki, Helsinki, Finland ⁸⁵Departments of Psychiatry and Psychotherapy, University of Cologne, Cologne, Germany ⁸⁶Departments of Neurodegenerative Diseases and Geriatric Psychiatry, University of Bonn, Bonn, Germany ⁸⁷DZNE Bonn, German Center for Neurodegenerative Diseases (DZNE), Bonn, Germany ⁸⁸Psychiatry and Glenn Biggs Institute for Alzheimer's and Neurodegenerative Diseases, UT Health San Antonio, San Antonio, TX, USA ⁸⁹Department of Mental Disorders, Norwegian Institute of Public Health, New York, NY, USA ⁹⁰Department of Medicine, Massachusetts General Hospital and Harvard Medical School, Boston, MA, USA ⁹¹Departments of Psychiatry and Psychotherapy, Charité Universitätsmedizin, Berlin, Germany ⁹²Department of University Health Care services - SMURB, Federal University of Bahia, Salvador, Brazil ⁹³Departments of Psychiatry and Psychotherapy, Medical Center - University of Freiburg, Freiburg, Germany ⁹⁴Department of Psychiatry, Amsterdam UMC Location Vumc, Amsterdam, The Netherlands ⁹⁵Departments of Psychiatry and The Behavioral Sciences, Keck School of Medicine of USC, Los Angeles, CA, USA ⁹⁶Psychiatric Genetics Unit, Group of Psychiatry, Mental Health and Addiction, Vall D'hebron Research Institute (VHIR), Barcelona, Spain ⁹⁷Department of Psychiatry, Hospital Universitari Vall D'hebron, Barcelona, Spain ⁹⁸Department of Instituto De Salud Carlos III, Biomedical Network Research Centre On Mental Health (CIBERSAM), Madrid, Spain ⁹⁹Department of Biology, Universitat De Barcelona, Barcelona, Spain ¹⁰⁰Departments of Clinical and Molecular Medicine, Norwegian University of Science and Technology, Trondheim, Norway ¹⁰¹K. G. Jebsen Center for Genetic Epidemiology, Norwegian University of Science and Technology, Trondheim, Norway ¹⁰²Departments of Molecular Medicine and Surgery, Karolinska Institutet, Stockholm, Sweden ¹⁰³Departments of Psychiatry, Pediatrics, and Pharmacology, Vanderbilt University Medical Center, Nashville, TN, USA ¹⁰⁴Department of Precision

Medicine, City of Hope, Monrovia, CA, USA ¹⁰⁵Laboratory of Clinical Science, NIMH Intramural Research Program, Bethesda, MD, USA ¹⁰⁶Departments of Research, Innovation and Education, Oslo University Hospital, Oslo, Norway ¹⁰⁷Departments of Medicine and Health Sciences, Norwegian University of Science and Technology, Trondheim, Norway ¹⁰⁸Department of Neurology, Oslo University Hospital, Oslo, Norway ¹⁰⁹Department of Computational Biology, Fudan University, Fudan, PRC ¹¹⁰Department of Bellvitge University, University of Barcelona, Barcelona, Spain ¹¹¹Psychosomatic Department, Windach Hospital of Neurobehavioural Research and Therapy, Windach, Germany ¹¹²Department of Psychiatry, University of North Carolina At Chapel Hill, Chapel Hill, NC, USA ¹¹³Department of Nutrition, University of North Carolina At Chapel Hill, Chapel Hill, NC, USA ¹¹⁴Departments of Rijksuniversiteit Groningen and Psychiatry, University Medical Center Groninge, Groningen, The Netherlands ¹¹⁵Department of Specialized Training, Drenthe Mental Health Care Institute, , ¹¹⁶Institute of Biomedical Technologies, Italian National Centre for Research, Segrate, Milano, Italy ¹¹⁷Child and Adolescent Psychiatry Department, APHP, Paris, France ¹¹⁸Department of Psychiatry, Institute of The Royal Netherlands Academy of Arts and Sciences (NIN-KNAW), Amsterdam, The Netherlands ¹¹⁹Department of Medicine, University of New South Wales, Randwick, NSW, Australia ¹²⁰Departments of Psychiatry and Psychotherapy, University of Göttingen, Göttingen, Germany ¹²¹Department of Psychiatry, New York State Psychiatric Institute, New York, NY, USA ¹²²Department of Psychiatry, Columbia University Medical Center, New York, NY, USA ¹²³Department of Psychiatry, Harvard Medical School, Boston, MA, USA ¹²⁴Departments of Psychiatry and Psychotherapy, University Medicine Greifswald, Greifswald, Greifswald ¹²⁵RR&D Center for Neurorestoration and Neurotechnology, Providence VA Medical Center, Providence, RI ¹²⁶Department of Psychiatry, University of Michigan, Ann Arbor, MI, USA ¹²⁷Brain and Mind Center, The University of Sydney, Sydney, NSW, Australia ¹²⁸Department of Biostatistics, Johns Hopkins Bloomberg School of Public Health, Baltimore, MD, USA ¹²⁹Institute of Population Health Sciences, National Health Research Institutes, , Taiwan ¹³⁰Institute of Neuroscience and Physiology, University of Gothenburg, Gothenburg, Sweden ¹³¹Bergen Center for Brain Plasticity, Haukeland University Hospital, Bergen, Norway ¹³²Department of Clinical Science, University of Bergen, Bergen, Norway ¹³³Departments of Addictology and Psychiatry, Univ Paris Est Créteil, AP-HP, Inserm, Paris, France ¹³⁴Department of Psychiatry, Stellenbosch University, Stellenbosch, South Africa ¹³⁵National Centre for Register-based Research, Aarhus University, Aarhus, Denmark ¹³⁶Centre for Integrated Register-based Research, Aarhus University, Aarhus, Denmark ¹³⁷Analytic and Translational Genetics Unit, Massachusetts General Hospital, Boston, MA, USA ¹³⁸Program In Medical and Population Genetics, Broad Institute of Harvard and MIT, Cambridge, MA, USA ¹³⁹Department of Psychiatric Genetics, Grupo Médico Carracci INMEGEN, Mexico City,

México ¹⁴⁰Department of Psychiatric Genetics, Instituto Nacional De Medicina Genómica, México City, Mexico ¹⁴¹CORE - Copenhagen Research Center for Mental Health, Copenhagen University Hospital, Copenhagen, Denmark ¹⁴²Department of Clinical Medicine, University of Copenhagen, Copenhagen, Denmark ¹⁴³Department of Psychiatry, Rutgers University, Piscataway, NJ, USA ¹⁴⁴Department of Psychiatry, Harvard University, Boston, MA, USA ¹⁴⁵Department of Psychiatry, Yale University, New Haven, CT, USA ¹⁴⁶Department of Clinical Genetics, VU University Medical Center Amsterdam, Amsterdam, The Netherlands ¹⁴⁷Department of Psychiatry, Hospital Universitari Vall D'hebron, Barcelona, Catalonia, Spain ¹⁴⁸Group of Psychiatry, Mental Health and Addictions, Vall D'hebron Research Institute (VHIR), Barcelona, Spain ¹⁴⁹Group 27, Biomedical Network Research Centre On Mental Health (CIBERSAM), Barcelona, Spain ¹⁵⁰Departments of Psychiatry and Forensic Medicine, Universitat Autònoma De Barcelona, Barcelona, Spain ¹⁵¹Department of Psychiatry, Sunnybrook Health Sciences Centre, , ¹⁵²Department of Psychiatry, Federal University of São Paulo (UNIFESP), São Paulo, Brazil ¹⁵³Departments of Psychiatry and Behavioral Neurosciences, Wayne State University School of Medicine, Detroit, MI, USA ¹⁵⁴Departments of Psychiatry and Behavioral Sciences, Baylor College of Medicine, Houston, TX, USA ¹⁵⁵Psychiatry and Neuroscience Institute, University of Cape Town, Cape Town, Western Cape, South Africa ¹⁵⁶Department of Psychiatry, University of British Columbia, Vancouver, BC, Canada ¹⁵⁷Department of Pharmacology, Northwestern University Feinberg School of Medicine, Chicago, IL, USA ¹⁵⁸Center for Genetic Medicine, Northwestern University Feinberg School of Medicine, Chicago, IL, USA ¹⁵⁹Department of Cardiology, University of Milan, Milan, Italy ¹⁶⁰Department of Mental Health Services, Copenhagen University Hospital, Copenhagen, Denmark ¹⁶¹GLOBE Institute, University of Copenhagen, Copenhagen, Denmark ¹⁶²Institute of Clinical Medicine, University of Oslo, Oslo, Norway ¹⁶³Departments of Child and Adolescent Psychiatry and Psychotherapy, University of Zurich, Zürich, Switzerland ¹⁶⁴Neuroscience Center Zurich, University of Zurich and The ETH Zurich, Zurich, Switzerland ¹⁶⁵Zurich Center for Integrative Human Physiology, University of Zurich, Zurich, Switzerland ¹⁶⁶Department of Psychology, University of Bergen, Bergen, Norway ¹⁶⁷Psychosis Research Unit, Aarhus University Hospital - Psychiatry, 8200 Aarhus N, Denmark ¹⁶⁸Psychiatric Genetics Unit, Vall D'hebron Research Institute (VHIR), Universitat Autònoma De Barcelona, Barcelona, Spain ¹⁶⁹Biomedical Network Research Centre On Mental Health (CIBERSAM), Barcelona, Spain. ³ Biomedical Network Research Centre On Mental Health (CIBERSAM), Instituto De Salud Carlos III, Madrid, Spain ¹⁷⁰Departments of Genetics, Microbiology and Statistics, University of Barcelona, Barcelona, Spain ¹⁷¹Center for Basics In Neuromodulation, University of Freiburg, Freiburg, Germany ¹⁷²Department of Medicine, University of Oslo, Oslo, Norway ¹⁷³Helsinki Institute of Life Science, Univer-

sity of Helsinki, Helsinki, Finland ¹⁷⁴Department of Psychiatry, Cumming School of Medicine, University of Calgary, Calgary, AB, Canada ¹⁷⁵Program In Genetics and Genome Biology, Hospital for Sick Children, Toronto, ON, Canada ¹⁷⁶Department of Cell Biology, SUNY Downstate Health Sciences University, Brooklyn, NY, USA ¹⁷⁷Department of Psychiatry, Amsterdam UMC Location AMC, Amsterdam, The Netherlands ¹⁷⁸Psychiatry and Genetics Institute, Center for OCD, Anxiety and Related Disorders, University of Florida, Gainesville, FL, USA ¹⁷⁹Department of Psychiatry, Center for Genomic Medicine, Massachusetts General Hospital, Harvard Medical School, Boston, MA, USA ¹⁸⁰Departments of Psychiatry and Community Health and Epidemiology, Dalhousie University, Halifax, NS, Canada

GWAS details for NORDiC-NOR & NORDiC-SWE

pre-GWAS Quality Control

NORDiC-SWE

We formed a case/control dataset by merging PLINK filesets for four different cohorts (one case-only, three control-only) using PLINK v1.90b3n. This merged fileset consisted of 647,335 variant calls across a total of 1107 cases and 3,500 controls.

We first identified a subset of samples that will be usable in the final GWAS based on a lack of cryptic relatedness patterns with other samples and likely European ancestry. In preparation for this we used PLINK v1.90b3n to extract common (MAF > 5%), and used the LD-pruned ($-indep\ 50\ 5\ 2$) subset of these variants for relatedness checks, implemented via PLINK's 'genome' function. As part of relatedness QC we first removed a total of 48 samples with mean $\pi_{\hat{}}$ values observed with other samples ≥ 0.02 , which we considered to be evidence of systemic issues with the sample including but not limited to overall high genotype missingness. Next we pruned instances of sample duplication, defined as $\pi_{\hat{}} \geq 0.95$. For a set of samples which based on these criteria are duplicates, we selected the one sample to keep based on which sample carried the lowest genotype missingness, as computed in PLINK. A total of 3 samples were removed in the duplicate pruning process. In the remaining samples we identified all pairs where a cryptic relatedness pattern (defined here as $\pi_{\hat{}} > 0.2$) is present. To resolve these relatedness issues in a manner that minimizes the total number of samples removed from the cohort, we used an iterative strategy that for each round, 1) defined rel_max as the maximum number of cryptic relationships observed across single samples, 2) removed samples where the number of cryptic relationships equaled rel_max , 3) recomputes rel_max in the pruned sample set. Once rel_max equals 1, then for each pairwise cryptic relationship, we selected the sample to keep based on which sample carried the lower overall genotype missingness, as computed in PLINK. A total of 102 samples that carried cryptic relatedness issues were marked for exclusion from the final GWAS, leaving behind 1074 cases and 3380 controls. To identify

the subset of samples that are of likely European ancestry, we utilized PEDDY v0.4.3, which allows for PCA of input samples with 1000 genomes sample data and subsequent classification per sample of its most likely general ethnicity. While PEDDY was originally designed primarily for exome and whole genome sequence data, it should be sufficient for identification of and pruning of samples that clearly are not of European ancestry. We found that a total of 6,039 variants overlapped between the merged PLINK fileset and the 1000 genomes data included in PEDDY, and used these to conduct PCA and PEDDY's classification algorithm. We kept all samples with an ancestry classification of EUR. From the relatedness and ethnicity classification steps we identified a total of 989 cases and 3200 controls suitable for the final NORDIC GWAS.

To prepare our merged cohort dataset for the GWAS pipeline, we pruned single variants from our relatedness-pruned dataset (1,074 cases, 3,380 controls) where there was suggestive evidence of technical biases or batch effects. For this we first collect cohort level allele frequency and genotype missingness values for the QC-passing subset of input samples, and look for instances where an input cohort has an extreme value which might be consistent with batch effects or technical problems. We defined variants as QC-failing if they met one of the following criteria: 1) maximum genotype missingness in a cohort > 0.02 ; 2) allele frequency < 0.001 in at least one cohort; 3) max – min allele frequency > 0.1 across all four cohorts; 4) max – min allele frequency > 0.03 across all three control cohorts; 5) genome-wide significant in a control vs. control synthetic GWAS. A total of 154,791 variants met at least one of these criteria were excluded, leaving us with a final case/control dataset consisting of genotype calls across 492,554 variants across the 1074 cases and 3,380 controls.

NORDiC-NOR

The pre-GWAS QC applied to the NORDiC-NOR dataset (482 cases, 343 controls in the raw data) was nearly identical to that applied to NORDiC-SWE data after the merging of separate genotype data, consisting of pruning of cryptic relatedness, marking of samples that are of likely European ancestry and pruning of the dataset for single variants where there was suggestive evidence of technical biases or batch effects. In our cryptic relatedness QC step we identified 4 samples that had a mean $\pi_{\hat{}}$ with other samples ≥ 0.1 , 74 samples that had evidence of being a sample duplicate ($\pi_{\hat{}} \geq 0.95$) and 8 samples from the remaining cohort with evidence of cryptic relatedness ($\pi_{\hat{}} \geq 0.2$), leaving behind 404 cases and 335 controls. We found a total of 6263 variants overlapped between the merged PLINK fileset and the 1000 genomes data included in PEDDY, and identified a total of 368 cases and 315 controls with likely European ancestry. We performed variant-level QC on a PC-pruned subset of 340 cases and 307 controls, defining variants as failing if they met one of the following criteria: 1) maximum genotype missingness in a cohort > 0.02 ; 2) allele frequency

of 0 in at least one cohort; 3) max – min allele frequency > 0.1 . A total of 136,525 variants met at least one of these criteria were excluded, leaving us with a final case/control dataset consisting of genotype calls across 479,358 variants. We used calls across these variants in samples that had been pruned for relatedness issues (not including standard pairwise relatedness issues as ricopili can detect these) as input for the GWAS (407 cases, 340 controls).

QC and imputation implemented in Ricopili

We used the ricopili pipeline to run an automated round of pre-imputation QC on the genotype data from 492,554 QC-passing variants across the full unpruned datasets of NORDiC-SWE (1107 cases and 3500 controls) and 479,358 QC-passing variants across NORDiC-Norway (407 cases and 340 controls), and conducted imputation on the genotype data using the Haplotype Reference Consortium (HRC) reference panel. All subsets of the analysis involved ricopili were done using ricopili v2018_Dec_7.001. The pre-imputation ricopili QC step involved a series of hard filters on variant and sample level data, including removing variants with pre-sample pruning call rate < 0.95 , samples with call rate < 0.98 , FHET outside of ± 0.20 , samples with discrepancies between reported and derived sex, and post sample-pruning variants that meet any of the following: 1) call rate < 0.98 , 2) missing difference > 0.02 , 3) invariant positions, 4) MAF > 0.01 , 5) HWE $p < 1e-6$ in controls, and 6) HWE $p < 1e-10$ in cases. After the QC described we were left with 481,323 QC-passing variants across 1077 cases and 3486 controls in NORDiC-SWE, and 469,618 QC-passing variants across 404 cases and 340 controls in NORDiC-Norway.

After sample and variant pruning we next used ricopili's impute_dirsub module to perform imputation using HRC genotypes as a reference panel. In our imputation run we used eagle v2.3.5 for pre-phasing, and minimac3 v2.0.1 for imputation. We derived 3 different imputed callsets from this process: 1) a set of high confidence imputed genotypes (2,771,425 in NORDiC-SWE, 3,043,464 in NORDiC-Norway), 2) a set of imputed best-guess genotypes with medium level accuracy (7,112,906 in NORDiC-SWE, 7,277,174 in NORDiC-Norway), and 3) a set of variants where imputation accuracy is lowered in order to increase the total number of variants included in the imputation (9,021,638 in NORDiC-SWE, 8,964,589 in NORDiC-Norway).

Supplementary Figures

Fig. S1. Genome-wide association results for the MTAG OCD with cases ascertained for another disorder as the primary phenotype (iPSYCH; Manhattan plot in (A) and quantile-quantile plot in (B)) and for the MTAG OCD analysis with the biobank cases (23andMe) as the primary phenotype (Manhattan plot in (C) and quantile-quantile plot in (D)). The x-axis in (A) and (C) shows the position in the genome (chromosomes 1-22), while the y-axis represents $-\log_{10}(p)$ values for the association of variants with OCD. The horizontal red line represents the threshold for genome-wide significance. Each dot represents one SNP that was tested in the GWAS, with green diamonds indicating the lead SNP in regions harboring a genome-wide significant SNP. In (B) and (D) the expected $-\log_{10}(p)$ under the null is plotted against the observed $-\log_{10}(p)$, qq-plots (B) and (D) belong to Manhattan lots (A) and (C), respectively. The shading indicates 95% confidence region under the null. Lambda indicates the genomic inflation factor.

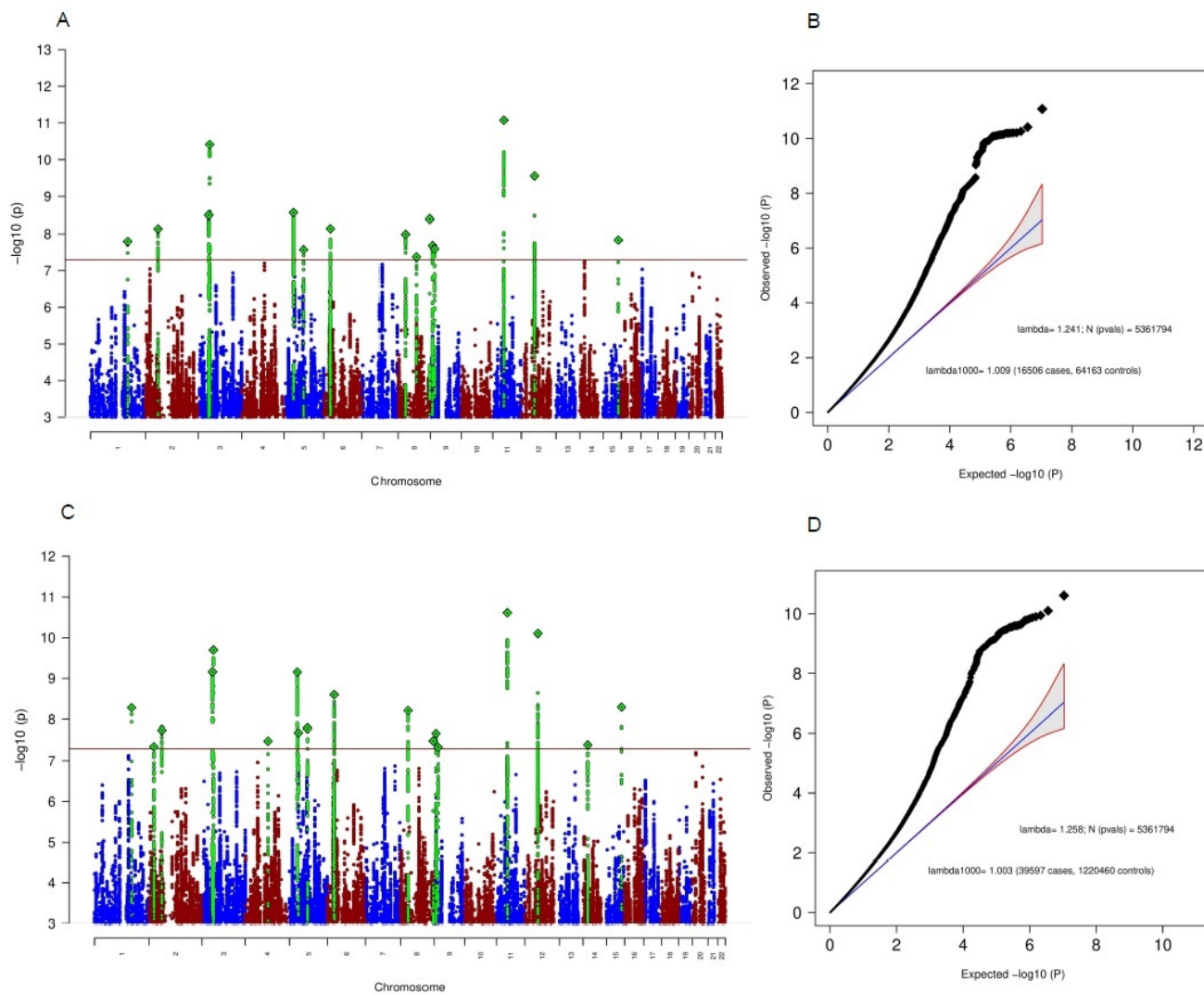
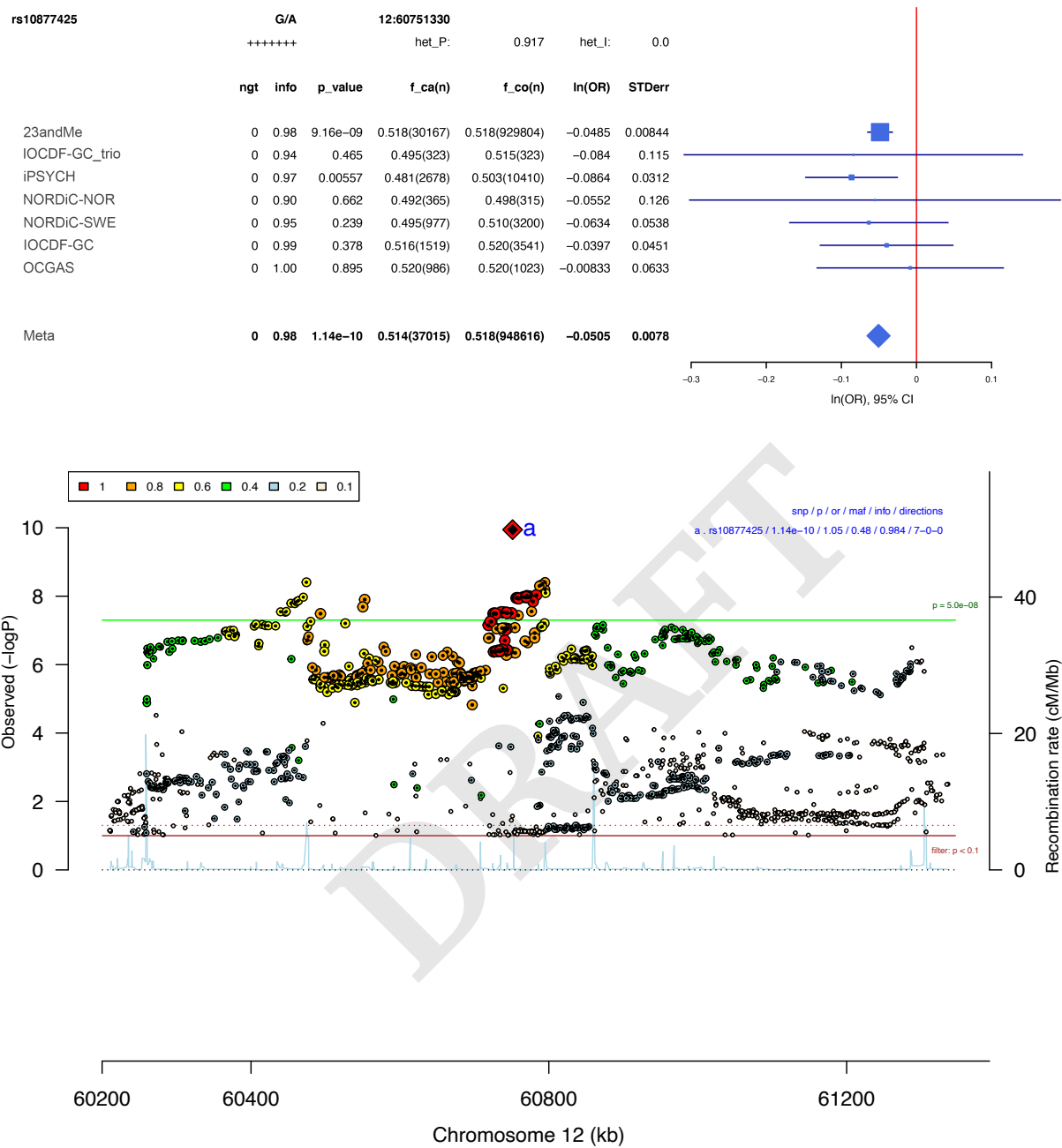


Fig. S2. Forest plot (top) and regional association plot (bottom) of SNP rs10877425. Forest plot: Shows the imputation score (info), p-value (p_value), A1 allele frequency in cases and number of cases (f_ca(n)), A1 allele frequency in controls and number of controls (f_co(n)), effect of the association (ln(OR)), and standard error of the effect (STDerr) for each individual dataset and the over-all meta-analysis. On the right side, effects (ln(OR)) and 95% confidence intervals (CI) are plotted. At the top, the direction of effect for each study is shown (+ for positive effect of A1, - for negative effect of A1), and results of a test of heterogeneity (het_P and het_I) of effect across the individual datasets are displayed. Regional association plot: The $-\log_{10}(P)$ of SNPs in the OCD meta-analysis GWAS is shown on the left y axis. The recombination rates expressed in centimorgans (cM) per Mb (Megabase) (blue line) are shown on the right y axis. Position in Mb is on the x axis. Only the SNPs with association p-value less than 0.1 were plotted. The lead SNP in the region is shown as a red diamond. Colour coding indicates LD to the lead SNP.



database: gwascatalog.Sep_2019.rp.txt, refGene.txt.Sep_2019.out

Fig. S3. Forest plot (top) and regional association plot (bottom) of SNP rs674094. Forest plot: Shows the imputation score (info), p-value (p_value), A1 allele frequency in cases and number of cases (f_ca(n)), A1 allele frequency in controls and number of controls (f_co(n)), effect of the association (ln(OR)), and standard error of the effect (STDerr) for each individual dataset and the over-all meta-analysis. On the right side, effects (ln(OR)) and 95% confidence intervals (CI) are plotted. At the top, the direction of effect for each study is shown (+ for positive effect of A1, - for negative effect of A1), and results of a test of heterogeneity (het_P and het_I) of effect across the individual datasets re displayed. Regional association plot: The $-\log_{10}(P)$ of SNPs in the OCD meta-analysis GWAS is shown on the left y axis. The recombination rates expressed in centimorgans (cM) per Mb (Megabase) (blue line) are shown on the right y axis. Position in Mb is on the x axis. Only the SNPs with association p-value less than 0.1 were plotted. The lead SNP in the region is shown as a red diamond. Colour coding indicates LD to the lead SNP.

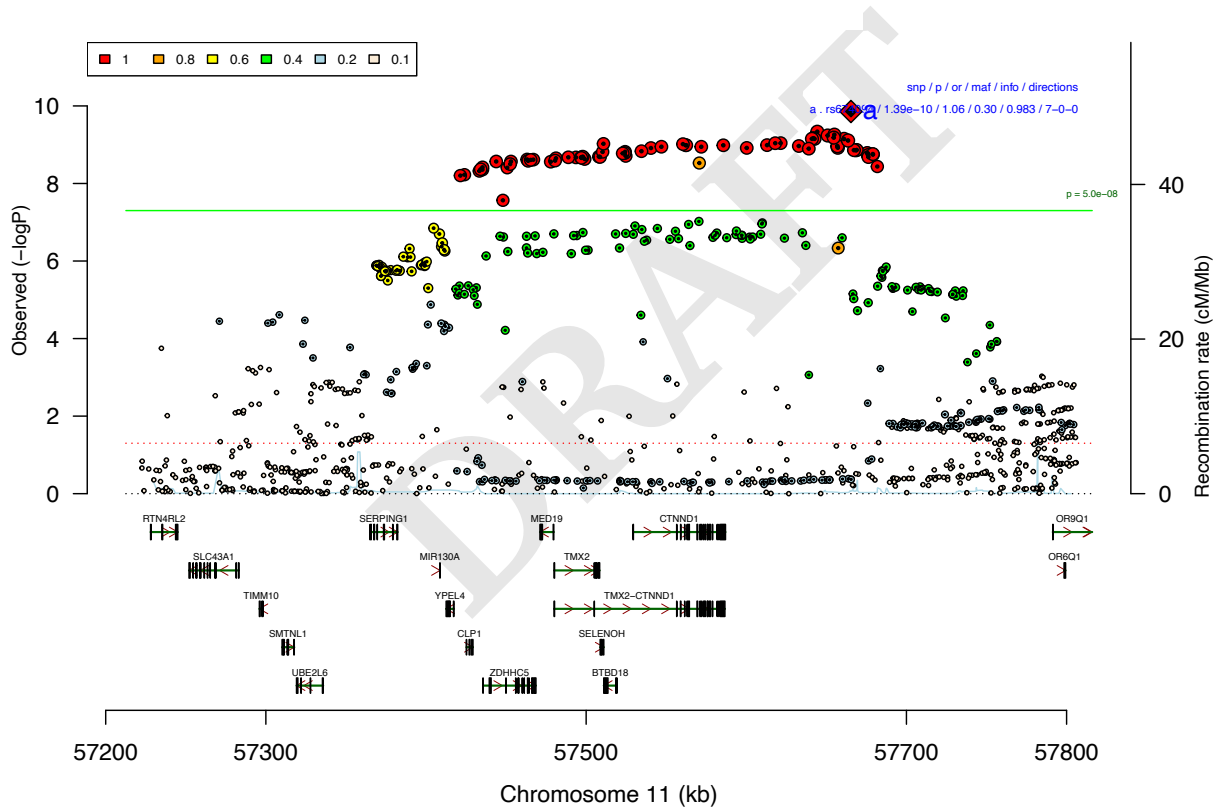
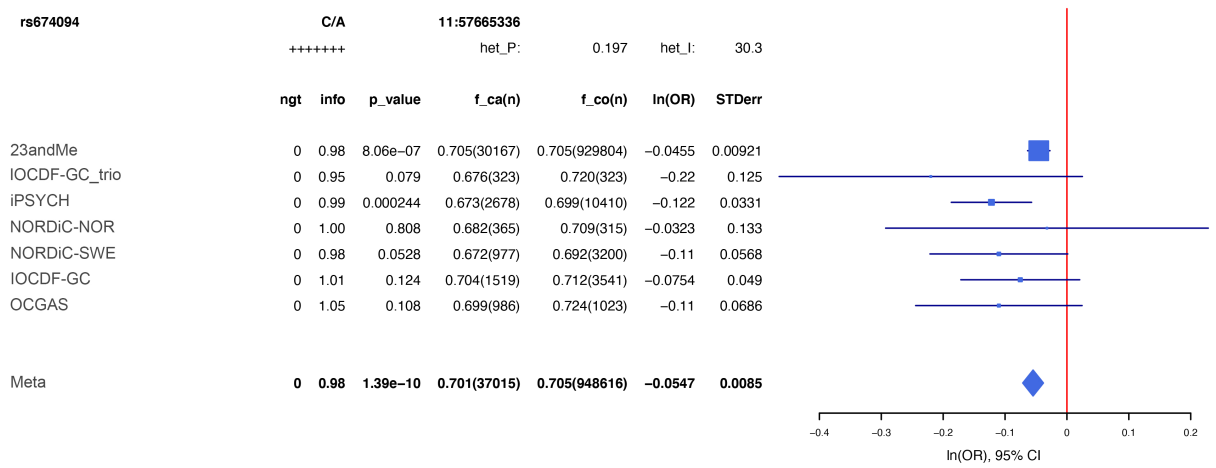


Fig. S4. Forest plot (top) and regional association plot (bottom) of SNP rs11953498. Forest plot: Shows the imputation score (info), p-value (p_value), A1 allele frequency in cases and number of cases (f_ca(n)), A1 allele frequency in controls and number of controls (f_co(n)), effect of the association (ln(OR)), and standard error of the effect (STDerr) for each individual dataset and the over-all meta-analysis. On the right side, effects (ln(OR)) and 95% confidence intervals (CI) are plotted. At the top, the direction of effect for each study is shown (+ for positive effect of A1, - for negative effect of A1), and results of a test of heterogeneity (het_P and het_I) of effect across the individual datasets re displayed. Regional association plot: The $-\log_{10}(P)$ of SNPs in the OCD meta-analysis GWAS is shown on the left y axis. The recombination rates expressed in centimorgans (cM) per Mb (Megabase) (blue line) are shown on the right y axis. Position in Mb is on the x axis. Only the SNPs with association p-value less than 0.1 were plotted. The lead SNP in the region is shown as a red diamond. Colour coding indicates LD to the lead SNP.

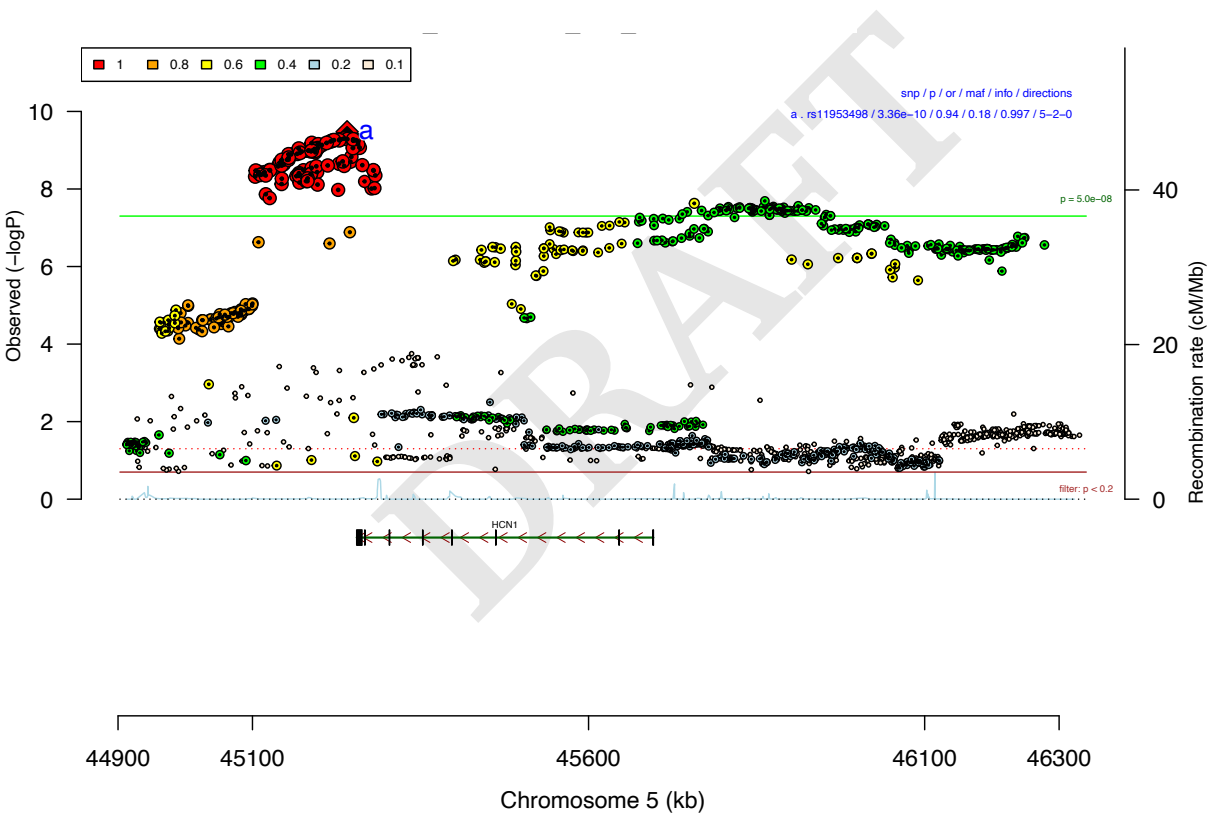
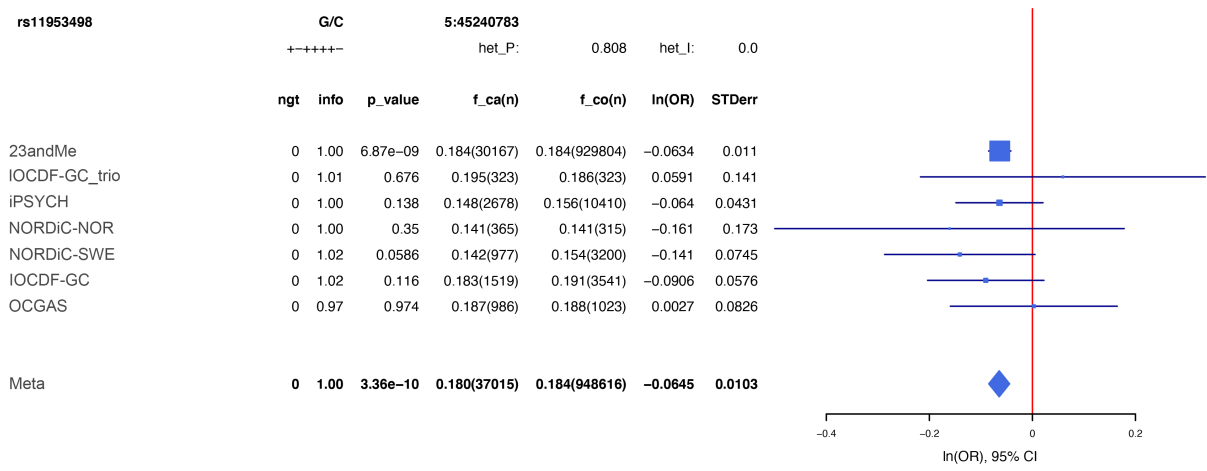


Fig. S5. Forest plot (top) and regional association plot (bottom) of SNP rs9840050. Forest plot: Shows the imputation score (info), p-value (p_value), A1 allele frequency in cases and number of cases (f_ca(n)), A1 allele frequency in controls and number of controls (f_co(n)), effect of the association (ln(OR)), and standard error of the effect (STDerr) for each individual dataset and the over-all meta-analysis. On the right side, effects (ln(OR)) and 95% confidence intervals (CI) are plotted. At the top, the direction of effect for each study is shown (+ for positive effect of A1, - for negative effect of A1), and results of a test of heterogeneity (het_P and het_I) of effect across the individual datasets re displayed. Regional association plot: The $-\log_{10}(P)$ of SNPs in the OCD meta-analysis GWAS is shown on the left y axis. The recombination rates expressed in centimorgans (cM) per Mb (Megabase) (blue line) are shown on the right y axis. Position in Mb is on the x axis. Only the SNPs with association p-value less than 0.1 were plotted. The lead SNP in the region is shown as a red diamond. Colour coding indicates LD to the lead SNP.

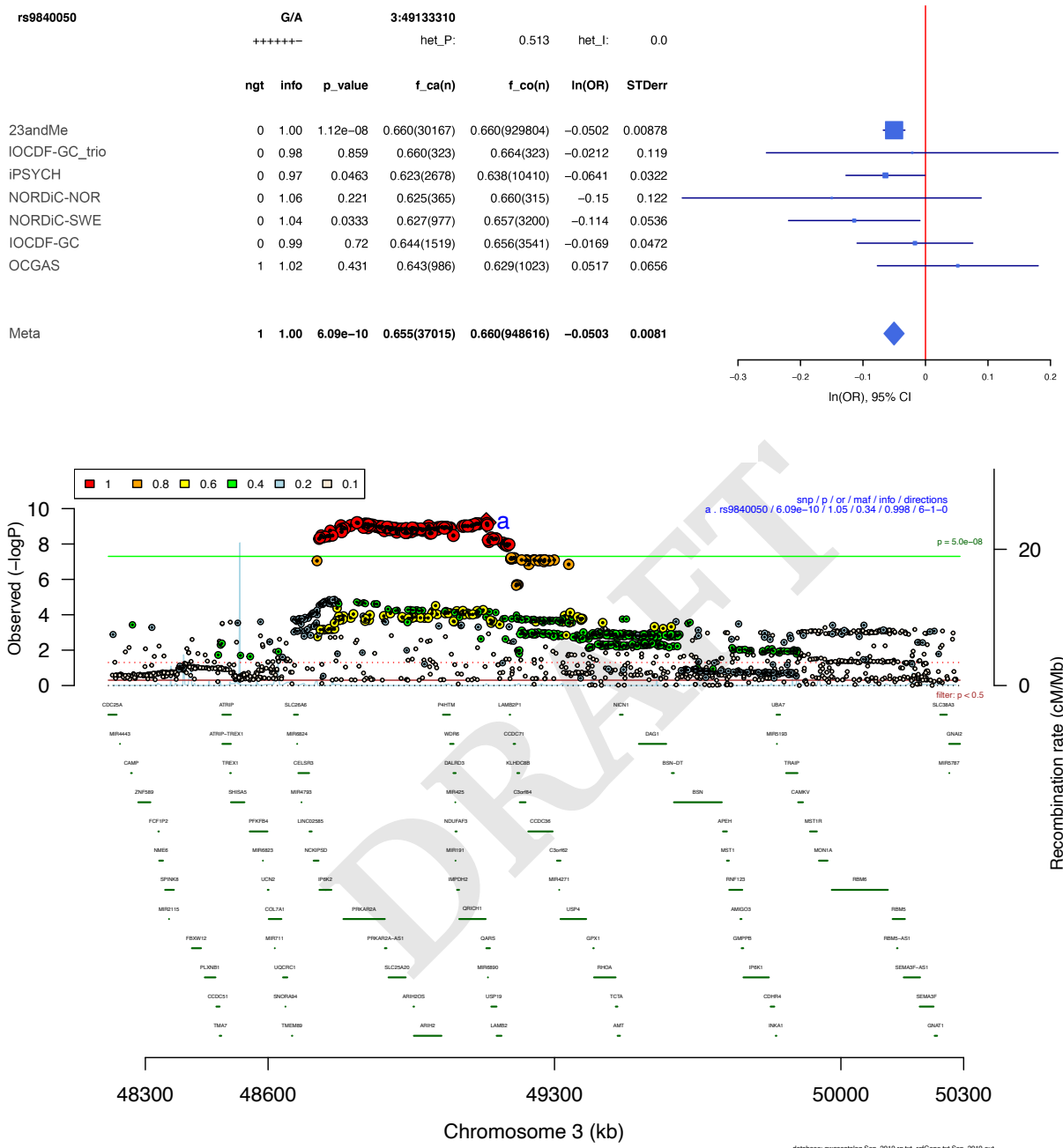


Fig. S6. Forest plot (top) and regional association plot (bottom) of SNP rs2564930. Forest plot: Shows the imputation score (info), p-value (p_value), A1 allele frequency in cases and number of cases (f_ca(n)), A1 allele frequency in controls and number of controls (f_co(n)), effect of the association (ln(OR)), and standard error of the effect (STDerr) for each individual dataset and the over-all meta-analysis. On the right side, effects (ln(OR)) and 95% confidence intervals (CI) are plotted. At the top, the direction of effect for each study is shown (+ for positive effect of A1, - for negative effect of A1), and results of a test of heterogeneity (het_P and het_I) of effect across the individual datasets re displayed. Regional association plot: The $-\log_{10}(P)$ of SNPs in the OCD meta-analysis GWAS is shown on the left y axis. The recombination rates expressed in centimorgans (cM) per Mb (Megabase) (blue line) are shown on the right y axis. Position in Mb is on the x axis. Only the SNPs with association p-value less than 0.1 were plotted. The lead SNP in the region is shown as a red diamond. Colour coding indicates LD to the lead SNP.

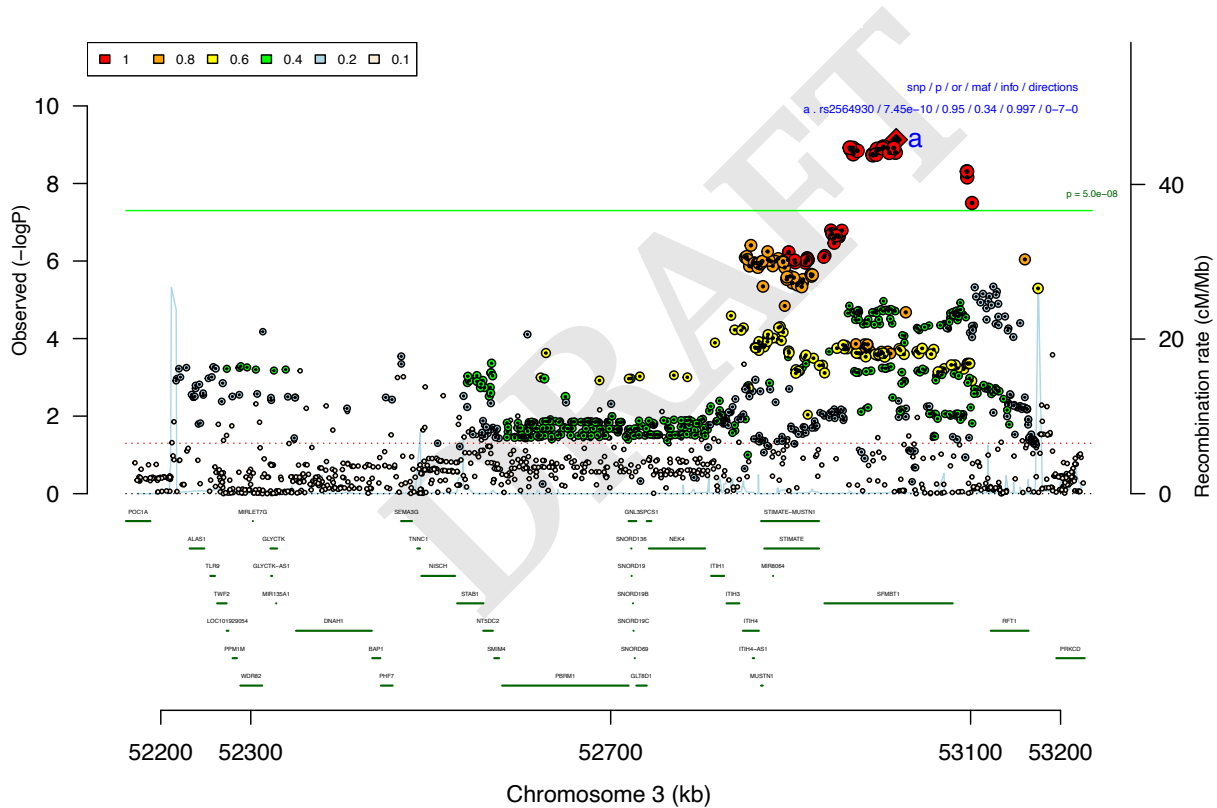
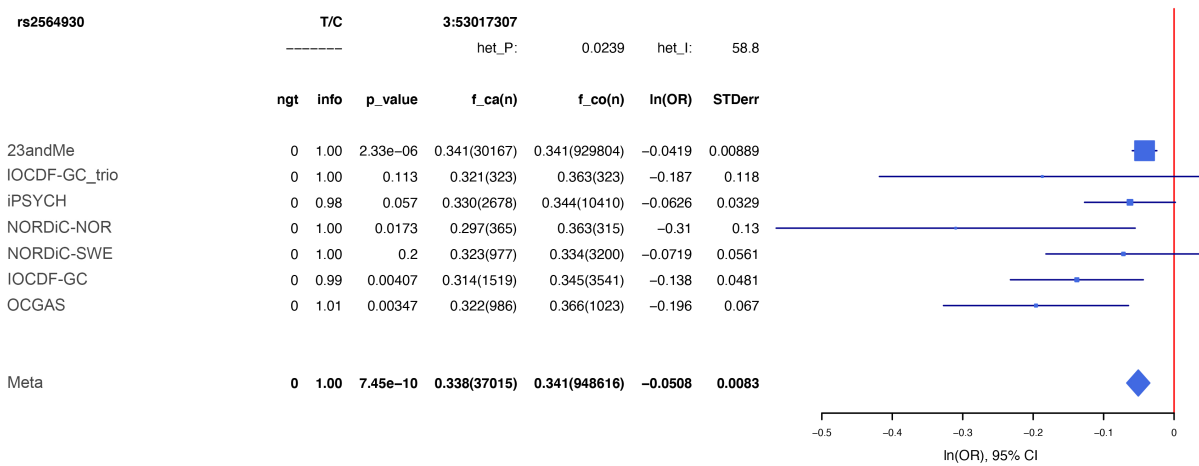


Fig. S7. Forest plot (top) and regional association plot (bottom) of SNP rs9265969. Forest plot: Shows the imputation score (info), p-value (p_value), A1 allele frequency in cases and number of cases (f_ca(n)), A1 allele frequency in controls and number of controls (f_co(n)), effect of the association (ln(OR)), and standard error of the effect (STDerr) for each individual dataset and the over-all meta-analysis. On the right side, effects (ln(OR)) and 95% confidence intervals (CI) are plotted. At the top, the direction of effect for each study is shown (+ for positive effect of A1, - for negative effect of A1), and results of a test of heterogeneity (het_P and het_I) of effect across the individual datasets re displayed. Regional association plot: The $-\log_{10}(P)$ of SNPs in the OCD meta-analysis GWAS is shown on the left y axis. The recombination rates expressed in centimorgans (cM) per Mb (Megabase) (blue line) are shown on the right y axis. Position in Mb are on the x axis. Only the SNPs with association p-value less than 0.1 were plotted. The lead SNP in the region is shown as a red diamond. Colour coding indicates LD to the lead SNP.

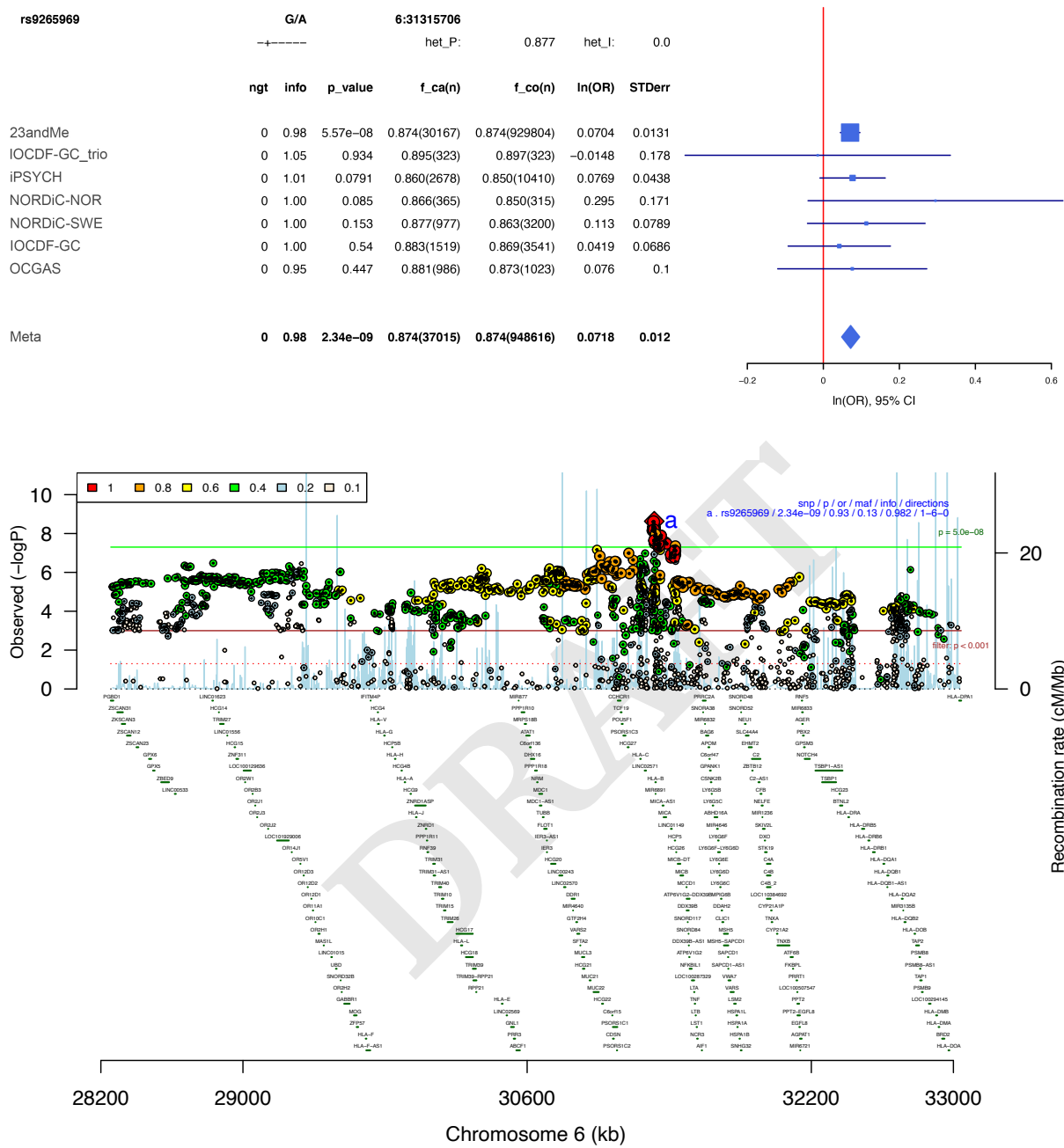


Fig. S8. Forest plot (top) and regional association plot (bottom) of SNP rs6660196. Forest plot: Shows the imputation score (info), p-value (p_value), A1 allele frequency in cases and number of cases (f_ca(n)), A1 allele frequency in controls and number of controls (f_co(n)), effect of the association (ln(OR)), and standard error of the effect (STDerr) for each individual dataset and the over-all meta-analysis. On the right side, effects (ln(OR)) and 95% confidence intervals (CI) are plotted. At the top, the direction of effect for each study is shown (+ for positive effect of A1, - for negative effect of A1), and results of a test of heterogeneity (het_P and het_I) of effect across the individual datasets re displayed. Regional association plot: The $-\log_{10}(P)$ of SNPs in the OCD meta-analysis GWAS is shown on the left y axis. The recombination rates expressed in centimorgans (cM) per Mb (Megabase) (blue line) are shown on the right y axis. Position in Mb is on the x axis. Only the SNPs with association p-value less than 0.1 were plotted. The lead SNP in the region is shown as a red diamond. Colour coding indicates LD to the lead SNP.

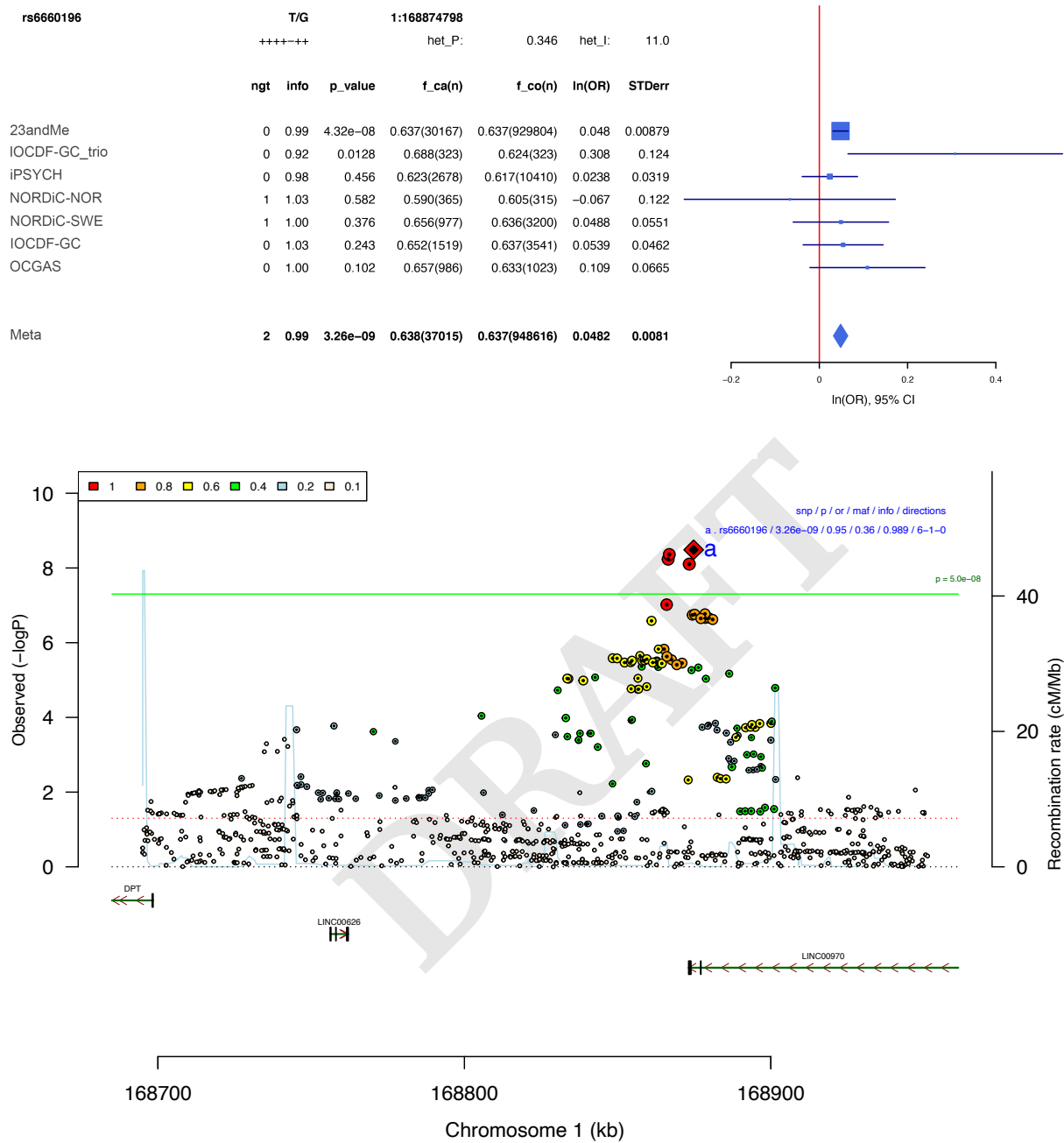


Fig. S9. Forest plot (top) and regional association plot (bottom) of SNP rs4702. Forest plot: Shows the imputation score (info), p-value (p_value), A1 allele frequency in cases and number of cases (f_ca(n)), A1 allele frequency in controls and number of controls (f_co(n)), effect of the association (ln(OR)), and standard error of the effect (STDerr) for each individual dataset and the over-all meta-analysis. On the right side, effects (ln(OR)) and 95% confidence intervals (CI) are plotted. At the top, the direction of effect for each study is shown (+ for positive effect of A1, - for negative effect of A1), and results of a test of heterogeneity (het_P and het_I) of effect across the individual datasets re displayed. Regional association plot: The $-\log_{10}(P)$ of SNPs in the OCD meta-analysis GWAS is shown on the left y axis. The recombination rates expressed in centimorgans (cM) per Mb (Megabase) (blue line) are shown on the right y axis. Position in Mb is on the x axis. Only the SNPs with association p-value less than 0.1 were plotted. The lead SNP in the region is shown as a red diamond. Colour coding indicates LD to the lead SNP.

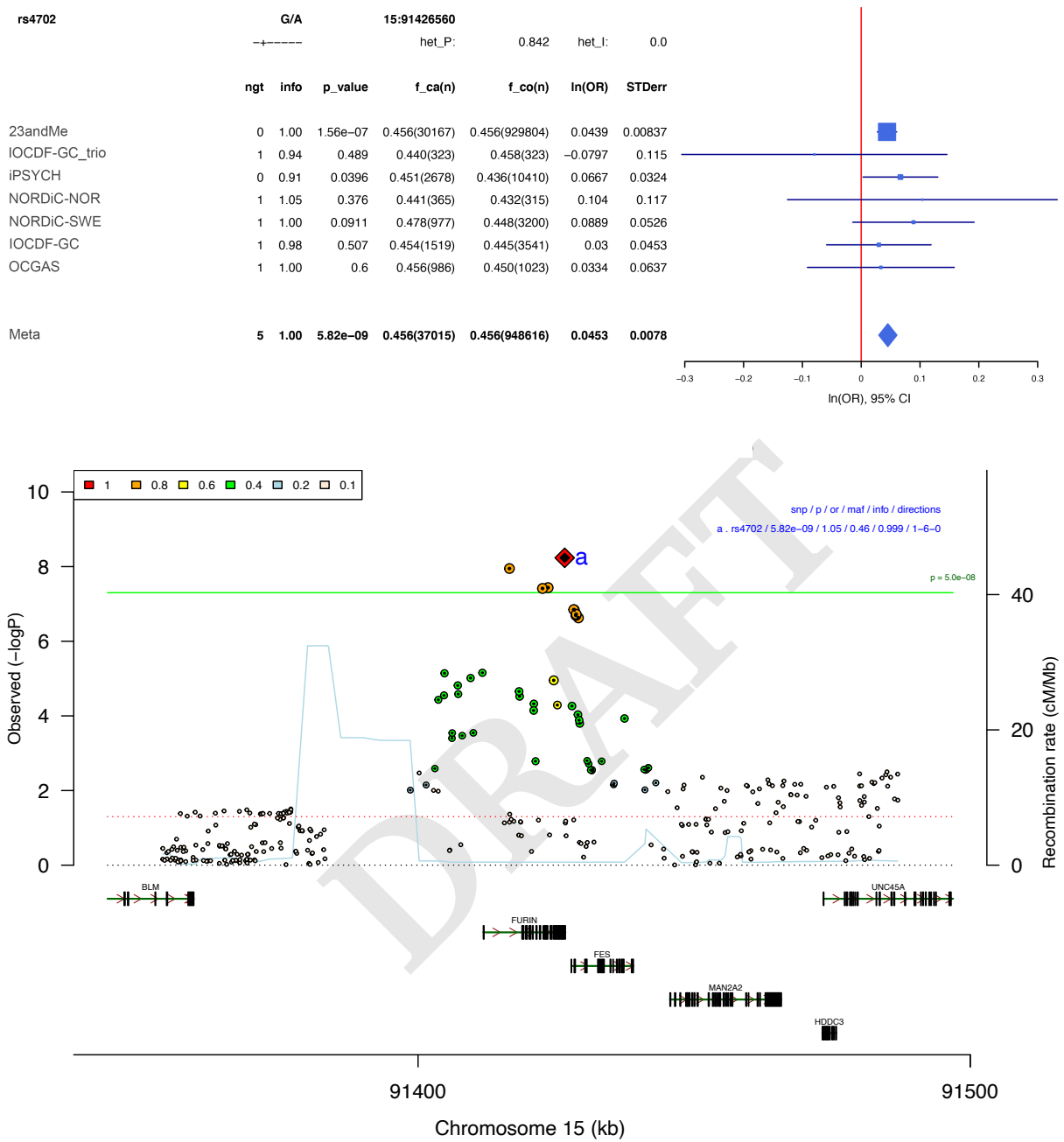


Fig. S10. Forest plot (top) and regional association plot (bottom) of SNP rs2198140. Forest plot: Shows the imputation score (info), p-value (p_value), A1 allele frequency in cases and number of cases (f_ca(n)), A1 allele frequency in controls and number of controls (f_co(n)), effect of the association (ln(OR)), and standard error of the effect (STDerr) for each individual dataset and the over-all meta-analysis. On the right side, effects (ln(OR)) and 95% confidence intervals (CI) are plotted. At the top, the direction of effect for each study is shown (+ for positive effect of A1, - for negative effect of A1), and results of a test of heterogeneity (het_P and het_I) of effect across the individual datasets re displayed. Regional association plot: The $-\log_{10}(P)$ of SNPs in the OCD meta-analysis GWAS is shown on the left y axis. The recombination rates expressed in centimorgans (cM) per Mb (Megabase) (blue line) are shown on the right y axis. Position in Mb is on the x axis. Only the SNPs with association p-value less than 0.1 were plotted. The lead SNP in the region is shown as a red diamond. Colour coding indicates LD to the lead SNP.

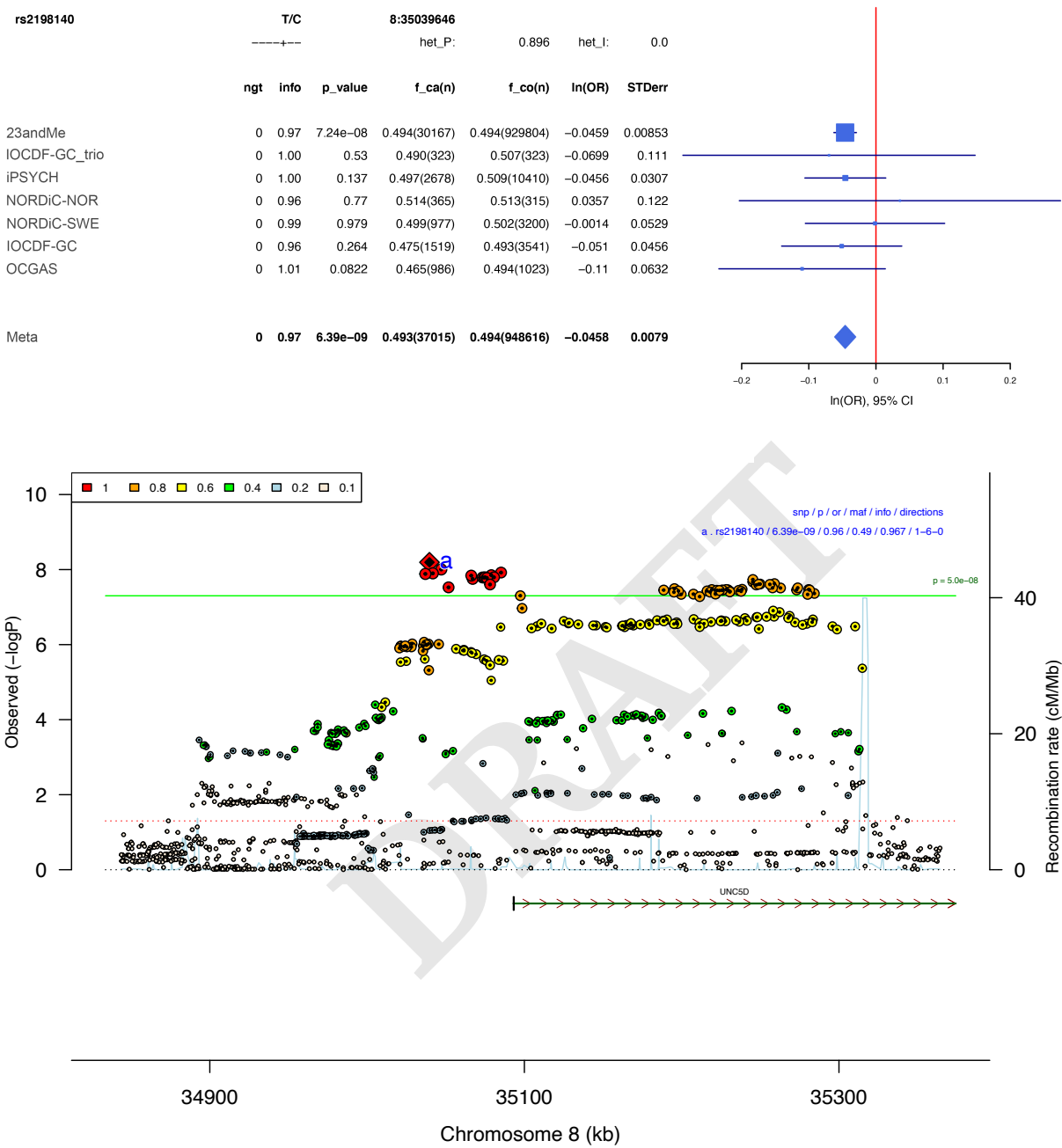


Fig. S11. Forest plot (top) and regional association plot (bottom) of SNP rs3899258. Forest plot: Shows the imputation score (info), p-value (p_value), A1 allele frequency in cases and number of cases (f_ca(n)), A1 allele frequency in controls and number of controls (f_co(n)), effect of the association (ln(OR)), and standard error of the effect (STDerr) for each individual dataset and the over-all meta-analysis. On the right side, effects (ln(OR)) and 95% confidence intervals (CI) are plotted. At the top, the direction of effect for each study is shown (+ for positive effect of A1, - for negative effect of A1), and results of a test of heterogeneity (het_P and het_I) of effect across the individual datasets re displayed. Regional association plot: The $-\log_{10}(P)$ of SNPs in the OCD meta-analysis GWAS is shown on the left y axis. The recombination rates expressed in centimorgans (cM) per Mb (Megabase) (blue line) are shown on the right y axis. Position in Mb is on the x axis. Only the SNPs with association p-value less than 0.1 were plotted. The lead SNP in the region is shown as a red diamond. Colour coding indicates LD to the lead SNP.

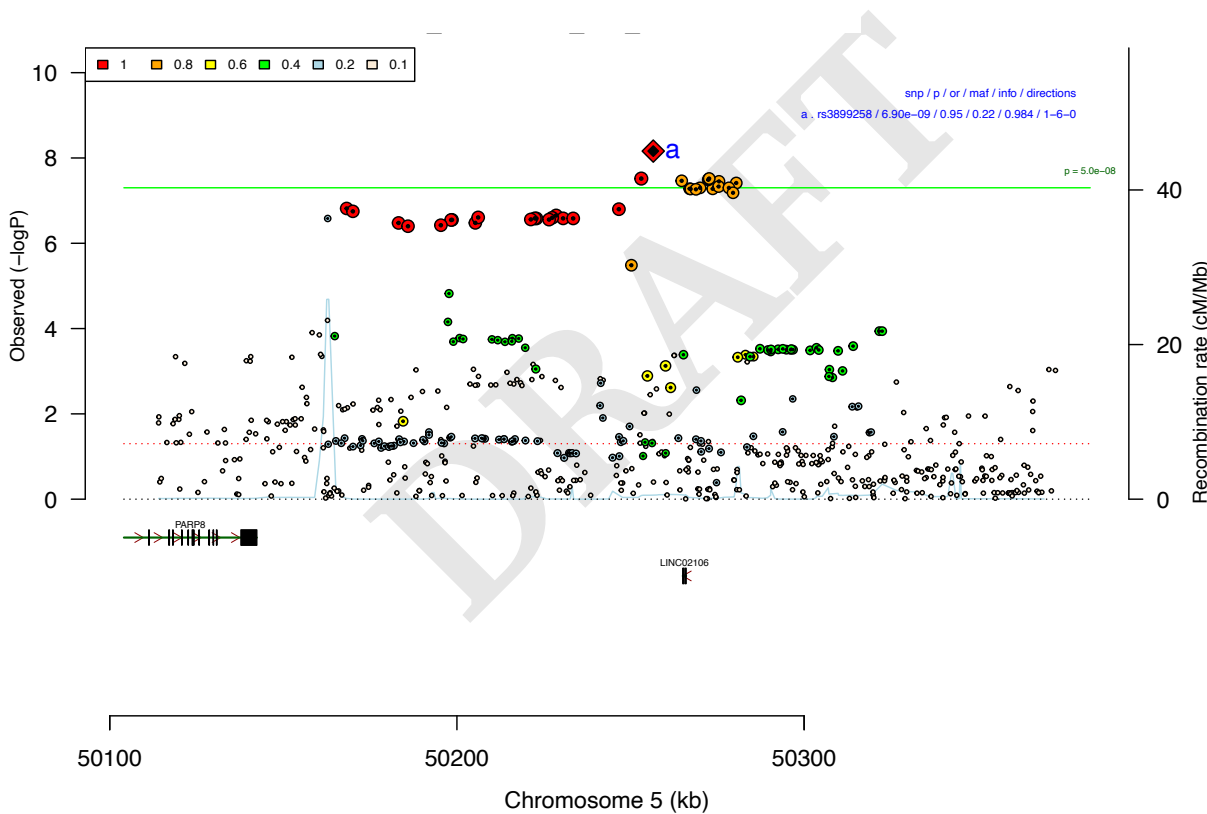
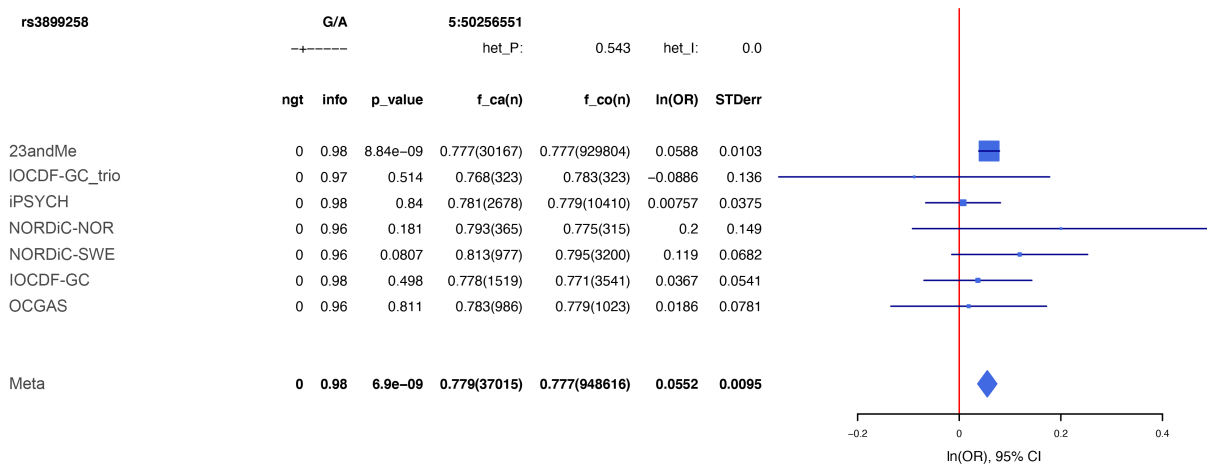


Fig. S12. Forest plot (top) and regional association plot (bottom) of SNP rs66818976. Forest plot: Shows the imputation score (info), p-value (p_value), A1 allele frequency in cases and number of cases (f_ca(n)), A1 allele frequency in controls and number of controls (f_co(n)), effect of the association (ln(OR)), and standard error of the effect (STDerr) for each individual dataset and the over-all meta-analysis. On the right side, effects (ln(OR)) and 95% confidence intervals (CI) are plotted. At the top, the direction of effect for each study is shown (+ for positive effect of A1, - for negative effect of A1), and results of a test of heterogeneity (het_P and het_I) of effect across the individual datasets re displayed. Regional association plot: The $-\log_{10}(P)$ of SNPs in the OCD meta-analysis GWAS is shown on the left y axis. The recombination rates expressed in centimorgans (cM) per Mb (Megabase) (blue line) are shown on the right y axis. Position in Mb is on the x axis. Only the SNPs with association p-value less than 0.1 were plotted. The lead SNP in the region is shown as a red diamond. Colour coding indicates LD to the lead SNP.

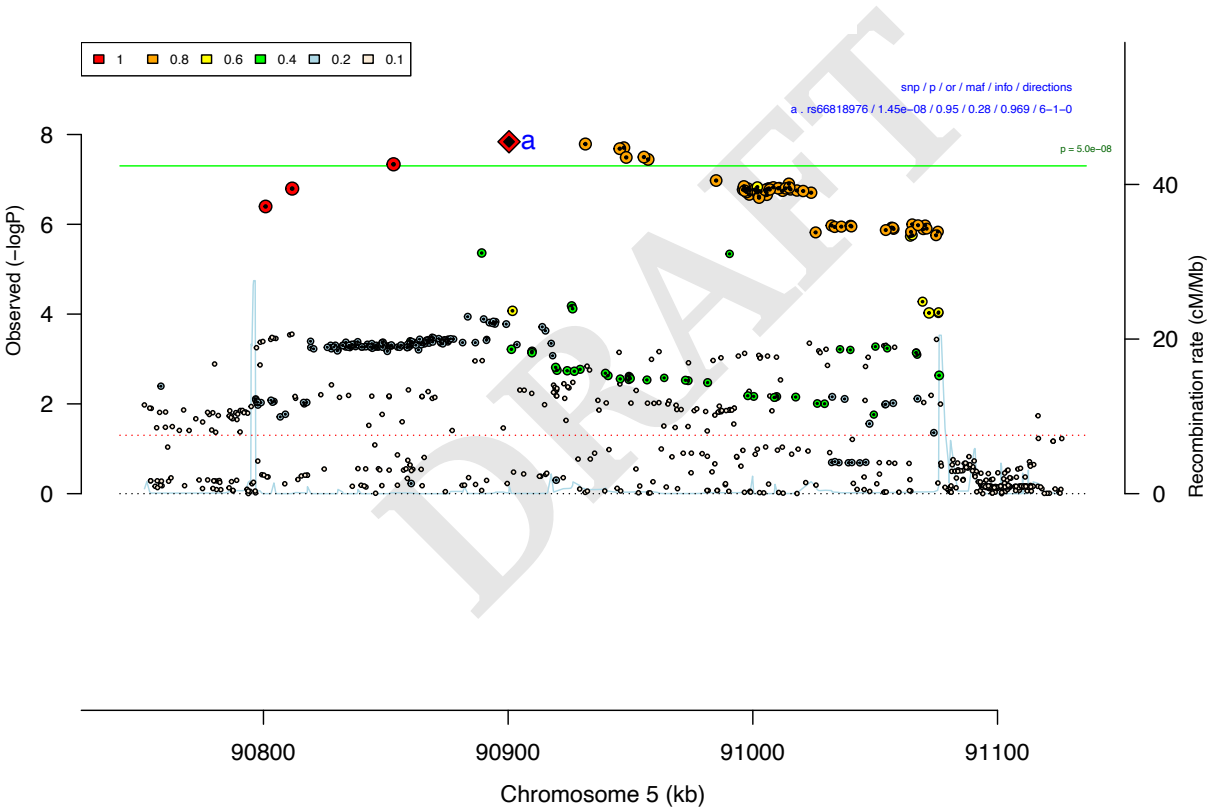
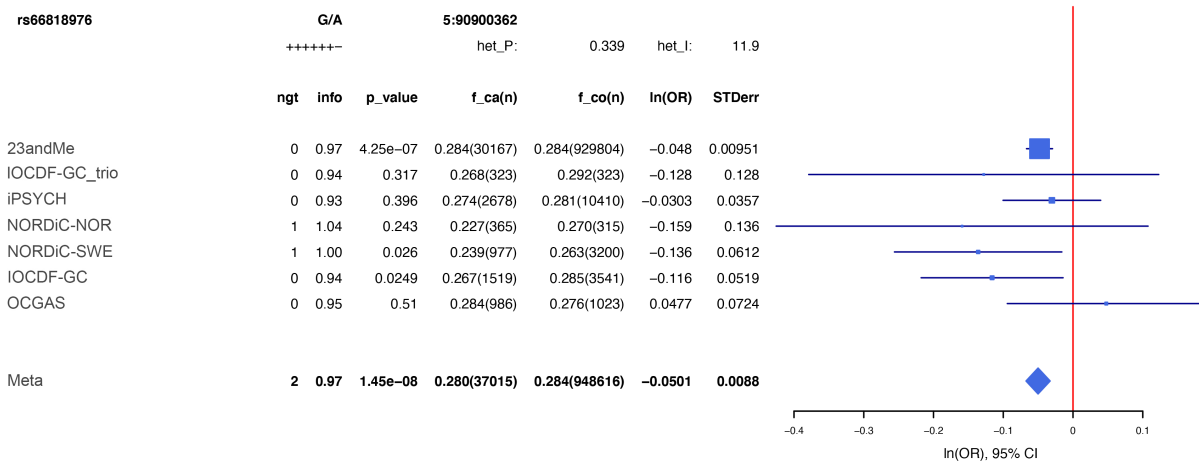


Fig. S13. Forest plot (top) and regional association plot (bottom) of SNP rs2836950. Forest plot: Shows the imputation score (info), p-value (p_value), A1 allele frequency in cases and number of cases (f_ca(n)), A1 allele frequency in controls and number of controls (f_co(n)), effect of the association (ln(OR)), and standard error of the effect (STDerr) for each individual dataset and the over-all meta-analysis. On the right side, effects (ln(OR)) and 95% confidence intervals (CI) are plotted. At the top, the direction of effect for each study is shown (+ for positive effect of A1, - for negative effect of A1), and results of a test of heterogeneity (het_P and het_I) of effect across the individual datasets re displayed. Regional association plot: The $-\log_{10}(P)$ of SNPs in the OCD meta-analysis GWAS is shown on the left y axis. The recombination rates expressed in centimorgans (cM) per Mb (Megabase) (blue line) are shown on the right y axis. Position in Mb is on the x axis. Only the SNPs with association p-value less than 0.1 were plotted. The lead SNP in the region is shown as a red diamond. Colour coding indicates LD to the lead SNP.

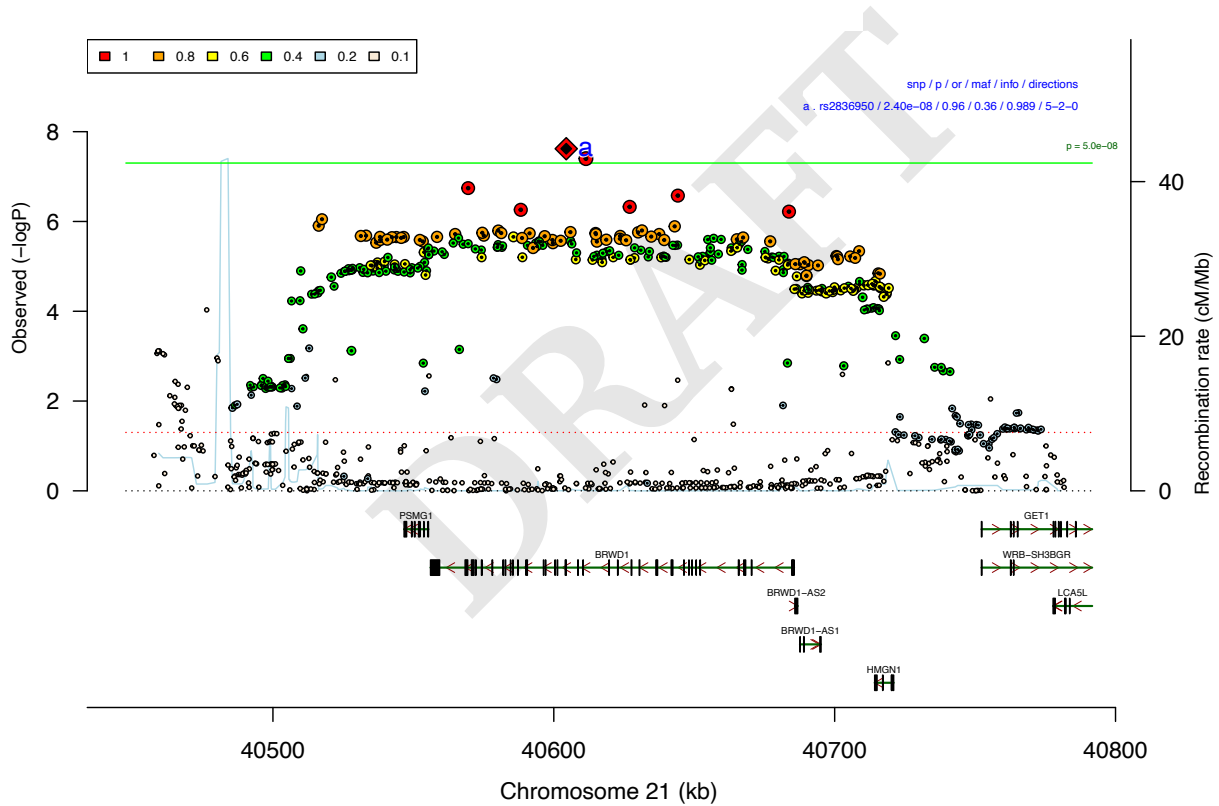
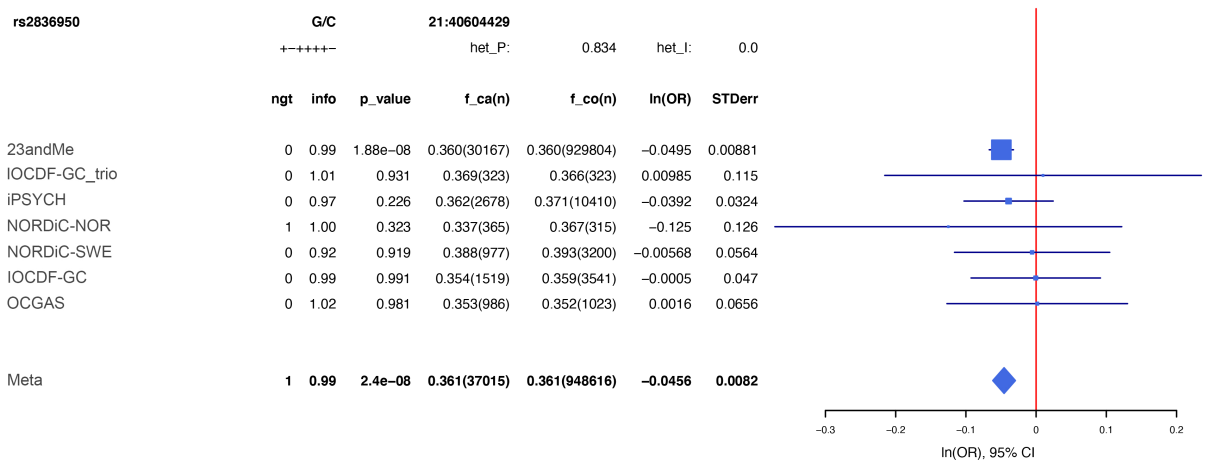


Fig. S14. Forest plot (top) and regional association plot (bottom) of SNP rs35518360. Forest plot: Shows the imputation score (info), p-value (p_value), A1 allele frequency in cases and number of cases (f_ca(n)), A1 allele frequency in controls and number of controls (f_co(n)), effect of the association (ln(OR)), and standard error of the effect (STDerr) for each individual dataset and the over-all meta-analysis. On the right side, effects (ln(OR)) and 95% confidence intervals (CI) are plotted. At the top, the direction of effect for each study is shown (+ for positive effect of A1, - for negative effect of A1), and results of a test of heterogeneity (het_P and het_I) of effect across the individual datasets re displayed. Regional association plot: The $-\log_{10}(P)$ of SNPs in the OCD meta-analysis GWAS is shown on the left y axis. The recombination rates expressed in centimorgans (cM) per Mb (Megabase) (blue line) are shown on the right y axis. Position in Mb is on the x axis. Only the SNPs with association p-value less than 0.1 were plotted. The lead SNP in the region is shown as a red diamond. Colour coding indicates LD to the lead SNP.

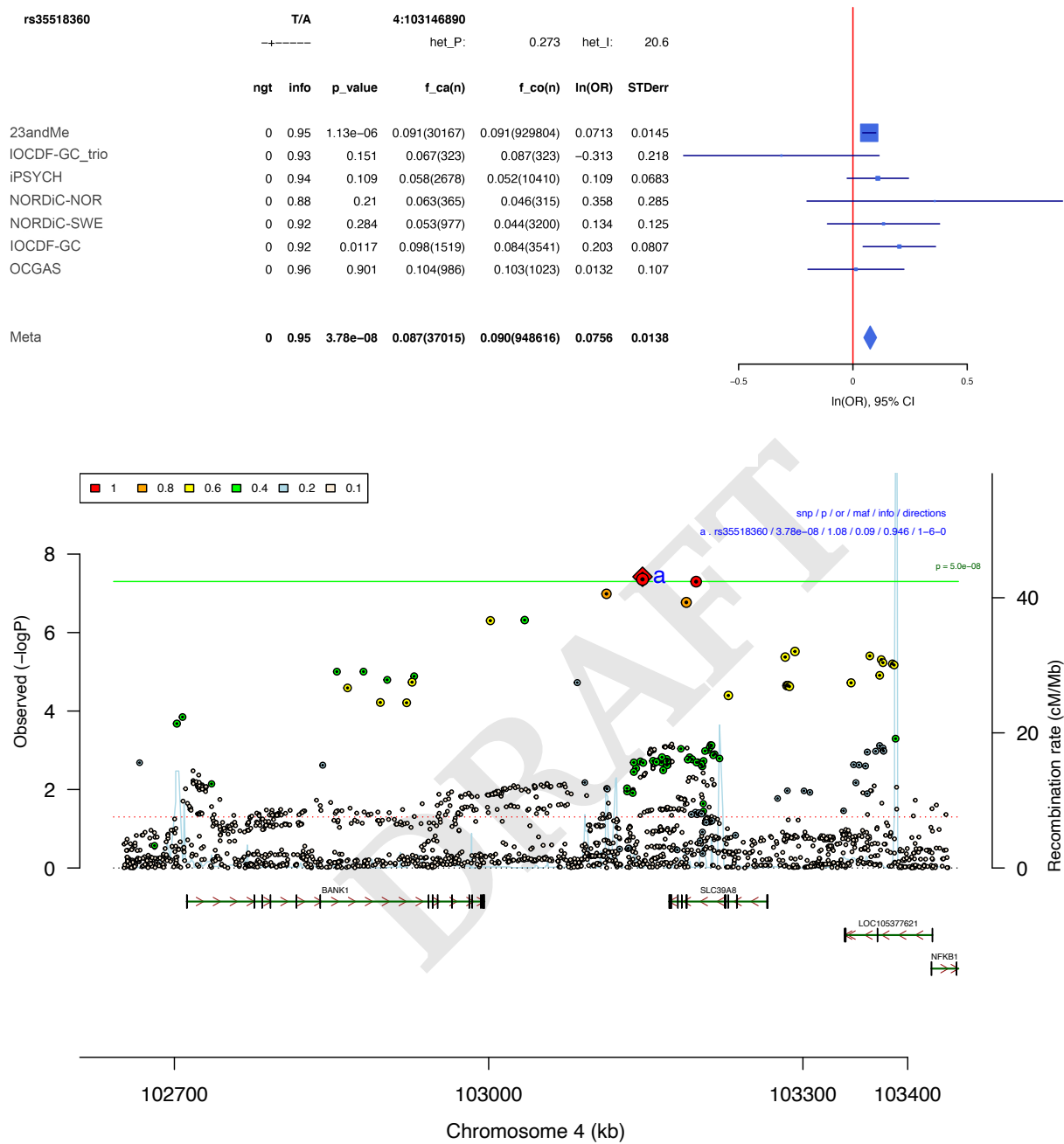


Fig. S15. Forest plot (top) and regional association plot (bottom) of SNP rs4460629. Forest plot: Shows the imputation score (info), p-value (p_value), A1 allele frequency in cases and number of cases (f_ca(n)), A1 allele frequency in controls and number of controls (f_co(n)), effect of the association (ln(OR)), and standard error of the effect (STDerr) for each individual dataset and the over-all meta-analysis. On the right side, effects (ln(OR)) and 95% confidence intervals (CI) are plotted. At the top, the direction of effect for each study is shown (+ for positive effect of A1, - for negative effect of A1), and results of a test of heterogeneity (het_P and het_I) of effect across the individual datasets re displayed. Regional association plot: The $-\log_{10}(P)$ of SNPs in the OCD meta-analysis GWAS is shown on the left y axis. The recombination rates expressed in centimorgans (cM) per Mb (Megabase) (blue line) are shown on the right y axis. Position in Mb is on the x axis. Only the SNPs with association p-value less than 0.1 were plotted. The lead SNP in the region is shown as a red diamond. Colour coding indicates LD to the lead SNP.

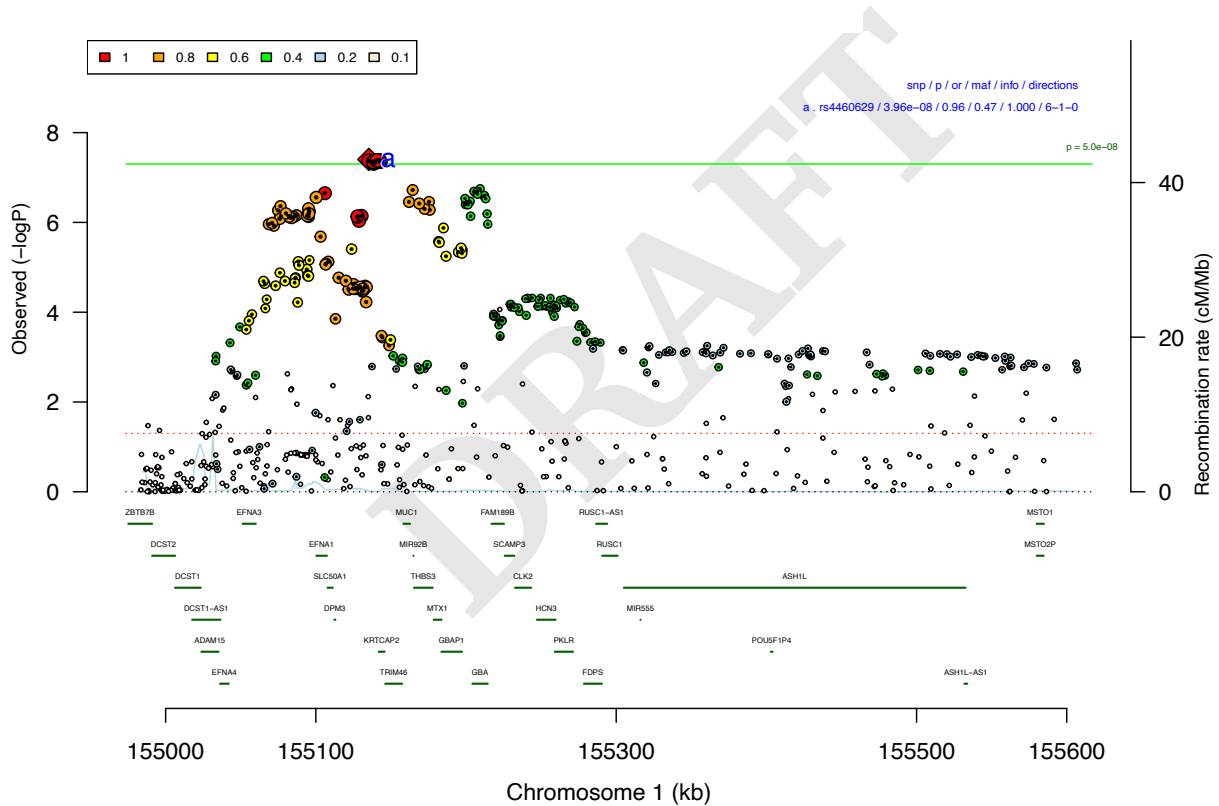
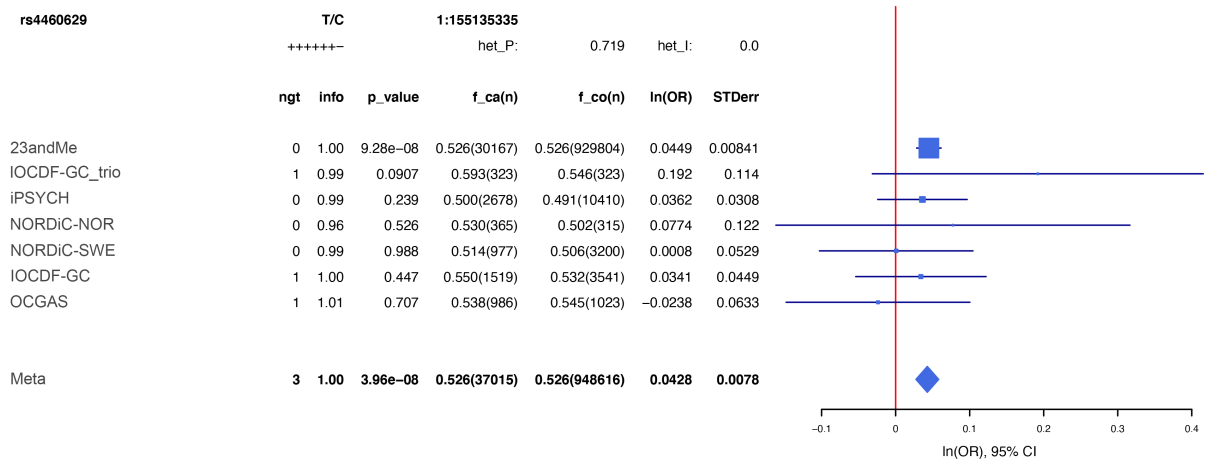


Fig. S16. Forest plot (top) and regional association plot (bottom) of SNP rs1922782. Forest plot: Shows the imputation score (info), p-value (p_value), A1 allele frequency in cases and number of cases (f_ca(n)), A1 allele frequency in controls and number of controls (f_co(n)), effect of the association (ln(OR)), and standard error of the effect (STDerr) for each individual dataset and the over-all meta-analysis. On the right side, effects (ln(OR)) and 95% confidence intervals (CI) are plotted. At the top, the direction of effect for each study is shown (+ for positive effect of A1, - for negative effect of A1), and results of a test of heterogeneity (het_P and het_I) of effect across the individual datasets re displayed. Regional association plot: The $-\log_{10}(P)$ of SNPs in the OCD meta-analysis GWAS is shown on the left y axis. The recombination rates expressed in centimorgans (cM) per Mb (Megabase) (blue line) are shown on the right y axis. Position in Mb is on the x axis. Only the SNPs with association p-value less than 0.1 were plotted. The lead SNP in the region is shown as a red diamond. Colour coding indicates LD to the lead SNP.

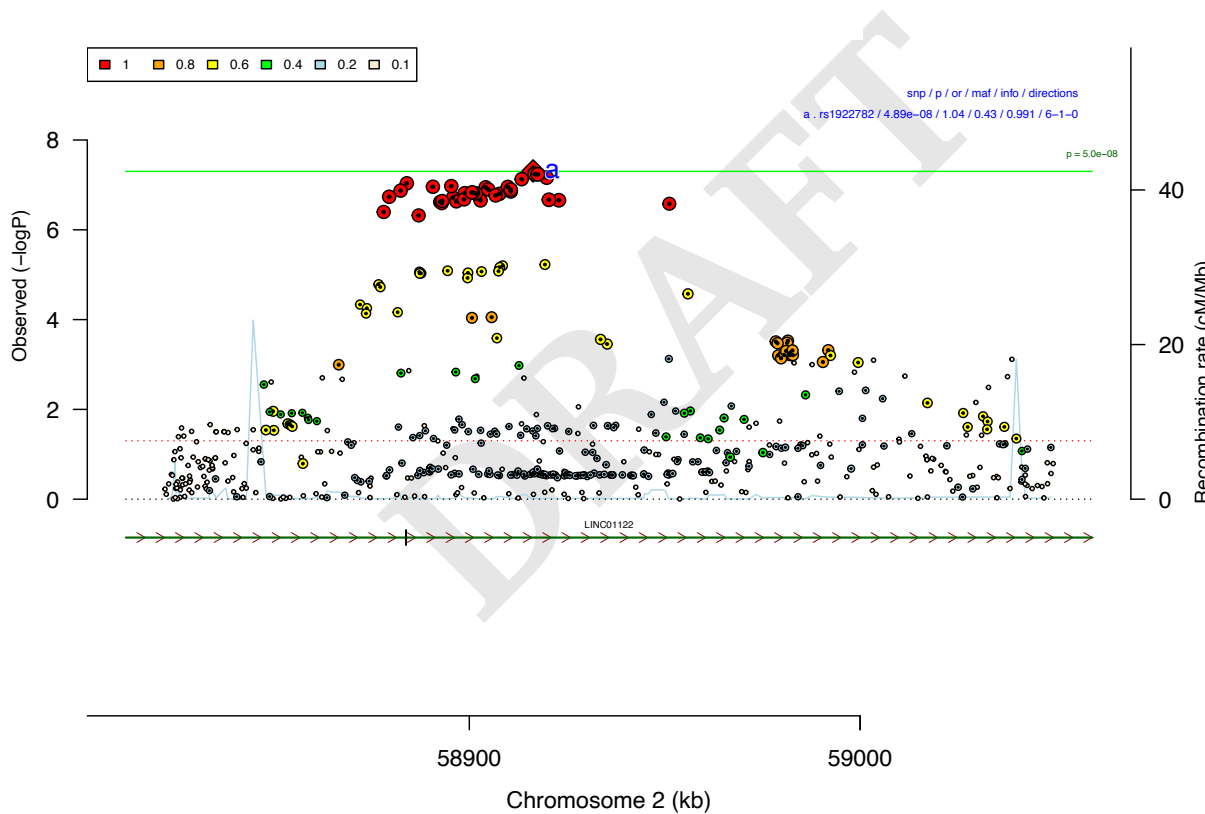
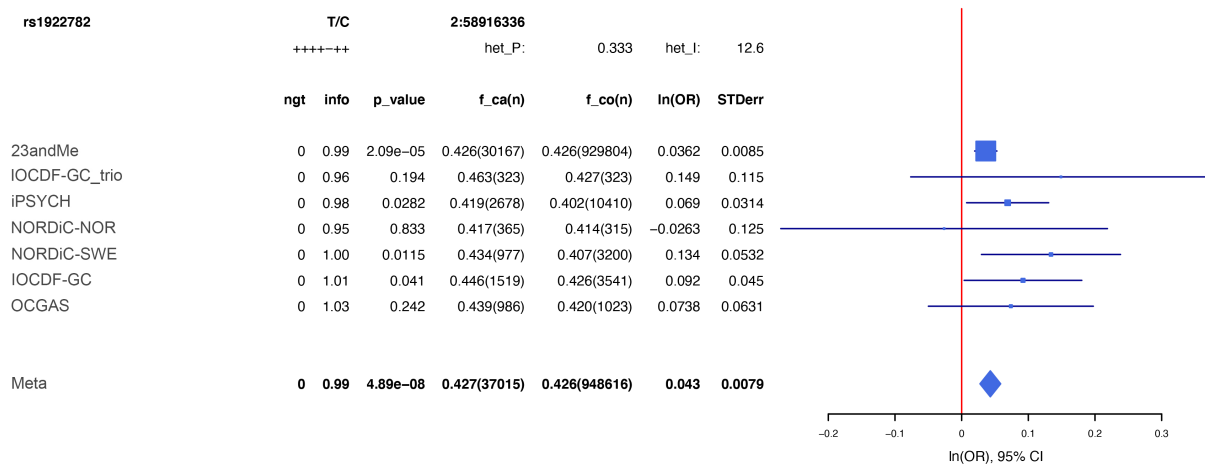
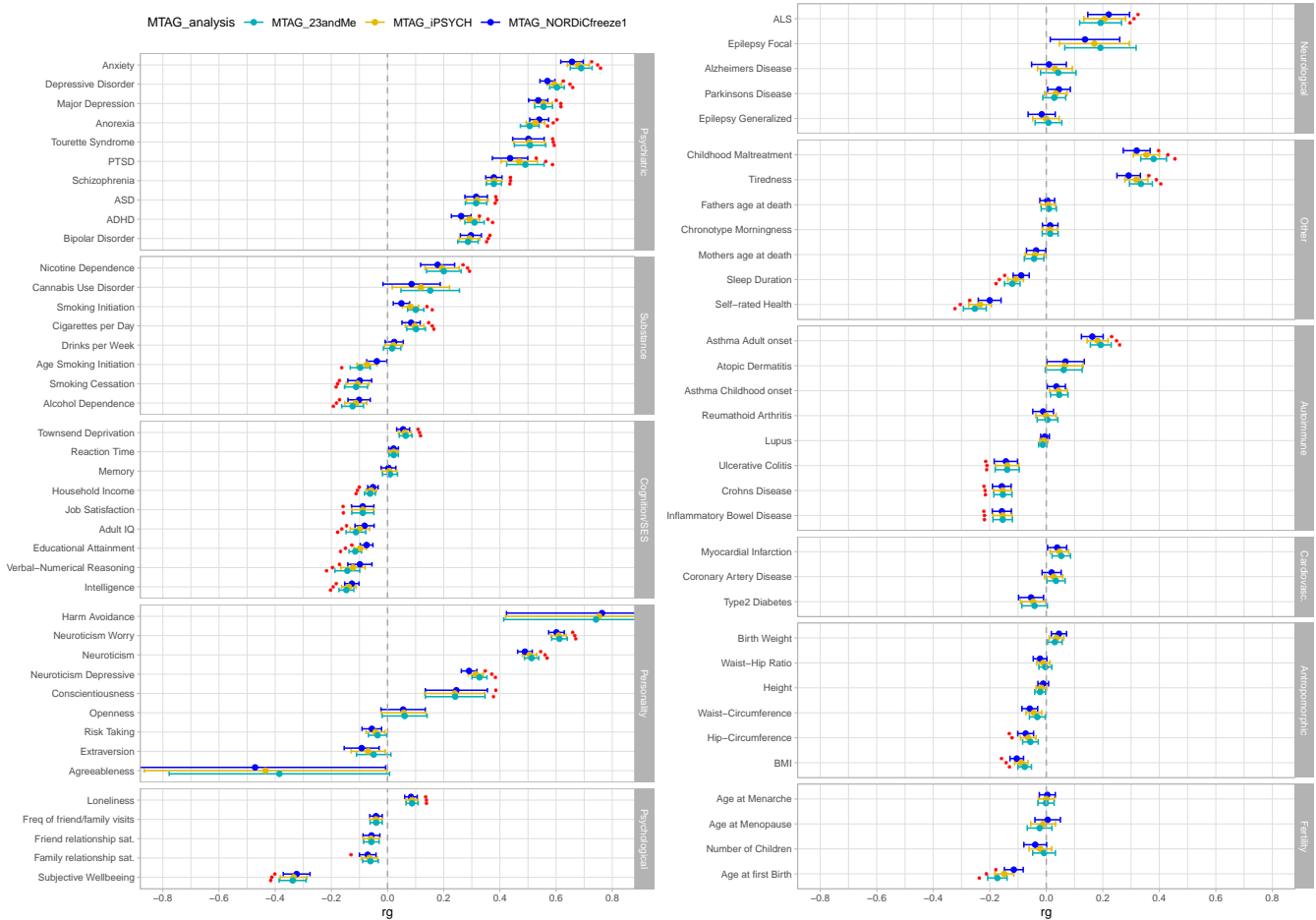


Fig. S17. Genetic correlations (rg) between OCD, divided into three sub-groups, and behavioral, cognitive, psychiatric, neurologic, immunologic, metabolic, and anthropomorphic phenotypes. Error bars represent standard errors and red asterisks indicate significant associations after FDR correction for multiple testing.



Fig. S18. Genetic correlations (r_g) between three MTAG analyses of OCD, and behavioral, cognitive, psychiatric, neurologic, immunologic, metabolic, and anthropomorphic phenotypes. Error bars represent standard errors and red asterisks indicate significant associations after FDR correction for multiple testing.



DR